Universität Hamburg

The neural cell adhesion molecule associates with and signals through p21-activated kinase 1 to regulate neuronal growth cone morphology in mice (*Mus musculus* Linnaeus, 1758)

Dissertation

von

Shen Li

Liaoning, China

zur Erlangung des akademischen Grades

Doktor der Naturwissenschaften Dr. rer. nat.

am Department Biologie der Fakultät für

Mathematik, Informatik und Naturwissenschaften

der Universität Hamburg

Hamburg, April 2009

Diese Arbeit wurde am im Institut für Biosynthese Neuraler Strukturen
des Zentrums für Molekulare Neurobiologie Hamburg angefertigt.

Gutachter: Prof. Dr. Melitta Schachner

Prof. Dr. Thorsten Burmester

Genehmigt vom Department Biologie
der Fakultät für Mathematik, Informatik und Naturwissenschaften
an der Universität Hamburg
auf Antrag von Frau Professor Dr. M. SCHACHNER
Weiterer Gutachter der Dissertation:
Herr Professor Dr. T. BURMESTER
Tag der Disputation: 29. Mai 2009

Hamburg, den 15. Mai 2009

Professor Dr. Jörg Ganzhorn
Leiter des Departments Biologie

Dr Jude Taylor
GSK
No. 3 699 Halei Rd
Pudong, Shanghai,
China 201203
PH: +86-61590814
Email: jude.m.taylor@gsk.com

Department of Biology,
University of Hamburg

April 29, 2009

I hereby declare that I have read the thesis entitled "The neural cell adhesion molecule associates with and signals through p21-activated kinase 1 to regulate neuronal growth cone morphology".

I am a native English speaker with a background in neuroscience and immunology. I consider the English in the thesis to be of a high standard and adequate for the authors PhD defense.

Yours sincerely,

Dr. Jude Taylor, PhD

GSK
Shanghai

TABLE OF CONTENTS

ABSTRACT

The neural cell adhesion molecule (NCAM) is a member of the immunoglobulin superfamily of cell adhesion molecules. Being the most prominent cell adhesion molecule in the nervous system, NCAM plays important roles in regulating neuronal morphology, growth and migration. NCAM dysfunction is linked to human brain disorders such as schizophrenia and bipolar disorder. However, the various ways by which NCAM evokes its cellular responses are not completely understood.

In the present study, p21-activated kinase 1 (Pak1) was identified as a new binding partner of the intracellular domain of NCAM. Paks are highly conserved serine / threonine protein kinases. Their activity is stimulated by the binding of active Rho family GTPases Rac and Cdc42 and lipids. They are very important for the cytoskeletal organization, transcription regulation, cell death and survival signaling and oxidant generation in phagocytic leukocytes.

It was revealed in this study that clustering of NCAM on growth cone membrane changed the phosphorylation pattern of Pak1, leading to activation of Pak1 and its effectors LIMK1 and cofilin. The phosphorylation status, kinase activity and levels of membrane associated Pak1 were abnormal in brains of NCAM-deficient mice. Expression and phosphorylation of LIMK1 and cofilin were dysregulated in the mutant as well. NCAM enhanced Pak1 activity by promoting formation of Pak1-Cdc42-PIX complexes at lipid rafts. Active Pak1 was rapidly released back to the cytosol to phosphorylate and activate LIMK1 which further phosphorylated cofilin and inhibited its filamentous actin severing and depolymerizing property. Increased levels of active non-phosphorylated cofilin in NCAM-deficient brains caused excessive actin depolymerization which resulted in morphological abnormalities of growth cones *in vitro*, including enlargement of growth cones and inhibition of filopodia formation and mobility.

In conclusion, the findings of this thesis work will contribute to a better understanding of the molecular mechanisms underlying NCAM-mediated cytoskeletal reorganization and neurite outgrowth.

ZUSAMMENFASSUNG

Das neurale Zelladhäsionsmolekül (NCAM) ist ein Mitglied der Zelladhäsionsmoleküle der Immunglobulin-Superfamilie. Als das prominenteste Zelladhäsionsmolekül im Nervensystem spielt NCAM eine wichtige Rolle in der Regulation der neuronalen Morphologie, des Wachstums und der Migration. Fehlfunktionen von NCAM werden mit psychiatrischen Erkrankungen wie Schizophrenie und bipolarer Störung in Verbindung gebracht. Die verschiedenen Wege auf denen NCAM diverse zelluläre Antworten auslöst, sind jedoch noch nicht vollständig aufgeklärt.

Im Rahmen dieser Arbeit wurde Pak1 (*p21-activated kinase 1*) als neuer Bindungspartner der intrazellulären Domäne von NCAM identifiziert. Paks sind stark konservierte Serin- / Threonin-Proteinkinasen, deren Aktivität durch die Bindung von aktiven GTPasen der Rho-Familie, Rac und Cdc42 und Lipiden stimuliert wird. Sie sind sehr wichtig für die Organisation des Zytoskeletts, Transkriptionsregulation, Zelltod und Zellüberleben sowie die Bildung von Oxidationsmitteln in phagozytierenden Leukozyten.

In dieser Studie konnte gezeigt werden, dass das Clustering von NCAM auf der Membran von Wachstumskegeln das Phosphorylierungsmuster von Pak1 beeinflusst. Dies führt zur Aktivierung von Pak1, was die Aktivierung von LIMK1 und Cofilin zur Folge hat. Der Phosphorylierungsstatus, die Kinaseaktivität und der Level von Membran-assoziiertem Pak1 sind abnormal in Gehirnen von NCAM-defizienten Mäusen. Die Expression und Phosphorylierung von LIMK1 und cofilin sind in der Mutante ebenfalls disreguliert. NCAM verstärkt die Aktivität von Pak1, indem es die Bildung des Pak1-Cdc42-PIX Komplexes in *lipid rafts* fördert. Aktives Pak1 wird schnell ins Zytosol freigesetzt, um dort LIMK zu phosphorylieren und aktivieren. LIMK1 phosphoryliert anschließend cofilin und hemmt dadurch dessen Fähigkeit, Aktinfilamente zu zerteilen und zu depolymerisieren. Der gesteigerte Level von aktivem, nicht-phosphoryliertem cofilin in NCAM-defizienten Gehirnen verursacht eine übermäßige Aktindepolymerisation, was *in vitro* zu morphologischen Abnormitäten der Wachstumskegel führt. Dies beinhaltet die Vergrößerung der Wachstumskegel und die Hemmung der Filopodienbildung sowie deren Mobilität.

Meine Ergebnisse tragen somit zum Verständnis der molekularen Mechanismen bei, die der NCAM-vermittelten Reorganisation des Zytoskeletts und dem Wachstum von Neuriten zugrunde liegt.

I. INTRODUCTION

I.1. CELL ADHESION MOLECULES (CAMS)

The nervous system is organized in a pattern of remarkable complexity and precision. A human brain contains roughly ten billion specialized cells called neurons (Williams and Herrup, 1988). A neuron is an elongated, asymmetric cell with a long axon and branching dendrites connecting it through synapses to other neurons. Formation of right connections between neurons depends on the controlled spatial and temporal expression of selective adhesion molecules on the neural cell surface (Shapiro et al., 2007). The development of the neuronal network is a complex multi-step process, which begins with neural induction, proliferation and migration of neural cells. It continues with determination of developmental fate, axon and dendrite formation, growth cone guidance and formation of synapses, elaboration of neurites and the programmed death of some neurons (Maness and Schachner, 2007).

Cell adhesion molecules (CAMs) are heavily involved in the development of the nervous system. Besides migration, neurulation (neural tube formation), neurite outgrowth, synapse formation and plasticity, CAMs play a crucial role in myelination as well as nerve regeneration after injury (Crossin and Krushel, 2000; Santuccione et al., 2005; Schuch et al., 1989). A CAM on one cell can directly bind to the same kind of CAM (homophilic binding) or to a different class of CAM (heterophilic binding). Association of CAMs on the same cell plasma membrane gives rise to homodimers or higher-order oligomers in the plane of the cell's plasma membrane are called *cis*-interactions. Binding of CAM oligomers on one cell to the same or different CAMs on an adjacent cell are called *trans*-interactions (Kiselyov et al., 2005).

Although originally defined by their ability to attach cells to each other and to the extracellular matrix (ECM), CAMs are now known to provide a means for the bidirectional transfer of information between the exterior and the interior of cells (Maness and Schachner, 2007). The cytosolic domains of CAMs recruit sets of multifunctional scaffold proteins (Leshchyns'ka et al., 2003; Pollerberg et al., 1987; Pollerberg et al., 1986). These adapters act as linkers that directly or indirectly connect CAMs to elements of the cytoskeleton. They can also recruit intracellular molecules that are involved in signaling pathways (Ditlevsen et al., 2008). In some cases, a complex aggregate of CAMs, adapter proteins, and other associated proteins is assembled at the inner surface of the plasma membrane.

Based on their structural characteristics CAMs are grouped into four major families: integrins, cadherins, the immunoglobulin superfamily (IgSF) and selectins. Integrins are mainly involved in cell-matrix adhesion, whereas cadherins and Ig superfamily of CAMs mainly mediate cell to cell attachment. The group of selectins is especially important for a variety of transient cell-cell interactions in the blood stream (Juliano, 2002; Lee and Benveniste, 1999). The importance of CAMs in cell adhesion has been directly demonstrated *in vitro* by application of specific CAM antibodies to cultured cells, which blocked adhesion between the cells (Akiyama et al., 1989; Beug et al., 1970; Rutishauser et al., 1978; Seilheimer and Schachner, 1988; Thiery et al., 1977).

I.1.1. The neural cell adhesion molecule NCAM

Multiple transmembrane proteins characterized by the presence of a variable number of immunoglobulin (IgG) repeats in their extracellular regions constitute the Ig superfamily of CAMs (IgCAMs). The Ig domain is a common protein motif, containing 70–110 residues, that was first identified in IgGs (Edelman and Poulik, 1961). Being the first member of this family described in the nervous system, NCAM was discovered independently by different groups (Jorgensen and Bock, 1974; Rutishauser et al., 1976; Thiery et al., 1977). Each of its five membrane-distal Ig-like domains has an intrachain disulfide bond that connects the two anti-parallel beta-sheets. Additionally, NCAM has two membrane-proximal domains that resemble regions of ECM component fibronectin termed fibronectin type 3-like domains (FNIII) (Fig. 2). NCAM plays a key role in neuronal development, synaptic plasticity and regeneration (Maness and Schachner, 2007). The importance of NCAM is emphasized by the fact that NCAM dysfunctions often lead to human neuropsychiatric and neurodegenerative disorders, such as schizophrenia, autism, anxiety disorders, depression and bipolar disorder (Arai et al., 2004; Gillian et al., 1994; Plioplys et al., 1990; Sullivan et al., 2007; Tsoory et al., 2008). Moreover, NCAM has gained much attention in cancer research because of its adhesive property (Zecchini and Cavallaro, 2008).

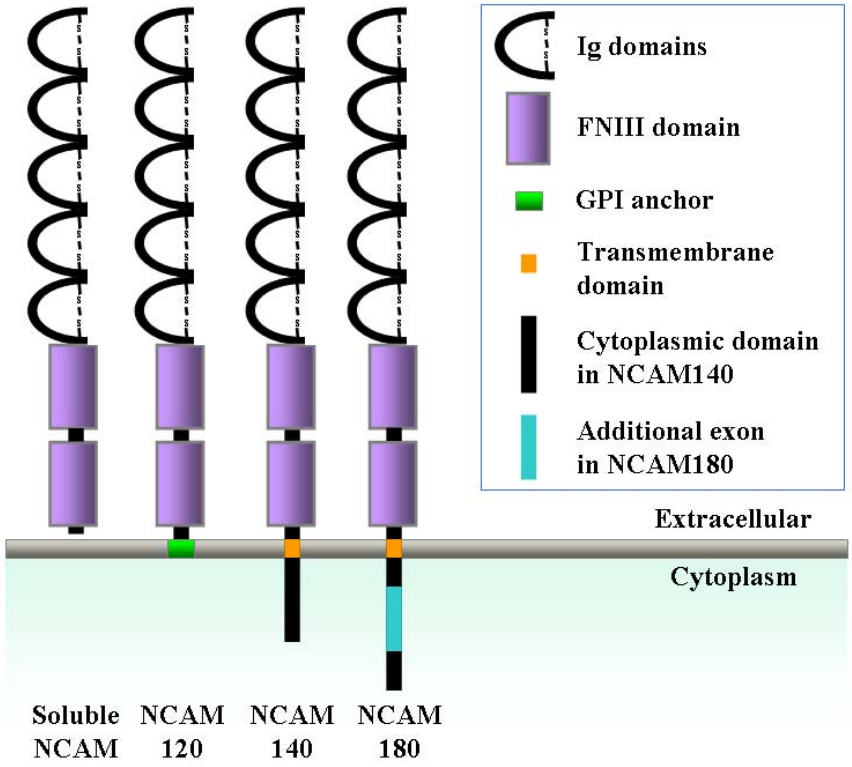

Fig. 1: **Major NCAM isoforms.** NCAM120, NCAM140 and NCAM180 consist of five immunoglobulin-like (Ig) domains and two fibronectin type 3-like (FNIII) domains in the extracellular part. NCAM120 is anchored to the plasma membrane owing to a glycosylphosphatidylinositol (GPI) anchor, whereas NCAM140 and NCAM180 are integral proteins that span the plasma membrane. The cytoplasmic domains of NCAM180 and NCAM140 differ in length due to an additional exon insert in NCAM180.

NCAM is encoded by a single gene, ncam1, which is located on chromosome 11 in humans (Nguyen et al., 1986; Walsh et al., 1986) and on mouse chromosome 9 (D'Eustachio et al., 1985). Due to alternative splicing, a variety of NCAM isoforms exist. NCAM180, NCAM140 and NCAM120 are three major isoforms denoted according to their apparent molecular weight on a SDS-PAGE gel (Goridis et al., 1983). These isoforms are similar in their extracellular domain but differ in their intracellular structure. NCAM120 consists solely of an extracellular part and is tethered to the membrane via a glycosylphosphatidylinositol (GPI) lipid anchor (Hemperly et al., 1986a) (Fig. 1). On the other hand, NCAM140 and NCAM180 are transmembrane proteins (Hemperly et al., 1986b) and NCAM180 differs from NCAM140 in having a 261-amino acid insert in the cytoplasmic region. Further isoforms can be generated by exclusion or inclusion of 6 small exons in the original transcript (Walmod et al., 2004). In addition to the membrane associated isoforms, secreted and soluble isoforms of NCAM were also reported (Bock et al., 1987; Gower et al., 1988; He et al., 1986; Hinkle et al., 2006). The soluble isoforms can be detected in human cerebrospinal fluid (CSF), serum and

amniotic fluid (Ibsen et al., 1983; Krog et al., 1992). Notably, an increase in the soluble isoform of NCAM in the CSF, the hippocampus as well as the prefrontal cortex is implicated in schizophrenia (Poltorak et al., 1995).

The diversity of NCAM is also generated by posttranslational modifications. The transmembrane isoforms can be reversibly palmitoylated at up to four cysteine residues in the intracellular juxtamembrane region (Little et al., 1998; Ponimaskin et al., 2008). Palmitoylation increases the hydrophobicity and enhances the attachment to special microdomains in the membrane, the so called lipid rafts. NCAM is part of the glycocalyx and can carry either N-glycosylations (Albach et al., 2004) or O-glycosylations (Ong et al., 2002a; Walsh et al., 1989). NCAM was the first vertebrate protein demonstrated to be glycosylated with polysialic acid (PSA), a negatively charged sugar derivative (Finne et al., 1983; Hoffman et al., 1982; McCoy et al., 1985). PSA attenuates the adhesive properties of NCAM (Cunningham et al., 1983; Sadoul et al., 1983) and modifies the functions of NCAM during neural migration, axon path finding and synaptic plasticity (Angata et al., 2004; Eckhardt et al., 2000; Weinhold et al., 2005). Polysialylation of NCAM decreases developmentally, changing NCAM from a plasticity promoting molecule to a stability generating molecule (Rutishauser et al., 1988).

NCAM is expressed on both neurons and glia. It appears early during embryonic development and persists into adulthood in the nervous system (Edelman, 1985). Interestingly, NCAM shows cell-specific expression pattern. The NCAM140 isoform is present in both neurons and glial cells, whereas NCAM120 is mainly expressed in glia (Bhat and Silberberg, 1988; Noble et al., 1985) and NCAM180 occurs predominantly in neurons late in development (Persohn et al., 1989). It is worth mentioning that NCAM is also expressed in non-neuronal tissue including muscle (Sanes et al., 1986), heart (Burroughs et al., 1991), pancreas and gonad (Moller et al., 1991). The subcellular localization also differs among the NCAM isoforms and might reflect the various functions that different NCAM isoforms support. During the development of a neuron, NCAM140 is the predominant isoform expressed in neurites, whereas in mature neurons it is localized to pre- and postsynaptic membranes. NCAM180 is mainly present in postsynaptic densities in the mature neuron (Persohn et al., 1989; Pollerberg et al., 1987; Schuster et al., 1998; Sytnyk et al., 2006).

The mechanism of NCAM homophilic interaction is still under debate. One hypothetical model is proposed on the basis of the crystal structure of the first three Ig modules of NCAM (Kiselyov et al., 2005). Briefly, two NCAM molecules on the same cell interact with high affinity by bending over each other and forming a cross through the first two Ig modules. When these NCAM *cis*-dimers aggregate between two opposing cells, they do so in either a "flat zipper" pattern or a "compact zipper" pattern. These homophilic interactions in turn induce heterophilic binding with various signaling molecules both extracellularly and intracellularly. Extracellularly, NCAM associates with other IgCAMs such as L1, the GPI anchored proteins transient axonal glycoprotein-1 (TAG-1) and prion protein (PrP), growth factors and growth factor receptors (FGFR, GDNF, GFRα, BDNF, PDNF), adenosine triphosphate (ATP) as well as several components of ECM (Horstkorte et al., 1993; Kiselyov et al., 2003; Milev et al., 1996; Paratcha et al., 2003; Probstmeier et al., 1989; Santuccione et al., 2005; Schmitt-Ulms et al., 2001; Vutskits et al., 2001; Zhang et al., 2004). NCAM initiates signaling transduction also by interaction with and activation of intracellular binding partners, e.g. non-receptor tyrosine kinase $p59^{fyn}$ (Beggs et al., 1997), receptor protein tyrosine phosphatase α (RPTPα) (Bodrikov et al., 2005) and multiple scaffolding molecules and cytoskeleton associated proteins such as spectrin, tubulin and growth-associated protein-43 (GAP-43) (Buttner et al., 2003; He and Meiri, 2002; Leshchyns'ka et al., 2003; Pollerberg et al., 1986). Depending on the accessibility of distinct binding partners NCAM can be locally involved in different processes.

I.1.2. NCAM in the process of neurite outgrowth

Different experimental approaches are employed to activate NCAM-mediated signaling pathways, which are collectively termed as NCAM stimulation. For instance, antibodies against NCAM extracellular domain successfully cluster NCAM molecules at the cell surface (Beggs et al., 1997). Besides, recombinant proteins comprising extracellular fragment of NCAM fused to the human IgG1 Fc-region are also shown to be capable of inducing NCAM homophilic binding and subsequent activation of NCAM related signal pathways (Doherty et al., 1995; Niethammer et al., 2002). NCAM-dependent signal transduction is also investigated with the help of pharmacological inhibitors of presumptive downstream molecules. NCAM does not possess any known catalytic activity *per se*, but it can evoke multiple signaling cascades depending on different interaction partners. NCAM modulates diverse biological functions including cell migration, differentiation, proliferation, survival, neurite outgrowth, the fasciculation of axons and the organization of synapses (Chung et al., 1991; Cremer et al.,

1997; Ditlevsen et al., 2003; Doherty et al., 1990b; Lindner et al., 1986; Neugebauer et al., 1988; Seilheimer and Schachner, 1988; Sytnyk et al., 2002; Vutskits et al., 2001). Among them, NCAM-mediated neurite extension is the most studied NCAM function to date. Both homophilic (Doherty et al., 1991a; Doherty et al., 1990b) and heterophilic (Williams et al., 1994a) interactions of NCAM can lead to the induction of intracellular signaling pathways thereby promoting neurite outgrowth.

Experiments making use of NCAM blocking antibodies give the first hint that NCAM might play a role in promoting neurite outgrowth. Treatment with NCAM antibodies hinders neurite outgrowth of retinal neurons grown on astrocytes (Neugebauer et al., 1988), dorsal root ganglion neurons grown on Schwann cells and fibroblast monolayers (Seilheimer and Schachner, 1988) and explants of chick retina grown on retinal glial cells (Drazba and Lemmon, 1990). These investigations indicate that NCAM-mediated neurite outgrowth can not be separated from its adhesive properties. In a later approach, neurons are cultured on monolayers of control or NCAM transfected cells and analyzed for their ability to extend neurites. By this means, NCAM is shown to stimulate neurite outgrowth from a variety of neuronal types (Doherty et al., 1991a; Doherty et al., 1990a; Doherty et al., 1990b; Doherty et al., 1991b). Interestingly, soluble fragments of some CAMs, such as NCAM and L1, are also shown to have the neurite outgrowth promoting properties (Doherty et al., 1995; Meiri et al., 1998). This put forward the notion that CAMs can increase neurite elongation through mechanisms other than adhesion. Thus, CAMs are believed to be not simply adhesive molecules but also could initiate signaling transduction.

It is well known that fibroblast growth factor receptor (FGFR), an IgSF receptor tyrosine kinase, plays an important role in NCAM-mediated neurite outgrowth (Niethammer et al., 2002; Saffell et al., 1997; Williams et al., 1994a). Due to the abundance of NCAM on the cell surface, about 85% of the FGFR molecules are estimated to be constantly involved in a transient binding with NCAM (Kiselyov et al., 2003). In order to activate FGFR, NCAM has to adopt *trans*-homophilic interaction, which increases the local concentration of NCAM-bound FGFR and facilitates its dimerization. Dimerized FGFR leads to *trans*-autophosphorylation and kinase activation (Schlessinger, 2000). One of FGFR's substrates is phospholipase Cγ (PLCγ) which binds the cytoplasmic phosphorylated residues of FGFR via its SH2 (src homology 2) domain and gets subsequently activated (Saffell et al., 1997). Activated PLCγ hydrolyzes phosphatidylinositol 4,5-bisphosphate (PIP2) to generates

inositol 1,4,5-trisphosphate (IP3) and diacylglycerol (DAG). These and further downstream second messenger trigger calcium influx from intracellular stores and extracellular space into the cytoplasm (Doherty et al., 1991a; Kiryushko et al., 2006; Ronn et al., 2002; Williams et al., 1994b). The increasing cellular calcium concentration induces further signaling cascades. A crucial serine / threonine protein kinase, protein kinase C (PKC), is also activated downstream of NCAM stimulation by the combination of increased Ca^{2+}, DAG and the negatively charged membrane phospholipid phosphatidylserine (Kolkova et al., 2000; Leshchyns'ka et al., 2003). Moreover, NCAM-induced neurite outgrowth is also reported to be dependent on another FGFR-mediated pathway, in which the adaptor protein FGFR substrate 2 (FRS2) and the docking protein ShcA are indispensable (Hinsby et al., 2004).

Although several interaction partners are shared between NCAM140 and NCAM180, they also bind preferentially to distinct signaling molecules, indicating that they might have different functions. NCAM140, but not NCAM180 or NCAM120, constitutively co-immunoprecipitates with the src family tyrosine kinase $p59^{fyn}$, and NCAM crosslinking by its antibodies induces transient $p59^{fyn}$ phosphorylation (Beggs et al., 1997; Kramer et al., 1999). In addition, when neurons from $p59^{fyn}$-deficient mice grow on fibroblasts expressing NCAM, they exhibit a reduction of neurite growth (Beggs et al., 1994). Pharmacological inhibition of src family kinases abolishes NCAM stimulated neurite outgrowth (Kolkova et al., 2000) and $p59^{fyn}$ activity decreases in NCAM deficient mice as compared to wild-type mice (Bodrikov et al., 2005). These data suggest a role of $p59^{fyn}$ in NCAM mediated signaling. Further investigation reveals that NCAM-$p59^{fyn}$ interaction is mediated via RPTPα (Bodrikov et al., 2005), which is a known activator of src family tyrosine kinases and is highly expressed in neurons and growth cones (Ponniah et al., 1999; Zheng et al., 1992). The increase in calcium concentration in response to NCAM-FGFR signaling strengthens the complex between NCAM140 and RPTPα via spectrin (Bodrikov et al., 2005). Upon NCAM activation and palmitoylation the complex redistributes into lipid rafts (Bodrikov et al., 2005; Niethammer et al., 2002). This event recruits and activates downstream signaling molecules such as the focal adhesion kinase (FAK) (Niethammer et al., 2002), which culminates in the activation of the mitogen activated protein kinase (MAPK) pathway (Schmid et al., 1999). These serine / threonine protein kinases regulate the activity of several transcription factors such as CREB, NFκB and c-fos. They enter the nucleus where they regulate the transcription of their target genes (Pawson and Scott, 1997).

Downstream of NCAM-mediated FGFR activation, PKC is activated as aforementioned. NCAM180 is shown to be a more potent PKCβ2-binding isoform relative to NCAM140, although PKCβ2 also co-immunoprecipitates to a lesser extent with NCAM140 (Leshchyns'ka et al., 2003). Spectrin binding is required for NCAM-PKC association, as a dominant–negative spectrin construct disrupts the co-immunoprecipitation of NCAM with PKCβ2 (Leshchyns'ka et al., 2003; Rodriguez et al., 1999). Upon NCAM activation, NCAM-spectrin-PKCβ2 complex redistributes to lipid rafts where PKC affects various growth-promoting substrates, for instance GAP-43 (Botto et al., 2007; Sheu et al., 1990). GAP-43 is a membrane associated and palmitoylated glycoprotein and is highly expressed in neurons in the developing nervous system. GAP-43 is enriched in axonal growth cones and functions eventually in the regulation of actin polymerization (Goslin et al., 1988; He et al., 1997; Meiri et al., 1998). Formation of the NCAM-spectrin-PKCβ2 complex can be enhanced by Ca^{2+} binding to spectrin (Ditlevsen et al., 2008). There are findings indicating that protein kinase A (PKA) (Jessen et al., 2001), calmodulin-dependent protein kinase II (CaMKII) (Bodrikov et al., 2008; Ditlevsen et al., 2007a; Williams et al., 1995), Phosphatidylinositol 3-kinase (PI3K) / Akt pathway (Ditlevsen et al., 2003; Neiiendam et al., 2004; Pedersen et al., 2004) and nitric oxide (NO) synthase / NO / cyclic guanosine monophosphate / protein kinase G pathway (Ditlevsen et al., 2007b) are as well implicated in NCAM-mediated neurite outgrowth.

I.1.3. The role of lipid rafts in NCAM-mediated neurite outgrowth

Lipid rafts are small (10-200 nm), heterogeneous, highly dynamic, sterol- and sphingolipid-enriched domains that compartmentalize cellular processes. Small rafts can sometimes be stabilized to form larger platforms through protein-protein and protein-lipid interactions (Pike, 2006). The lipid raft hypothesis, initially proposed by Simons & Ikonen (Simons and Ikonen, 1997) introduces a modified paradigm to the Singer-Nicolson fluid mosaic model (Singer and Nicolson, 1972). Lipid rafts are viewed as critical sites for cellular signaling, protein and lipid trafficking and viral and toxin entry. Most of our current knowledge concerning the function of rafts comes from two operational definitions: depletion of cell cholesterol with methyl-β-cyclodextrin, and isolation of membrane fractions that are insoluble in cold detergent, e.g. Triton X-100 (Edidin, 2001).

Membrane domains can organize signal transduction events by concentrating interacting molecules on both sides of the membrane, thus speeding up binding during signaling and preventing inappropriate crosstalk between pathways (Simons and Ikonen, 1997). This notion is supported by the fact that various signaling molecules are enriched in rafts, such as, GPI-anchored proteins (Danielsen and van Deurs, 1995; Sargiacomo et al., 1993), doubly acylated tyrosine kinases of the src family (Casey, 1995), cholesterol-linked and palmitoylated proteins (Resh, 1999; Rietveld et al., 1999) and α-subunits of heterotrimeric G proteins (Resh, 1999). It is becoming apparent that NCAM translocation into lipid rafts is of central importance in the regulation of the signaling cascades downstream of NCAM (Bodrikov et al., 2005; Bodrikov et al., 2008; Leshchyns'ka et al., 2003; Niethammer et al., 2002; Santuccione et al., 2005).

NCAM120 is mainly raft-associated owing to its GPI anchor, whereas the transmembrane isoforms NCAM180 and NCAM140 are found mostly in the non-raft fraction (He et al., 1986; Niethammer et al., 2002). However, the raft localization of the transmembrane isoforms is dynamically regulated. The importance of lipid rafts in NCAM-mediated signal transduction is firstly exemplified in transfected Chinese hamster ovary (CHO) cells. NCAM140 mediated FAK activation is abolished upon disruption of raft structures by cholesterol depletion and upon exclusion of NCAM140 from lipid rafts by mutation of the palmitoylation sites (Niethammer et al., 2002). In a later study, a dominant-negative spectrin construct is reported to disrupt NCAM-spectrin-PKCβ2 complex formation and raft-association, with a subsequent inhibition of the NCAM-mediated neurite outgrowth (Leshchyns'ka et al., 2003).

It is shown that clustering of NCAM promotes its redistribution to lipid rafts and the formation of a NCAM-RPTPα-CaMKIIα complex, resulting in serine phosphorylation of RPTPα by CaMKIIα (Bodrikov et al., 2008). Overexpression of a dominant negative RPTPα mutant interferes with NCAM-induced neuronal process extension (Bodrikov et al., 2008). Moreover, PrP, a GPI-linked protein and a directly binding partner of NCAM, potentiates the recruitment and stabilization of NCAM in lipid rafts and regulates $p59^{fyn}$ activity. Disruption of the interaction between PrP and NCAM by NCAM-deficiency or PrP-deficiency or treatment with antibodies against PrP impairs neurite outgrowth (Santuccione et al., 2005). Proteins that regulate the cytoskeleton downstream of NCAM, e.g. GAP-43, are shown to localize mainly in lipid rafts indicating that lipid rafts are local organizers of the cytoskeleton (del Pozo et al., 2004; Laux et al., 2000; Michaely et al., 1999).

I.2. THE NEURONAL GROWTH CONE AND THE GROWTH CONE CYTOSKELETON

The ability of neurons to extend neurites over long distances in response to environmental guidance signals is made possible by the growth cone, a highly motile structure found at the leading edge of neuronal processes. It was firstly described by the Spanish histologist Santiago Ramón y Cajal in 1890 as "a concentration of protoplasm of conical form, endowed with amoeboid movements" (y Cajal, 1890a; y Cajal, 1890b). The sensory, motor, integrative and adaptive functions of growing axons and dendrites are all contained within this specialized structure. The shapes of growth cones vary widely, but generally three major cytoplasmic domains can be distinguished. The peripheral domain is composed of a broad, flat membrane extension called the lamellipodium, and at the edges of it an extension of multiple long, finger-like projections called filopodia. The central domain contains organelles, and a transition zone is located between the peripheral and central domains. A bundle of microtubules form the backbone of the axon (Suter and Forscher, 2000) (Fig. 2).

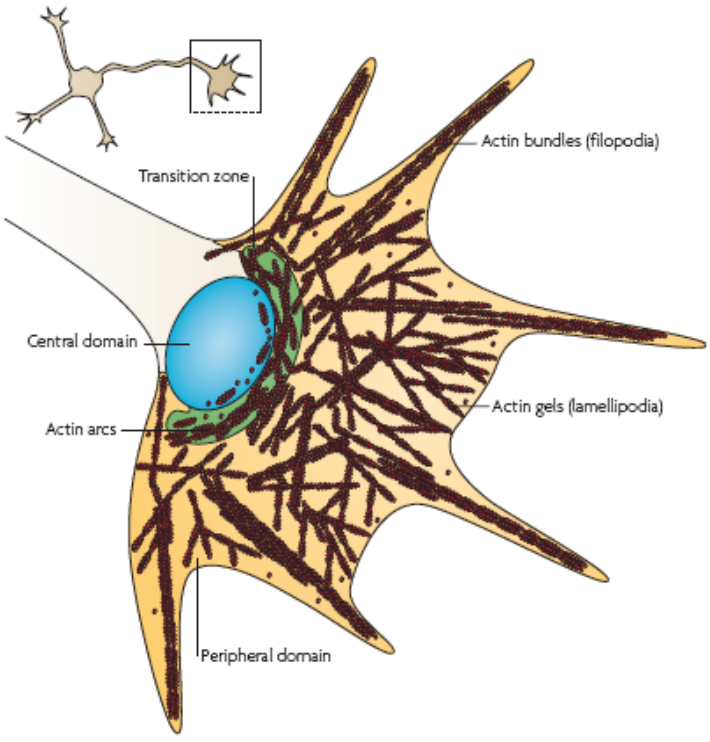

Fig. 2: **Cytoskeletal organization of a growth cone** (Pak et al., 2008). The growth cone can be divided into three distinct regions: the peripheral domain (in yellow), the central domain (in blue) and the transition zone (in green). In the peripheral domain, linear actin bundles comprise filopodia (microspikes), which protrude outward, and mesh-like gels comprise lamellipodia (veils), which are located between the filopodia. The central domain is rich in microtubules (not shown). In the transition zone, transverse bundles of actin filaments (actin arcs) are present.

Both lamellipodia and filopodia are formed by polymerization of actin (Pak et al., 2008). Actin cytoskeleton plays a pivotal role in morphological development and structural plasticity of neurons (Luo, 2002). In response to different stimuli, actin forms a variety of higher-order structures. In the case of growth cones, lamellipodia are made up of short branches of actin filaments forming a network. Each actin filament has branches at an angle of 70°, with the barbed (rapid growing) end towards the cell membrane. On the other hand, filopodia are made up of 15–20 long actin filaments with their barbed ends towards the filopodia tips (Lewis and Bridgman, 1992). Actin assembles into filaments at the growing tip of the growth cone and disassembles at the end of the actin filament. Microtubules continue to extend during this process, to keep up with the advancing growth cone. Actin networks move forward to drive growth cone advancement, thus tightly regulated assembly and dynamics of actin is required to control neurite outgrowth velocity and direction (Pak et al., 2008). This highly coordinated process is modulated by a seemingly bewildering range of associated proteins and other factors, among them the best known regulators are Rho-family small GTPases (Tanaka et al., 1995; Wen and Zheng, 2006), as will be described in more detail in the next chapter.

I.3. REGULATION OF ACTIN CYTOSKELETON BY PAK1 PATHWAY

I.3.1. Rho family small GTPases

Even though the molecular mechanisms that control the cytoskeletal organization are only beginning to be elucidated, it is quite clear that a family of small GTPases, called the Rho GTPases, play a pivotal role in this process in all cell types. Rho GTPases are monomeric G-proteins of about 20–25 kDa in mass. They have been described as "molecular switches" that transduce extracellular stimulation to intracellular downstream effectors. The Rho family in mammals represents a group of 23 gene products (Wherlock and Mellor, 2002). Rho GTPases participate in the regulation of the cytoskeleton dynamics, cell polarity, gene transcription, cell cycle progression, vesicular transport and a variety of enzymatic activities (Zhao and Manser, 2005). Especially, the founding members of Rho family GTPases, Rho, Rac and Cdc42, are key regulators of actin dynamics that lead to organized actin-based structures associated with the structure and motility of cells. Rho, Rac and Cdc42 were first identified in an *Aplysia* cDNA library (Madaule and Axel, 1985). High amounts of RhoA, RhoB, Rac1 and Cdc42 mRNAs are detected in adult rat hippocampus, cerebellum, brainstem, thalamus and neocortex (Olenik et al., 1997). This widespread expression suggests a critical involvement of the Rho GTPases in neuronal function.

The first evidence of the function of Rho-family GTPases came from the experiments involving Cdc42, which was identified in a temperature-sensitive *Saccharomyces cerevisiae* mutant as an essential element for budding (Adams et al., 1990; Pfenninger et al., 1983). Using fibroblasts as model system, it was shown that Rho activation causes the assembly of actin stress fibers and focal adhesion (large integrin clusters) (Ridley and Hall, 1992). Rac induces lamellipodium formation and membrane ruffling (Ridley et al., 1992), whereas Cdc42 controls filopodia extension and growth cone turning (Nobes and Hall, 1995; Shin et al., 2002) (Fig. 3). All three GTPases regulate the assembly of focal contacts and thus the adhesion properties of the cell to ECM (Nobes and Hall, 1995). In the nervous system Rho GTPases regulate neuronal processes that involves plasticity of the cytoskeleton, like neurite outgrowth, neuronal polarity, neuronal migration, growth cone guidance and the function of synapses (Dickson, 2001; Luo, 2000). In general, RhoA and Cdc42 / Rac have antagonistic effects on neurite formation and outgrowth (Luo, 2000). Rac1 and Cdc42 likely promote neurite outgrowth through the formation of lamellipodia and filopodia at growth cones, respectively (Kim et al., 2002; Kuhn et al., 1998; Lamoureux et al., 1997; Luo, 2002; Luo et al., 1994). In contrast, RhoA mediates growth cone collapse and neurite retraction with concomitant cell rounding (Jalink et al., 1994; Kranenburg et al., 1999; Shamah et al., 2001). Some guidance molecules could operate by coordinating activation and deactivation of multiple Rho GTPases. Accumulating evidence suggests that the balance of Rho GTPase activities is required for the control of neurite extension (Nikolic, 2002).

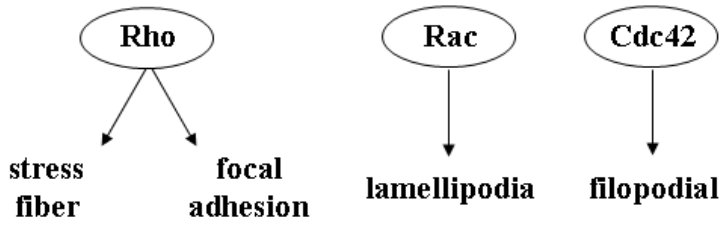

Fig. 3: **Rho GTPase in control of actin cytoskeletal organization in fibroblasts.**

In order to execute their proper function, the activity of Rho GTPases is spatiotemporal regulated by cycling between two conformational states: an active, GTP-bound, and an inactive, GDP bound form. This is accomplished by three types of regulatory proteins. Guanine nucleotide exchange factors (GEFs) promote GDP release and GTP binding, thus activating Rho GTPases (Bateman and Van Vactor, 2001; Vetter and Wittinghofer, 2001; Zheng, 2001). GTPase-activating proteins (GAPs) negatively regulate GTPases by catalyzing the hydrolysis of GTP to GDP (Scheffzek et al., 1998; Zalcman et al., 1999). GDP dissociation inhibitors

(GDIs) hold the Rho GTPase in an inactive state by inhibiting GDP release (Olofsson, 1999; Sasaki and Takai, 1998).

I.3.2. Guanine nucleotide exchange factor PIX

Numerous GAPs and GEFs have been identified and characterized, which are potential targets for intracellular signaling cascades and could serve to integrate the signals that lead to Rho GTPase activation. In addition to enzymatic activity, they possess protein–protein and phospholipid-interacting domains that restrict their function to defined subcellular locations (Bernards, 2003; Rossman et al., 2005). PIX (Pak-interactive exchange factor) / Cool (cloned-out of library) family proteins are GEFs for both Cdc42 and Rac, which are isolated as direct interactors of Pak (p21-activated kinase) (Bagrodia et al., 1998; Manser et al., 1998), and are also first reported as p85SPR (SH3 domain-containing proline-rich protein) (Oh et al., 1997). Of the two isoforms, α-PIX is expressed primarily in hematopoetic cells and muscles (Manser et al., 1998), whereas β-PIX is ubiquitously expressed and is subjected to extensive splicing, such as β-PIX-a / β1-PIX, β-PIX-b, β-PIX-bL, β-PIX-c, β-PIX-d / β2-PIX, with β-PIX-b and β-PIX-c predominantly expressed in the nervous system (Kim et al., 2000; Kim et al., 2001; Koh et al., 2001; Park et al., 2004).

PIX molecules are Dbl-family exchange factors for Rho proteins, defined by possessing a Dbl homology (DH) domain in tandem with a Pleckstrin homology (PH) domain (Zheng et al., 1996). The intracellular localization of Rho GEFs is often achieved by specific domains which associate with other proteins or phospholipids at the cell membrane. The DH domain typically represents the motif for binding the Rho family GTPases and stimulating GDP / GTP exchange, whereas the PH domain mediates the appropriate cellular localization of the protein (Hart et al., 1994; Whitehead et al., 1997; Zheng et al., 1996). PIX family proteins contain multiple protein–protein interaction motifs that dictate their localization and function. Both α-PIX and the predominant splice variants of β-PIX harbor a GIT (G-protein-coupled receptor kinase-interacting targets)-binding domain (Bagrodia et al., 1999; Di Cesare et al., 2000; Turner et al., 1999; Zhao et al., 2000b) which is important for the formation of focal complexes, and a coiled-coil motif that mediates dimerization and seems to be essential for cytoskeletal organization (Kim et al., 2001; Koh et al., 2001). The PIX family binds tightly through an N-terminal SH3 domain to an atypical proline-rich Pak sequence and co-localizes with Pak to form activated Cdc42 / Rac1 complexes (Bagrodia et al., 1998; Manser et al., 1998). This interaction not only is important for Pak localization but also is implicated in Pak activation and

nucleotide exchange of Rac and Cdc42. Pak activation leads to autophosphorylation of Pak at Ser199, which then decreases the affinity of Pak to PIX. The PIX / Pak interaction thus drives Pak to cycle between membrane association and the cytosol (Mott et al., 2005; Zhao et al., 2000a).

I.3.3. Serine / Threonine protein kinase Pak

Pak family serine / threonine protein kinases are the first identified Rho effectors. Paks play fundamental roles in a wide range of cellular processes, including cell morphology, motility, survival, gene transcription, apoptosis and hormone signaling (Arias-Romero and Chernoff, 2008). Paks have been linked to numerous pathological conditions and human diseases including human cancer (Vadlamudi and Kumar, 2003), X-linked mental retardation (Allen et al., 1998; Bienvenu et al., 2000), William's syndrome (Luo, 2000) and HIV infectivity (Cullen, 1996). Paks are evolutionarily highly conserved from yeast to mammals where six members are known (Nikolic, 2002). On the basis of biochemical and structural features, the Paks of higher eukaryotes have been classified into two groups: Pak1, Pak2 and Pak3 have been assigned to group I, whereas Pak4, Pak5 and Pak6 belong to group II (Bokoch, 2003; Jaffer and Chernoff, 2002). Examination of expression patterns has revealed that Pak1 is highly expressed in the brain, muscle and spleen whereas Pak2 is ubiquitously expressed and Pak3 predominantly resides in the brain (Manser et al., 1994; Teo et al., 1995).

Pak1 binds to and is activated by Rac1, Rac2, Rac3 (Knaus et al., 1998; Manser et al., 1994; Mira et al., 2000) and Cdc42 (Manser et al., 1994), but does not bind RhoA / B / C / E / G. Conserved residues within the N-terminal PBD (p21-binding domain) are involved primarily in binding and activation by these GTPases (Fig. 4). The minimal sequence responsible for Cdc42 and Rac binding, the so-called CRIB domain (Cdc42 and Rac interactive binding domain), has been traced down to amino acid 75-90 in Pak1 molecule (Burbelo et al., 1995), and the sequences in the flanking KI (kinase inhibitory) domain contribute to overall binding affinity (Knaus et al., 1998; Lei et al., 2000; Sells et al., 1997). The C-terminal catalytic domains of Pak1, Pak2 and Pak3 are at least 93 % identical among the three kinases. Other notable features of the N-terminal regulatory region of group I Paks include two conserved canonical PXXP SH3-binding motifs and a conserved non-classical SH3-binding site for PIX (Manser et al., 1998). The first (most N-terminal) conserved SH3-binding site binds the adaptor protein Nck (Bokoch et al., 1996), whereas the second site is able to interact with Grb2 (growth factor receptor bound protein 2) (Puto et al., 2003).

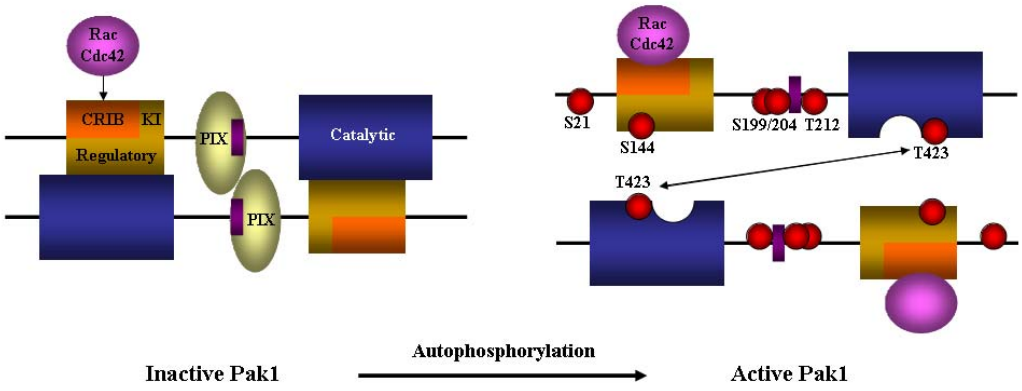

Fig. 4: **A model for PAK1 activation** (modified from (Zhao and Manser, 2005))**.** The auto-inhibited kinase is arranged in a head-to-tail fashion, in which the catalytic domain (blue) binds the KI domain (yellow) and is supported by associated PIX dimers. Upon Cdc42 / Rac binding, the kinase undergoes a conformational change that allows autophosphorylation (red circles). Phosphorylation of Ser144 serves to disable the KI-domain–kinase interaction, while phosphorylation of Ser199/204 reduces the affinity for PIX. Phosphorylation of the activation-loop Thr423 may occur in *trans* as indicated, or may involve a third-party kinase such as PDK1. p35 / CDK5 phosphorylates Pak1 at Thr212 and inhibits Pak1 kinase activity.

Pak1 exists as a homodimer in solution and in cells with the kinase in a *trans*-inhibited conformation (Fig. 4) with the N-terminal inhibitory portion of one Pak1 molecule binding and inhibiting the catalytic domain of the other (Lei et al., 2000; Parrini et al., 2002). Pak1 KI domain residues contribute to this inhibitory interface (Lei et al., 2000). Structural data as well as genetic and biochemical studies have shown that the binding of group I Paks to activated GTPases causes a major change in the conformation of the KI domain. This disrupts its interaction with the catalytic domain allowing autophosphorylation that is required for switching to an active state (Benner et al., 1995; Gatti et al., 1999; Leeuw et al., 1998; Lei et al., 2000; Morreale et al., 2000; Thompson et al., 1998; Zhao et al., 1998). All group I Paks contain a conserved threonine residue in the kinase domain (corresponding to Thr423 in Pak1). Phosphorylation of this residue seems to be a key event for their full activation and maintaining the kinases in a catalytically competent state (Gatti et al., 1999; Yu et al., 1998; Zenke et al., 1999). Autophosphorylation of Pak1 at Ser144 (a conserved residue in the KI domain) contributes to kinase activation, while autophosphorylation sites Ser199/204 (Pak1) serve to downregulate the PIX–Pak interaction (Chong et al., 2001). Another extensively studied phosphorylation site on Paks is Thr212. The p35-bound form of the cell-cycle regulatory protein cyclin-dependent kinase 5 (CDK5) phosphorylates Pak1 at Thr212 and inhibits Pak1 kinase activity in a cell-cycle-dependent manner (Nikolic et al., 1998; Rashid et al., 2001). The cyclin B-bound form of CDC2 has also been reported to phosphorylate mammalian Pak1

(Banerjee et al., 2002; Thiel et al., 2002) and *Xenopus laevis* Pak2 (Cau et al., 2000) at Thr212.

Paks are stimulated by many upstream signaling pathways including membrane bound growth-factor receptors, cytokine receptors (Zhang et al., 1995), integrin cell-adhesion complexes (Rosenberger and Kutsche, 2006) and G-protein-coupled receptors (Knaus et al., 1995; Price et al., 1998). These signaling pathways activate GEFs, which then stimulate GTP loading on Cdc42 or Rac1. Being a predominantly cytoplasmic protein, membrane recruitment of Pak1 via SH-containing adaptor proteins such as NCK (Bokoch et al., 1996; Lu et al., 1997), Grb2a (Puto et al., 2003) or PIX (Manser et al., 1998), or mimicked by the addition of membrane targeting sequences (Daniels et al., 1998) results in stimulation of the kinase. These adaptors bring Pak proteins into close proximity with various interacting proteins and bio-active lipids such as sphingosine and could activate Pak in a GTPase-independent manner (Bokoch et al., 1998; King et al., 2000b). GIT1 associates indirectly with Paks via PIX, and serves as a potent activator of Paks through a Rho GTPase-independent mechanism (Loo et al., 2004).

An important Pak1 function that has aroused great research interest is the regulation of actin dynamics. The first evidence that Pak might be involved in cytoskeletal rearrangment by Rac or Cdc42 comes from the micro-injection of activated Pak1 into fibroblasts which quickly induces the formation of lamellipodia, filopodia and membrane ruffles (Sells et al., 1997). In response to growth factors or activated Rac, in v-src transformed fibroblasts and in wounded cells, Pak1 redistributes into membrane ruffles, where it co-localizes with polymerized actin (Dharmawardhane et al., 1997). In addition, the expression of constitutively active forms of Pak1 causes the loss of actin stress fibers, increases focal adhesion turnover and increases motility (Manser et al., 1997; Sells et al., 1997). In *Drosophila*, Pak is enriched in the leading edge of embryonic epithelial cells undergoing dorsal closure and regulates the formation of focal complexes (Harden et al., 1996). Pak activity is required to localize β-PIX and Rac to the front of the cell (Cau and Hall, 2005).

Paks have been assigned an important role in regulating neurite growth process in several systems. Rac-Pak complex was shown to co-localize and associate with CDK5 / p35 at neuronal growth cone leading edge (Nikolic et al., 1998) and is essential for the proper regulation of the cytoskeleton during neurite outgrowth and remodeling (Nikolic et al., 1998;

Rashid et al., 2001). Targeting of Pak to the plasma membrane causes nerve growth factor (NGF)-independent neurite outgrowth in PC12 cells, whereas a dominant negative Pak blocks NGF-dependent neurite extension (Daniels et al., 1998). In addition, Rac / Cdc42-Pak signaling pathway drives polarized outgrowth of the actin cytoskeleton in the developing neurite, which plays a pivotal role in regulating morphological alterations in neuronal cells (Daniels et al., 1998). More recent research demonstrate that Pak1 regulates axon specification and outgrowth in differentiating hippocampal neurons (Jacobs et al., 2007). And Pak1 controls the correct morphology, orientation, and radial migration of neurons in the cerebral cortex (Causeret et al., 2008). Pak was also shown to mediate axon targeting in *Drosophila* photoreceptor and olfactory neurons (Ang et al., 2003; Hing et al., 1999).

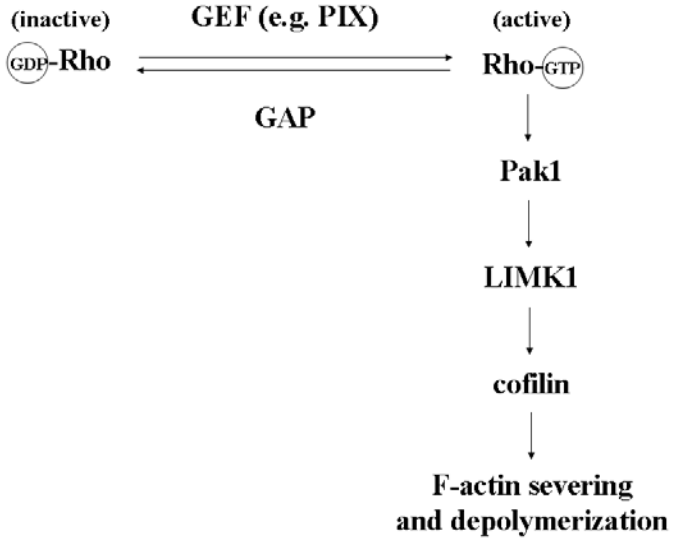

Fig. 5: **Regulation of actin polymerization by Pak1 pathway.** Rho GTPases (Cdc42 or Rac) are activated by exchange of GDP for GTP, catalysed by guanine nucleotide exchange factors (GEFs, e.g. PIX). They are inactivated by GTP hydrolysis, catalysed by GTPase-activating proteins (GAPs). In their active, GTP-bound conformation, GTPases bind to and activate Pak1. Pak1 can then phosphorylate and activate LIMK1, which in turn phosphorylates and inactivates cofilin. Unphosphorylated cofilin stimulates severing and depolymerization of filamentous actin (F-actin).

The basis of Pak1 on regulation of neurite outgrowth is not completely understood, but several Pak1 substrates functioning in controlling of cytoskeletal dynamics might account at least part of the effect. To date, more than 30 direct targets of group I Paks have been identified. Some of the most extensively characterized substrates of Pak1 and Pak2 are MLCK (myosin light-chain kinase), BAD (Bcl-2 / Bcl-X_L-antagonist, causing cell death), LIMK (LIM domain kinase), Merlin and MAPK (Arias-Romero and Chernoff, 2008). Among them, LIMK is believed to be a major Pak1 effector on actin cytoskeletal organization (Fig. 5).

I.3.4. Pak effectors LIMK and cofilin

3.4.1. LIMK

LIMK family of serine protein kinases, which include LIMK1 and LIMK2, were cloned in search of novel protein kinases (Bernard et al., 1994; Mizuno et al., 1994), and were found to be involved in the regulation of actin polymerization and microtubule disassembly (Stanyon and Bernard, 1999). The genomic structures of the murine LIMK1 and LIMK2 genes are well conserved, and the two mouse LIMKs share 50 % overall amino acid identity. In addition to the kinase domain at the C-terminal, they include three protein–protein interaction motifs: two LIM double zinc finger domains at the N-terminal of the molecule followed by a PDZ domain (Edwards and Gill, 1999; Stanyon and Bernard, 1999). LIMK proteins are ubiquitously expressed in mouse tissue, with the highest levels of LIMK1 found in the neurons of adult mouse and human brains and in the developing mouse nervous system (Foletta et al., 2004). In epithelial cells these proteins are found in both the cytoplasm and nucleus. Surprisingly, the subcellular localization of LIMK1 and LIMK2 differs greatly. LIMK1 localizes mainly at focal adhesions, while LIMK2 is found in punctae that resemble endosomes (Acevedo et al., 2006). The activity of LIMKs is regulated by phosphorylation of threonine residue 508 in the activation loop of the kinase domain of LIMK by Pak and Rho-kinase (ROCK) (Dan et al., 2001a; Edwards et al., 1999; Maekawa et al., 1999). LIMKs are further phosphorylated after homodimer formation and *trans*-phosphorylation of the kinase domain.

LIMK1 is a key component of a signal transduction network that connects extracellular stimuli to changes in cytoskeletal structure. Overexpression of LIMK1 in a variety of cultured cell types results in accumulation of filamentous actin (F-actin) (Arber et al., 1998; Yang et al., 1998). Loss of LIMK activity inhibits Rac- and Cdc42-induced actin polymerization. There is also evidence that LIMK inactivation inhibits lamellipodium extention (Sumi et al., 1999; Yang et al., 1998; Zebda et al., 2000). The LIMK1 knockout mice develop normally and are fertile, but exhibit abnormalities in dendritic spine morphology and in synaptic function, including enhanced hippocampal long-term potentiation. They also showed altered fear responses and deficiency in spatial learning (Meng et al., 2002). Mice lacking both LIMK genes are also healthy and fertile. However, they are more severely impaired in both ADF / cofilin phosphorylation and excitatory synaptic function in the CA1 region of the hippocampus than the LIMK1 deficient mice (Meng et al., 2004). The abnormalities in dendritic spine morphology in the LIMK1 deficient mice correlate with the findings that LIMK1 levels control

neurite length of cultured hippocampal neurons. Increased levels of LIMK1 resultes in increased neurite length, while down regulation of LIMK1 levels greatly reduces the length of neurites in cultured primary neurons (Tursun et al., 2005). Hetero-deletion of the LIMK1 locus and adjacent genes is associated with Williams Syndrome, which is characterized by mild mental retardation and defects in visuospatial constructive cognition (Frangiskakis et al., 1996). Recently, LIMK1 was also shown to be implicated in Alzheimer's disease pathology (Heredia et al., 2006).

3.4.2. Cofilin

Members of the ADF (actin-depolymerizing factor) / cofilin family are ubiquitously expressed actin-binding proteins. ADF is originally isolated from embryonic chick brain and named for its ability to depolymerize low concentrations of F-actin to monomeric actin (G-actin) (Bamburg et al., 1980). Cofilin is purified from porcine brain and named for its ability to bind and co-sediment with F-actin (co-filamentous with actin) (Nishida et al., 1984). Every eukaryotic cell expressing actin also expresses one or more members of this family. Vertebrates express ADF, cofilin-1 (isoform found in non-muscle tissue) and cofilin-2 (isoform first identified in muscle). ADF and cofilin from the same species have about 70 % amino-acid sequence identity (Bamburg and Bernstein, 2008).

From yeast to mammals, cofilin plays an essential morphogenetic role by promoting the rapid turnover of actin filaments through severing F-actin and depolymerizing actin filaments from the pointed (slower-growing) ends, in doing so, cofilin increases the actin monomer pool (Bamburg et al., 1999). Cofilin activity is subjected to complex regulation. One principal mechanism is its inhibition by phosphorylation on Ser3. The phosphorylated form does not bind to either G- or F-actin and hence is referred to as inactive. This inactivation can mainly be carried out by LIMKs. The dephosphorylation of ADF / cofilin is regulated by several phosphatases, including PP1, PP2A and PP2B (Meberg et al., 1998). Slingshot is a recently discovered family of phosphatases that have apparent specificity for ADF / cofilin (Niwa et al., 2002). Cofilin-null mice are embryonic lethal at least in part due to migration defects, while tissue-specific silencing of cofilin in the brain reveals its requirement for the formation of the cortical layers.

Highly orchestrated cytoskeletal remodeling accounts for the precise growth cone dynamics during morphogenic processes. Consequently, changes in the signaling pathways that control cytoskeletal organization can result in developmental defects and cause neural disorders. Characterization of the signaling cascades controlling cytoskeletal rearrangement elicited by cell migration and cell adhesion will greatly contribute to our knowledge of neural development and pave a way for novel clinical strategies towards improved diagnosis and therapeutic treatment of diseases that affect the central nervous system.

II. AIMS OF THE STUDY

NCAM is a member of the immunoglobulin superfamily cell adhesion molecules and plays a crucial role in various aspects of neuronal development such as cell migration, axonal growth, path finding and fasciculation, as well as synapse formation (Maness and Schachner, 2007). It is now quite clear that NCAM can signal through several different signaling cascades leading to MAPK pathway activation, which has the potential to modulate related gene expression. It seems that different NCAM interaction partners are segregated into functionally and physically distinct membrane microdomains. Lipid rafts are important players in the control of both the nature and the strength of NCAM-mediated intracellular signals. Each of the three major NCAM isoforms is engaged in distinct membrane proximal complexes with signaling molecules and cytoskeletal components (Bodrikov et al., 2005; Bodrikov et al., 2008; Leshchyns'ka et al., 2003; Niethammer et al., 2002).

We are interested in elucidating the molecular mechanism that NCAM utilizes to fullfil its function. Being a multifunctional molecule, NCAM can activate several signaling cascades to accomplish one task. For instance, in order to promote neurite outgrowth NCAM can selectively complex with FGFR, $p59^{fyn}$ or PKC. We want to find answers to the questions how distinct information is integrated upon NCAM stimulation and how activation of particular intracellular pathways can result in different cellular outcomes and how cross talk and convergence of several signaling pathways are organized and regulated to achieve specificity and flexibility of intracellular signals.

Yeast-two hybrid screening gave the first hint that Pak1 could be a new binding partner of NCAM, which may lie downstream of NCAM signaling. The prerequisite of this project is to confirm the physiological binding between NCAM and Pak1. And if these proteins also work together what could be their cellular responses. Since Pak1 is also heavily implicated in the regulation of neuronal development, it is interesting to test whether Pak1 mediates NCAM function in promoting neurite outgrowth, especially through modulation of actin cytoskeletal dynamics, a well studied role of Pak1. It is also worthy to investigate whether lipid rafts are important for the biological consequences elicited by NCAM and Pak1 interaction. In our study we identified a novel signaling pathway downstream of NCAM involved in the direct modification of actin cytoskeletal organization.

III. MATERIALS AND METHODS

III.1. MATERIALS

III.1.1. Chemicals and materials

All chemicals (in p.a. quality) and materials were purchased from the following companies and are listed below in alphabetical order:

Abcam (Cambridge, UK); Amersham Pharmacia Biotech Europe GmbH (Freiburg, Germany); BD Biosciences (Heidelberg, Germany); Beckman Coulter GmbH (Krefeld, Germany) including Beckman Instruments, Inc.; BIOCAT GmbH (Heidelberg, Germany); Biochrom AG (Berlin, Germany); BIOMOL Feinchemikalien GmbH (Hamburg, Germany); Bio-Rad Laboratories GmbH (Munich, Germany); BioVision, Inc. (Mountain View, California, USA) via BIOCAT GmbH; Calbiochem (EMD Chemicals, Inc., Gibbstown, New Jersey, USA) via Merck Biosciences GmbH; Carl Roth GmbH & Co. KG (Karlsruhe, Germany); CHEMICON via Millipore GmbH; Cell Signaling Technology, Inc. (Danvers, Massachusetts, USA) via New England Biolabs GmbH; Cytoskeleton, Inc. (Denver, CO, USA); Dianova GmbH (Hamburg, Germany); Frema Reform (Lüneburg, Germany); Herolab GmbH Laborgeräte (Wiesloh, Germany); Invitrogen GmbH (Karlsruhe, Germany); Jackson ImmunoResearch laboratories, Inc. via Dianova GmbH; KMF Laborchemie Handels-GmbH via VWR International GmbH; MACHEREY-NAGEL GmbH & Co. KG (Düren, Germany); Mallinckrodt Baker (Griesheim, Germany); Merck Biosciences GmbH (Bad Soden am Taunus, Germany); Millipore GmbH (Eschborn, Germany); New England Biolabs GmbH (Frankfurt am Main, Germany); Nunc GmbH & Co. KG (Thermo Fischer Scientific, Wiesbaden, Germany); PAA Laboratories GmbH (Cölbe, Germany); Pierce/Perbio Science Deutschland GmbH (Bonn, Germany); Pineda Antikörper-Service (Berlin, Germany); Polysciences Europe GmbH (Eppelheim, Germany); QIAGEN GmbH (Hilden, Germany); R&D Systems GmbH (Wiesbaden-Nordenstadt, Germany); Roche Diagnostics GmbH (Mannheim, Germany); Santa Cruz Biotechnology, Inc. (Heidelberg, Germany); SERVA Electrophoresis GmbH (Heidelberg, Germany); Sigma-Aldrich Chemie GmbH (Taufkirchen, Germany); Tebu-bio (Offenbach, Germany); Th. Geyer Hamburg GmbH & Co. KG (Hamburg, Germany); Upstate via Millipore GmbH; VWR International GmbH (Hannover, Germany). Cell culture material was ordered from Greiner Bio-One GmbH (Frickenhausen, Germany) via Hassa-Laborbedarf GmbH (Lübeck, Germany).

III.1.2. Buffers and solutions

General buffers and stock solutions are listed below. Bi-distilled water (ddH_2O) was used for preparation unless indicated otherwise.

Blocking buffer I *(for immunoblotting)*	4 % (w/v) skimmed milk powder (Frema Reform) in PBS
Blocking buffer II *(for immunoblotting)*	5 % (w/v) bovine serum albumin (BSA) (Sigma-Aldrich Chemie GmbH) in TBS
Cell lysis and F-actin stabilization buffer (LAS buffer) *(for F-actin / G-acin in vivo assay)*	50 mM PIPES buffer, pH 6.9 50 mM NaCl 5 mM $MgCl_2$ 5 mM EGTA 5 % (v/v) glycerol 0.1 % (v/v) Nonidet P-40 (NP-40) 0.1 % (v/v) Triton X-100 0.1 % (v/v) TWEEN 20 0.1 % (v/v) β-mercaptoethanol
Cracking buffer *(for preparation of yeast extracts)*	40 mM Tris-HCl, pH 6.8 8 M (w/v) Urea 5 % (w/v) SDS 0.1 mM EDTA 1 mM PMSF 0.4 mg/ml bromophenol blue 1 % (v/v) β-mercaptoethanol
Dilution buffer (2x) *(for growth cone stimulation assay)*	44 mM HEPES buffer, pH 7.3 100 mM sucrose 200 mM NaCl 2.4 mM $MgCl_2$ 10 mM KCl 2.4 mM NaH_2PO_4 20 mM glucose

DNA sample buffer (5x) *(for DNA agarose gels)*	20 % (v/v) glycerol in 1x TAE 0.025 % (w/v) Orange G
Ethidium bromide staining solution *(for DNA agarose gels)*	10 µg/ml ethidium bromide in 1x TAE (0.025 mM in 1x TAE)
Homogenization buffer *(for whole brain homogenization and membrane fraction isolation)*	0.32 M sucrose 5 mM Tris-HCl, pH 7.4 1 mM $MgCl_2$ 1 mM $CaCl_2$ 1 mM $NaHCO_3$ 0.1 mM PMSF
Homogenization buffer *(for growth cone fraction isolation)*	0.32 M sucrose 1 mM $MgCl_2$ 5 mM Tris-HCl, pH 7.4
Kinase buffer *(for Pak1 kinase assay)*	25 mM Tris-HCl, pH 7.5 10 mM $MgCl_2$ 5 mM β-glycerophosphate 0.1 mM Na_3VO_4 2 mM DTT
Phosphate buffered saline (PBS)	136 mM NaCl 10 mM Na_2HPO_4 2.7 mM KCl 1.8 mM KH_2PO_4 pH 7.3
Phosphate buffered saline/TWEEN (PBST) *(for immunoblotting)*	PBS 0.1 % (v/v) TWEEN 20
Radio immunoprecipitation assay (RIPA) buffer *(for co-immunoprecipitation)*	50 mM Tris-HCl, pH 7.5 150 mM NaCl 1 mM $Na_4P_2O_7$ 1 mM NaF 2 mM Na_3VO_4 1 % (v/v) NP-40 1 mM PMSF

Resolving gel *(for SDS-PAGE)*	375 mM Tris-HCl, pH 8.8 0.1 % (w/v) SDS 0.02 % (w/v) APS 0.1 % (v/v) TEMED Acrylamide/Bis solution (29:1) according to % of gel required
SDS-PAGE running buffer *(for SDS-PAGE)*	25 mM Tris 200 mM glycine 0.1 % (w/v) SDS
SDS sample buffer (5x) *(for SDS-PAGE)*	310 mM Tris-HCl, pH 6.8 25 % (v/v) glycerol 10 % (w/v) SDS 4.5 % (v/v) β-mercaptoethanol 0.015 % (w/v) bromphenol blue
Stacking gel *(for SDS-PAGE)*	125 mM Tris-HCl, pH 6.8 0.13 % (w/v) SDS 0.05 % (w/v) APS 0.2 % (w/v) TEMED 4 % Acrylamide/Bis solution (29:1)
Stripping buffer *(for immunoblotting)*	25 mM glycine-HCl, pH 2.2 1 % (w/v) SDS
Sucrose, 0.75 M *(for growth cone fraction isolation)*	0.75 M sucrose 1 mM $MgCl_2$ 5 mM Tris-HCl, pH 7.4
80 % Sucrose stock solution in ddH_2O *(for growth cone isolation)*	80 % (w/v) sucrose in ddH_2O
80 % Sucrose stock solution in Na_2CO_3 *(for lipid raft isolation)*	80 % (w/v) sucrose in 0.2 M Na_2CO_3
10 % Sucrose in TBS *(for lipid raft isolation)*	10 % (v/v) sucrose (from sucrose stock in Na_2CO_3) in TBS

30 % Sucrose in TBS *(for lipid raft isolation)*	30 % (v/v) sucrose (from sucrose stock in Na_2CO_3) in TBS
1 % Triton X-100 *(for lipid raft isolation)*	1 % (v/v) Triton X-100 (Sigma-Aldrich Chemie GmbH) in TBS
Transfer buffer *(for SDS-PAGE)*	25 mM Tris-HCl, pH 8.3 200 mM glycine 0.001 % (w/v) SDS 10 % (v/v) Methanol
Tris buffered saline (TBS)	50 mM Tris-HCl, pH 7.4 150 mM NaCl
Tris buffered saline/TWEEN (TBST) *(for immunoblotting)*	TBS 0.1 % (v/v) TWEEN 20
Tris acetate EDTA (TAE) buffer (50x) *(for DNA agarose gels)*	2 M Tris-acetate, pH 8.0 100 mM EDTA

III.1.3. Primary antibodies

Anti-actin (20-33)	Rabbit polyclonal antibody (Sigma-Aldrich Chemie GmbH), Raised against a synthetic actin N-terminal peptide, Immunoblotting: 1:1000 in 4 % milk in PBS
Anti-Pak1 (N-20)	Rabbit polyclonal antibody (Santa Cruz Biotechnology), Raised against a peptide mapping at the N-terminus of Rat Pak1, Immunoblotting: 1:500 in 4 % milk in PBS
Anti-Phospho-Pak1 (Thr423) / Pak2 (Thr402)	Rabbit polyclonal antibody (Cell Signaling Technology), Raised against a synthetic phospho-peptide (KLH-coupled) corresponding to residues surrounding Thr423 of human Pak1, Immunoblotting: 1:1000 in 5 % BSA in TBST
Anti-Phospho-Pak1 (Thr212) clone PK-18	Mouse monoclonal antibody (Sigma-Aldrich Chemie GmbH), Raised against a synthetic peptide corresponding to amino acids 203-217 (pThr212) of human Pak1, Immunoblotting: 1:2500 in 5 % BSA in TBST

Anti-Phospho-Pak1 (S199 / 204) / Pak2 (Ser192 / 197)	Rabbit polyclonal antibody (Cell Signaling Technology), Raised against a synthetic phospho-peptide (KLH-coupled) corresponding to residues surrounding serine 199/204 of human Pak1, Immunoblotting: 1:1000 in 5 % BSA in TBST
Anti-LIMK1 (C-10)	Mouse monoclonal antibody (Santa Cruz Biotechnology), Raised against amino acids 136-219 of human LIMK1, Immunoblotting: 1:200 in 4% milk in PBS
Anti-Phospho-LIMK1 (Thr508) / LIMK2 (Thr505)	Rabbit polyclonal antibody (Cell Signaling Technology), Raised against a synthetic phospho-peptide (KLH-coupled) corresponding to residues surrounding Thr508 of human LIMK1, Immunoblotting: 1:1000 in 5 % BSA in TBST
Anti-cofilin	Mouse monoclonal antibody (BD Biosciences), Raised against a synthetic peptide corresponding to N-terminal amino acids 3-98 of mouse cofilin, , Immunoblotting: 1:2500 in 4% milk in PBS
Anti-Phospho-cofilin (Ser3)	Rabbit polyclonal antibody (Sigma-Aldrich Chemie GmbH), Raised against a synthetic phosphor-peptide corresponding to amino acids 2-9 (pSer3) of human cofilin, with a C-terminal added cysteine, conjugated to KLH, Immunoblotting: 1:2500 in 5 % BSA in TBST
Anti-Phospho-tyrosine hydroxylase (Ser40)	Rabbit polyclonal antibody (AbD serotec), Raised against an amino acid sequence within tyrosine hydroxylase which includes phosphorylated Ser 40, Immunoblotting: 1:1000 in 4 % milk in PBS
Anti-tyrosine hydroxylase	Rabbit polyclonal antibody (AbD serotec), Raised against rat tyrosine hydroxylase, Immunoblotting: 1:1000 in 4 % milk in PBS
Anti-PIX	Rabbit polyclonal antibody (CHEMICON), Raised against β-Pix-GST fusion protein corresponding to the SH3 domain of β-Pix, Immunoblotting: 1:2500 in 4 % milk in PBS

Anti-Cdc42	Rabbit polyclonal antibody (Cell Signaling Technology), Raised against a synthetic peptide (KLH-coupled) corresponding to residues surrounding Lys135 of human Cdc42, Immunoblotting: 1:1000 in 4 % milk in PBS
Anti-contactin/F3	Goat polyclonal antibody (R&D Systems GmbH), Raised against a recombinant human contactin-1, Immunoblotting: 1:500 in 4 % milk in PBS
Anti-GAPDH	Mouse monoclonal antibody (CHEMICON), Raised against GAPDH from rabbit muscle, Immunoblotting: 1:2000 in 4 % milk in PBS
Anti-L1	Rabbit polyclonal antibody (produced in the laboratory of Prof. M. Schachner), Raised against the extracellular domain of mouse L1-Fc (Rolf et al, 2003), Immunoblotting: 1:5000 in 4 % milk in PBS
Anti-NCAM	Rabbit polyclonal antibody (produced in the laboratory of Prof. M. Schachner), Raised against NCAM from mouse brain, Immunoblotting: 1:5000 in 4 % milk in PBS
Anti-NCAM (clone 5b8)	Mouse monoclonal IgG_1 from Developmental Studies Hybridoma Bank, University of Iowa, USA
Anti-NCAM (clone H28)	Rat monoclonal antibody, Raised against the extracellular domain of mouse NCAM, the hybridoma cell line producing the H28 antibody was developed in the laboratory of Dr. Goridis (Centre National de la Recherche Scientifique UMR 8542, Paris, France), used as cell culture supernatant
Anti-NCAM (clone P61)	Rat monoclonal antibody (Dr. Goridis, Developmental Biology Institute of Marseille, Marseille, France), Recognizes an intracellular determinant expressed by NCAM180 and NCAM140, Immunoblotting: 1:500 in 4 % milk in PBS

Anti-NCAM chicken (Pineda)	Chicken polyclonal antibody (Pineda Antikörper-Service), Raised against the extracellular domain of mouse NCAM-Fc, Chicken preimmune serum (Pineda Antikörper-Service) For clustering of NCAM on growth cone membrane: 1:400
Anti-NCAM rabbit (Pineda)	Rabbit polyclonal antibody (Pineda Antikörper-Service), Raised against the extracellular domain of mouse NCAM-Fc, Rabbit pre-immune serum (Pineda Antikörper-Service) For clustering of NCAM on growth cone membrane: 1:400
Anti-α-tubulin (clone DM1A)	Mouse monoclonal antibody (Sigma-Aldrich Chemie GmbH), Raised against chick brain α-tubulin, Immunoblotting: 1:1000 in 4 % milk in PBS
Anti-β-tubulin (clone E7)	Mouse monoclonal antibody (Developmental Studies Hybridoma Bank, The University of Iowa, Iowa City, Iowa, USA)
IgG, rabbit	IgG from rabbit serum (Sigma-Aldrich Chemie GmbH)
IgG, rat	IgG from rat serum (Sigma-Aldrich Chemie GmbH)

III.1.4. Secondary antibodies

Secondary antibodies were purchased from Jackson ImmunoResearch laboratories, Inc. The antibodies used for Western blot were coupled to horse radish peroxidase (HRP) and purified by immuno-affinity chromatography. The antibodies were used in dilutions of 1:20,000 in 4 % milk in PBS or in 5 % BSA in TBST. For indirect immunofluorescence Cy2, Cy3 and Cy5 conjugated antibodies were used (diluted 1:200 – 1:300 in 1 % BSA in PBS).

III.1.5. DNA and protein standards

1 kb DNA Ladder	Invitrogen GmbH
Precision Plus Protein All Blue Standards (10 bands of 10-250 kDa, pre-stained in blue)	Bio-Rad Laboratories GmbH
Precision Plus Protein Dual Color Standards (10 bands of 10-250 kDa, pre-stained in blue and red)	Bio-Rad Laboratories GmbH

III.1.6. Yeast and bacterial strains

Yeast and bacterial strains were purchased from Invitrogen GmbH and competent for transformation with plasmid DNA.

Strain	***Description***
Saccharomyces cerevisiae MaV203	*MATα, leu2-3,112, trp1-901, his3Δ200, ade2-101, cyh2^R, can1^R, gal4Δ, gal80Δ, GAL1::lacZ, HIS3$_{UASGAL1}$::HIS3@LYS2, SPAL10::URA3*
Escherichia coli MAX Efficiency DH5α Competent Cells	F- φ80*lac*ZΔM15 Δ(*lac*ZYA-*arg*F) U169 *rec*A1 *end*A1 *hsd*R17 (r_k-, m_k+) *pho*A *sup*E44 λ- *thi*-1 *gyr*A96 *rel*A1
Escherichia coli ElectroMAX DH10B Cells	F- *mcr*A Δ(*mrr-hsd*RMS-*mcr*BC) φ80*lac*ZΔM15 Δ*lac*X74 *rec*A1 *end*A1 *ara*D139 Δ(*ara, leu*)7697 *gal*U *gal*K λ- *rps*L *nup*G
Escherichia coli One Shot *ccd*B Survival T1 Phage-Resistant Cells	F- *mcr*A Δ(*mrr-hsd*RMS-*mcr*BC) φ80*lac*ZΔM15 Δ*lac*X74 *rec*A1 *ara*Δ139 Δ(*ara-leu*)7697 *gal*U *gal*K *rps*L (Str^R) *end*A1 *nup*G *tonA::*P$_{trc}$-*ccd*A

III.1.7. Yeast and bacterial media

Yeast and bacterial media were autoclaved. Antibiotics were added to warm media later.

YPAD medium	10 g/l Bacto-yeast extract 20 g/l Bacto-peptone 100 mg/l adenine sulfate 20 g/l dextrose Adjust pH to 6.0 with HCl
YPAD plates	20 g/l agar in YPAD Medium
Synthetic complete (SC) dropout medium	6.7 g/l yeast nitrogen base without amino acids 1.35 g/l dropout amino acid powder mix 20 g/l glucose Adjust pH to 5.9 with NaOH

SC dropout plates	20 g/l agar in SC dropout medium
Luria Bertani (LB) medium	10 g/l Bacto-tryptone 10 g/l NaCl 5 g/l yeast extract
LB ampicillin medium	100 mg/l ampicillin in LB Medium
LB ampicillin plates	20 g/l agar in LB Medium 100 mg/l ampicillin
LB gentamicin medium	10 mg/l gentamicin in LB Medium
LB gentamicin plates	20 g/l agar in LB Medium 10 mg/l gentamicin
LB kanamycin medium	25 mg/l kanamycin in LB Medium
LB kanamycin plates	20 g/l agar in LB Medium 25 mg/l kanamycin
Super Optimal broth with Catabolite repression (SOC) medium	20 g/l tryptone 5 g/l yeast extract 10 mM NaCl 2.5 mM KCl 10 mM $MgCl_2$ 10 mM $MgSO_4$ 20 mM glucose

III.1.8. Primary cell culture media and material

Sterile polystyrene cell culture plates and flasks were purchased from Greiner Bio-One GmbH. The material was free from heavy metal, non-pyrogenic and non-cytotoxic.

Culture medium *(primary neurons)*	Neurobasal-A medium (Invitrogen GmbH) Supplemented with: 1x B-27 supplement (Invitrogen GmbH) 2 mM GlutaMAX-supplement (Invitrogen GmbH) 2 ng/ml basic FGF-2 (R&D Systems GmbH)

Dissection solution *(primary neurons)*	Neurobasal-A medium (Invitrogen GmbH) Supplemented with: 1x B-27 supplement (Invitrogen GmbH) 2 mM GlutaMAX-supplement (Invitrogen GmbH)
Digestion solution *(primary neurons)*	Neurobasal-A medium (Invitrogen GmbH) Supplemented with: 1x B-27 supplement (Invitrogen GmbH) 0.2 mg/ml DNase I (Sigma-Aldrich Chemie GmbH) 2 mg/ml Papain (Sigma-Aldrich Chemie GmbH)
Dissociation solution *(primary neurons)*	Neurobasal-A medium (Invitrogen GmbH) Supplemented with: 1x B-27 supplement (Invitrogen GmbH) 0.2 mg/ml Dnase I (Sigma-Aldrich Chemie GmbH)
Fixing solution (10x)	4 % (v/v) Paraformaldehyde (PFA) in PBS

III.1.9. Inhibitors

Pak inhibitor, PAK18	PAK18 is composed of the cell permeant TAT peptide sequence and an 18-mer Pro-rich PIX-interacting motif of Pak that disrupts PIX-Pak interaction and blocks Pak activation (Calbiochem)
Methyl-β-cyclodextrin (MCD)	Selectively deletes cholesterol and leads to lipid raft disassembly (Sigma-Aldrich Chemie GmbH)
Complete protease inhibitor cocktail, EDTA-free (50x)	Protease inhibitor cocktail tablets, EDTA-free (Roche Diagnostics GmbH), 1 tablet in 1 ml ddH_2O
PhosStop phosphatase inhibitor cocktail (10x)	Phosphatase inhibitor cocktail tablets, (Roche Diagnostics GmbH), 1 tablet in 1 ml ddH_2O

III.1.10. Plasmids

Yeast expression vectors:

pDONR201	Gateway-adapted vector designed to generate *att*L-flanked entry clones containing gene of interest following recombination with an *att*B expression clone or an *att*B PCR product
pDEST32	DNA Binding Domain (DB) Gateway Destination Vector. This vector is used to clone the known gene of interest in frame with the sequence encoding the DNA binding domain of the GAL4 protein
pEXP-AD502	Activation Domain (AD) Gateway Expression Vector. This plasmid is used to construct a cDNA or genomic library for identifying proteins (AD-Y) that interact with the fusion protein (DB-X)
pPC86	Activation Domain (AD) Expression Vector. This plasmid is used to construct a cDNA or genomic library for identifying proteins (AD-Y) that interact with the fusion protein (DB-X)
pDEST32-NCAM140-ICD	For expression of NCAM140 intracellular domain in yeast (GenBank accession number X15051)
pDEST32-NCAM180-specific	For expression of NCAM180 specific segment in yeast (GenBank accession number X15051)

Mammalian cell expression vectors:

pCGC	Mammalian expression vector (kindly provided by Dr. T. Ohshima, Laboratory for Developmental Neurobiology, Brain Science Institute, Japan)
pCAG-GFP-CAG-myc-CA-Pak1	For expression of catalytically active (CA) Pak1 mutant (Pak1 T423E) (kindly provided by Dr. T. Ohshima)

pCAG-GFP-CAG-HA-DN-Pak1	For expression of dominant negative (DN) Pak1 (mouse Pak1 amino acid 67-150). The DN sequence binds to the catalytic domain of Paks and blocks autophosphorylation and consequent activation of these kinases (kindly provided by Dr. T. Ohshima)

III.1.11. Primers

Small letters present gene-specific sequences whereas the flanking sequences in the vector are presented in capital letters.

Oligonucleotides	**Sequence**
NCAM 140/180ICD-5’	5'-GGGG ACA AGT TTG TAC AAA AAA GCA GGC Ttg gac atc acc tgc tac ttc ct-3'
NCAM 140/180ICD-3’	5'-GGGG AC CAC TTT GTA CAA GAA AGC TGG GTa tca tgc ttt gct ctc att ctc tttt-3'
NCAM 180-specific-5’	5'-GGGG ACA AGT TTG TAC AAA AAA GCA GGC Tag ctg cct gcc gac acc aca g-3'
NCAM 180-specific-3’	5'-GGGG AC CAC TTT GTA CAA GAA AGC TGG GTt tcg gtc ttt gct ggt gcg gga g

III.1.12. Mouse strains

In this study 1-to-3-day-old wild-type (C57BL/6J) and NCAM-deficient mice (Cremer et al., 1994) were used. NCAM-deficient mice were back-crossed for at least nine generations onto the C57BL/6J background. Animals used for biochemical experiments were C57BL/6J and NCAM-deficient littermates obtained from heterozygous breeding. To prepare cultures of primary neurons wild-type and NCAM-deficient mice from homozygous breeding pairs were used. The genotypes of mutant and wild-type mice were determined using polymerase chain reaction (PCR) with template DNA isolated from tail biopsies. The animals were housed in plastic cages under standard conditions (12h:12h light/dark cycle with light on at 06:00, off at 18:00; 21 ± 2°C room temperature, free access to food and water).

III.1.13. Centrifuges

Beckman Optima XL-80 Ultracentrifuge with SW32Ti, SW40Ti, SW55Ti and SW80Ti rotors	Beckman Instruments GmbH (Munich, Germany)
Eppendorf Centrifuge 5804 R	Eppendorf AG (Hamburg, Germany)
Eppendorf Centrifuge 5810 R	Eppendorf AG (Hamburg, Germany)
Sorvall RC50*plus* centrifuge with SLA3000, SLA 1500, SA600 and HB-6 rotors	Kendro (Hanau, Germany)

III.2. METHODS

III.2.1. Molecular biological methods

2.1.1. Maintenance of yeast strains

Yeast strains were cultured and handled according to Guthrie and Fink (Guthrie and Fink, 1991). Yeast strains were stored in YPAD or SC dropout medium with 25 % glycerol at -80°C. To recovery frozen strains and prepare working stock plate, a small portion of the frozen glycerol stock was streaked onto a YPAD or SC dropout agar plate, and incubated at 30°C until the yeast colonies reached ~2 mm in diameter. To prepare liquid overnight culture, fresh 2-3 mm diameter yeast colonies were thoroughly dispersed in 5 ml YPAD or SC dropout meadium and incubated at 30°C for 16-18 h with shaking at 230-270 rpm.

2.1.2. Transformation of yeast

100 ng DNA was used to transform 100 µl aliquot of MaV203 competent cells. After addition of 600 µl PEG/LiAC solution, cells were incubated for 30 min in a 30°C water bath with occasional inversion to mix the components. Subsequently, 35.5 µl of DMSO was added and cells were heat shocked for 20 min in a 42°C water bath. After a brief centrifugation at 200 g for 5 s, pelleted cells were resuspended in 1 ml of autoclaved 0.9 % NaCl and plate onto appropriate plates, followed by further incubation for 60 to 72 h at 30°C.

2.1.3. Maintenance of bacterial strains

Bacterial strains were maintained according to Sambrook and colleagues (Sambrook et al., 1989). Bacteria were stored as glycerol stocks in LB medium containing 25 % (v/v) glycerol

at -80°C. An aliquot of this stock was streaked on an LB plate including the appropriate antibiotic and incubated overnight at 37°C. Plates were stored for up to 6 weeks at 4°C.

2.1.4. Transformation of bacteria

Competent bacteria were transformed with plasmid DNA according to Sambrook and coworkers (Sambrook et al., 1989). To 100 µl of bacteria 100 ng of plasmid DNA were added and incubated for 30 min on ice. After a heat shock at 42°C for 50 s and subsequent incubation on ice for 10 min, 0.5 ml of SOC medium was added and incubated at 37°C for 40 min. 50 µl cells were plated on LB agar plates containing the appropriate antibiotic. Plates were incubated at 37°C overnight.

2.1.5. Plasmid isolation

For preparation of large quantities of DNA, the QIAGEN Plasmid Maxi Kit (QIAGEN GmbH) was used. To prepare the starter culture a single colony was inoculated in 2 ml LB medium containing the appropriate antibiotics and grew at 37°C for 8 h with constant agitation. Afterwards, 1 ml of the starter culture was added to 400 ml LB medium containing antibiotics and the culture was incubated at 37°C with constant agitation overnight for 12-16 h. Cells were harvested in a Sorvall centrifuge at 6,000 g for 15 min at 4°C and DNA was isolated as described in the manufactures protocol. Finally, the DNA pellet was resuspended in 600 µl of pre-warmed (70°C) Tris-HCl (10 mM, pH 8.0) and the DNA concentration was determined.

2.1.6. Restriction digestion of DNA

Restriction enzyme digests were performed by incubating the DNA with an appropriate amount of enzymes, the respective buffer as recommended by the supplier, and at the optimal temperature for the specific enzyme for 2 h. The digest assay was set up as reactions with a total volume of 20 µl. If two enzymes were incompatible with each other, the DNA was digested successively with the enzymes. The restriction was terminated by addition of sample buffer and applied on an agarose gel.

2.1.7. Polymerase chain reaction (PCR)

Amplification of DNA fragments was performed in a 50 µl reaction mixture with thin-walled PCR tubes in MWG-PCR cyclers. Turbo-Pfu-Polymerase and the appropriate reaction buffer were obtained from Stratagene. The following reaction mixture was used:

Template	2-10 ng
Primer-5' (10pM)	1 µl
Primer-3' (10pM)	1 µl
Nucleotides (dNTPs) (20 mM)	1 µl
PCR-buffer (10 x)	5 µl
Turbo-pfu-Polymerase	2.5 U
ddH_2O	up to 50 µl

The PCR was performed with the following step gradient:

1) Initial denaturing	94°C	1 min
2) Denaturing	94°C	1 min
3) Annealing	T_m-4°C	1 min
4) Synthesis	72°C	1 min/ 1 kb DNA
5) Termination	72°C	10 min
6) Cooling	4°C	

The amplification procedure (steps 2-4) was repeated 30 times.
The melting temperature of the primers depends on the GC content and was calculated by the following formula:

$$T_m = 4 \times (G+C) + 2 \times (A+T)$$

If the two primers had different melting temperatures, the lower one was adopted. Afterwards, the quality of the PCR product was monitored by gel electrophoresis and the PCR product was purified with the rapid PCR purification kit (Invitrogen GmbH).

2.1.8. DNA gel electrophoresis

DNA fragments were separated by horizontal electrophoresis in DNA electrophoresis chambers (Bio-Rad Laboratories GmbH) using agarose gels. The percentage of agarose in the gel varied according to the expected size of DNA fragments. Agarose gels were prepared by heating agarose in 1x TAE buffer until agarose was dissolved. After agarose was cooled down to approximately 60°C it was filled into DNA gel trays. The polymerized gel was covered with 1x TAE buffer and the DNA samples mixed with DNA sample buffer were pipetted into the sample pockets. The gel was run at constant voltage at 100 V until the Orange G dye had reached the end of the gel. Subsequently, the gel was stained in an ethidium bromide staining solution for 30 min and documented using the E.A.S.Y. UV light documentation system (Herolab GmbH Laborgeräte).

2.1.9. Determination of DNA concentration

DNA concentrations were determined by spectrophotometric measurements in quartz cuvettes. The absolute volume necessary for measurement was 50 µl. For determining the concentration of DNA preparations, the eluate was diluted appropriately with sterile distilled water. Concentrations were determined by measuring the absorbance at 260 nm (for DNA) and 280 nm (for proteins). Absorbance at 260 nm had to be higher than 0.1 but less than 0.6 for reliable determinations. The concentration of DNA was calculated from the absorbance at 260 nm, given that 50 µg/ml of double stranded DNA has an absorbance of 1.0 at 260 nm. A ratio of 260 nm and 280 nm in the range of 1.8-2.0 monitored a sufficient purity of the DNA preparation.

2.1.10. Preparation of yeast extracts (Urea / SDS method)

100 ul of 60°C cracking buffer (supplemented with 1x Complete protease inhibitor) was applied to cell pellets obtained from 7.5 OD_{600} units of cells. Following by an addition of 80 µl glass beads, samples were heated at 70°C for 10 min and vigorously vortexed for 1 min. The supernatants collected after 5 min of centrifugation at 14,000 rpm at 4°C were boiled in a 100°C water bath for 5 min and vortexed vigorously for 1 min. After a second time centrifugation at 14,000 rpm at 4°C for 5 min, the supernatants were collected and combined with the previous supernatants, boiled at 100°C for 7 min and loaded on a gel.

2.1.11. Yeast two-hybrid screening

To identify NCAM-interacting proteins, yeast two-hybrid screening was performed with the ProQuest Two-Hybrid System (Invitrogen GmbH) in *Saccharomyces cerevisiae* strain MaV203 following the manufacturer's protocol. As bait, a DNA fragment encoding either C-terminal intracellular domain (ICD) 386 amino acids of mouse NCAM140 or 261 amino acids of mouse NCAM180 specific segment was PCR amplified from a NCAM expression vector using primers containing *att*B sites and mobilized into the pDONR201 vector by BP recombination reactions. Subsequent LR recombination reaction transferred NCAM140-ICD and NCAM180 specific sequence to destination vector pDEST32 in frame with Gal4 DNA-binding domain (DB). Expression of the NCAM-ICD-GAL4-DB fusion proteins in the transformed yeast strain was confirmed by Western blot analysis, showing immuno-staining with an anti-NCAM antibody (P61). The resulting strain expressing NCAM140-ICD or NCAM180 specific vector did not auto-activate the different reporter genes. pDEST32-NCAM140-ICD or

pDEST32-NCAM180-specific was co-transformed with a mouse brain cDNA library cloned in the pray vector pPC86 containing Gal4 activation domain (Invitrogen GmbH). Potential positive clones were selected with the aid of a series of positive and negative yeast controls supplied with the kit by accessing the growth of transformants on SC dropout plates: SC-Leu-Trp-His + 3-aminotriazole (3-AT; 30mM for NCAM140-ICD and 10 mM for NCAM180 specific), SC-Leu-Trp-Ura and SC-Leu-Trp + 0.2 % 5-fluoroorotic acid, and by evaluation of the X-gal assay. Plasmid DNA prepared from the yeast strain was transformed into *E. coli* to produce enough recombinant DNA for subsequent sequencing. Positive clones were confirmed by re-transforming the MaV203 yeast strain with isolated plasmids and testing again the reporter gene expression.

III.2.2. Protein biochemical methods

2.2.1. Determination of protein concentration

The protein concentrations of cell lysates or brain homogenates were determined by using the BCA protein Assay Kit (KMF Laborchemie Handels-GmbH). The reagent was prepared according to manufacturer's instructions. 200 µl of reagent were applied to 10 µl of cell lysate or brain homogenate in a microtiter plate and incubated for 30 min at 37°C. BSA standards ranging from 100 µg/ml to 2 mg/ml were simultaneously incubated. Samples and standards were analyzed in triplicate. Copper ions in the reagent are reduced by proteins in the sample proportional to the amount of protein. The reduced copper ions form a purple colored complex with bicinchoninic acid (BCA). Its absorbance was measured at 562 nm using the µQuant microplate spectrophotometer (BioTek Instruments Inc., Winooski, Vermont, USA, KC junior software). Protein concentration was then determined by correlating the relative absorbance to the BSA standards.

2.2.2. SDS-PAGE

Proteins were separated by discontinuous SDS-PAGE using the Mini-PROTEAN II system (Bio-Rad Laboratories GmbH). Either 1 mm or 1.5 mm thick gels, which were composed of a resolving gel with 8 %, 10 %, 12 % or 16 % acrylamide and a narrow stacking gel with 4 % acrylamide, were used for discontinuous SDS-PAGE. After complete polymerization of the gel, the chamber was assembled as described in the manufacturer's protocol. Samples were mixed with 5x SDS sample buffer followed by boiling at 100°C for 10 min. In a next step, protein marker and samples were loaded. The gel was run in SDS-PAGE running buffer at constant voltage of 90 V with a Bio-Rad PowerPac power supply (Bio-Rad Laboratories

GmbH) until the bromphenol blue line had reached the end of the gel. Gels were then subjected to Western blotting.

2.2.3. Electrophoretic transfer of proteins (Western blotting)

Proteins separated by SDS-PAGE were transferred from the gel onto a 0.2 µm Protran BA83 nitrocellulose membrane (VWR International GmbH) using a Mini Trans-Blot apparatus (Bio-Rad Laboratories GmbH). The blotting sandwich was assembled according to the manufacturer's protocol. Proteins were electrophoretically transferred in transfer buffer at constant voltage (80 V for 2 h or 35 V overnight at 4°C) using the Bio-Rad PowerPac power supply (Bio-Rad Laboratories GmbH). The protein standard served as molecular weight marker was also used for monitoring the efficiency of the protein transfer.

2.2.4. Immunochemical detection of electrophoretically transferred proteins

After electrophoretic transfer membranes were removed from the sandwich, placed with the protein binding side up into glass vessels, washed once in PBST and incubated in blocking buffer for 1 h at room temperature. Afterwards, the primary antibody was added at the desired dilution and incubated for 2 h at room temperature or overnight at 4°C. The primary antibody solution was removed and membrane was washed five times for 10 min with PBST under constant shaking. The appropriate secondary antibody was applied for 1.5 h at room temperature. The membrane was washed again five times for 10 min with PBST. Immuno-reactive bands (complexes composed of protein bound to nitrocellulose membrane, primary antibody, and secondary HRP-coupled antibody) were visualized using the ECL Western Blotting Detection Reagents (Amersham Pharmacia Biotech Europe GmbH), SuperSignal West Pico or SuperSignal West Dura reagents (Pierce, Perbio Science Deutschland GmbH). Membrane was soaked in detection solution (1:1 mixture of solutions I and II) and placed between transparent plastic foils. Afterwards it was exposed to Kodak BioMax light-1 films (Kodak, Sigma-Aldrich Chemie GmbH) in the dark for varying time intervals. Signals on the film were developed and fixed with Kodak GBX processing chemicals for autoradiography films (Kodak, Sigma-Aldrich Chemie GmbH).

2.2.5. Densitometric evaluation of band intensity

To quantify the signal intensity the developed films were scanned with a resolution of 400 dpi. The digitized pictures were analyzed using the image processing software TINA 2.09 (open

source, University of Manchester, UK) or Scion Image for Windows (Scion Corporation, Frederick, Maryland, USA). Data were analyzed with the student's *t*-test. The results are shown as the mean ± SEM (standard error of the mean).

2.2.6. Stripping and reprobing of Western blots

To detect consecutively proteins on an immunoblot, the blot was stripped from bound primary and secondary antibodies. Therefore membranes were incubated with stripping buffer for 15 min at room temperature under constant shaking followed by washing twice in PBST. Before incubation with antibodies membranes were blocked.

2.2.7. Co-immunoprecipitation

For co-immunoprecipitation experiments, samples containing 1 mg of total protein were lysed with cold RIPA buffer, containing protease inhibitor cocktail, for 1 h at 4°C. Lysates were centrifuged for 15 min at 20,000 g at 4°C. Supernatants were cleared with protein A / G-agarose beads (Santa Cruz Biotechnology) for 3 h at 4°C to reduce unspecific binding. Afterwards, beads were removed by centrifugation at 600 g for 5 min at 4°C. The supernatant was incubated with the corresponding antibodies or non-specific IgG overnight at 4°C, followed by precipitation with protein A / G-agarose beads for 3 h at 4°C. The beads were pelleted and washed four times with lysis buffer and three times with TBS. The proteins were finally eluted from beads with 5x SDS sample buffer by boiling at 100°C for 10 min. The samples were analyzed by Western blotting. Co-immunoprecipitation was performed in cooperation with Dr. Leshchyns'ka.

2.2.8. Subcellular fractionation by differential density gradient centrifugation

2.2.8.1 Preparation of brain homogenate

Wild-type and NCAM deficient mice were decapitated and whole brains were removed from skulls on ice. To obtain uniform homogenates, brains were homogenized using a Potter homogenizer with 15 strokes in ice cold homogenization buffer. The buffer was supplemented with a protease inhibitor cocktail and a phosphatase inhibitor cocktail. All experimental steps were performed on ice.

2.2.8.2 Isolation of soluble fractions and membrane fractions from total brain homogenates

Brain homogenates were centrifuged at 1,000 g for 10 min to spin down large elements, mainly cell perikarya whose processes have been sheared off, and nuclei. Pellets and supernatants were carefully separated. Thereafter, the supernatants were centrifuged at 100,000 g for 30 min. The finally obtained supernatants were enriched in cytosolic proteins and termed soluble fractions. The pellets were resuspended in a minimal volume of TBS buffer and used as total membrane fractions. Protease inhibitor cocktail and phosphatase inhibitor cocktail were added to all fractions and the total protein content was estimated. Samples for SDS-PAGE were prepared and membrane fractions were further processed to isolate lipid raft fractions (see 2.2.8.3).

2.2.8.3 Isolation of lipid raft fractions from total brain homogenates

Lipid raft fractions were isolated as described (Leshchyns'ka et al., 2003). Lipid rafts were obtained from the membrane fractions of wild-type and NCAM deficient mouse brains. All steps were performed on ice. Protein concentrations of wild-type and NCAM deficient membrane fractions were estimated and equal protein amounts of both fractions were used as starting material. Maximum 500 µl of membrane fractions were mixed with the 4x volume of ice-cold 1 % Triton X-100 in TBS in polyallomer tubes (14x95 mm, V=14 ml; Beckman Instruments GmbH) for the SW40Ti Beckman rotor and incubated for 20 min on ice. The extracted membranes were mixed with an equal volume of 80 % sucrose in 0.2 M Na_2CO_3 to a final sucrose concentration of 40 %. To create discontinuous gradients the material was overlaid with 2 ml 30 % sucrose in TBS and 1 ml 10 % sucrose in TBS. The gradient was further overlaid with TBS buffer and centrifuged at 230,000 g for 17 h. After centrifugation the lipid raft fractions were collected at the top of the gradient of 10 % sucrose, resuspended in TBS buffer and pelleted down by centrifugation at 100,000 g for 1 h. The pellets were resuspended in minimum volume of TBS which contained protease inhibitor cocktail. The total protein content was estimated (see 2.2.1) and samples for SDS-PAGE were prepared (see 2.2.2).

2.2.8.4 Isolation of growth cone fractions from total brain homogenates

Isolation of growth cone fractions was performed according to Pfenninger and coworkers (Pfenninger et al., 1983). Growth cones were isolated from 3 brains of 1-3-day-old mice. All

experimental steps were performed on ice. Mouse brains were dissected on ice and homogenized with few strokes in 10 ml homogenization buffer for growth cone isolation containing protease inhibitor cocktail. The homogenates were centrifuged at 1,660 g for 15 min. The low speed supernatants were carefully tipped off and used further, whereas the low speed pellets, containing nuclei and cell perikarya, were discarded. The discontinuous sucrose density gradients were prepared in thin-wall polyallomer tubes (13x51 mm, V=5 ml; Beckman Instruments GmbH) for the SW55Ti Beckman rotor. The supernatants were centrifuged on a gradient of 0.75 / 2.66 M sucrose at 242,000 g for 30 min. The interface between the load and 0.75 M sucrose consisted of growth cone particles. This layer was collected, resuspended in homogenization buffer and centrifuged at 100,000 g for 40 min to pellet down the growth cone fraction. The pellet was resuspended in homogenization buffer containing protease inhibitor cocktail. The particles lying between 0.75 M and 2.66 M sucrose were also collected and pelleted down and were named other membranes.

2.2.8.5 Isolation of lipid raft fractions from growth cones and other membranes

Lipid raft fractions were isolated from equal protein contents of wild-type growth cones and other membrane fractions as described in 2.2.8.2 and 2.2.8.4.

2.2.9. Clustering of NCAM with NCAM antibodies at the surface of isolated growth cones

1.3 ml of ice-cold growth cone fraction was collected from the interface between the loading homogenates and 0.75M sucrose as described in 2.2.8.4 and was mixed with 0.5 ml cold 2x dilution buffer and, after 30 min, with a further 0.8 ml of the same buffer added. Growth cones were then separated into equal aliquots and treated with either NCAM antibodies or pre-immune serum for 5 min, 15min or 30 min at 37°C with constant gentle shaking. The reaction was terminated by addition of 5x SDS-PAGE sample buffer. The phosphorylation of Pak1, LIMK1 and cofilin was analyzed by SDS-PAGE and Western blot with individual antibodies against the phosphorylated form of these proteins. The membranes were then stripped and re-probed with anti-Pak1, anti-LIMK1 and anti-cofilin antibodies to verify that the same amounts of protein were used for each stimulation group. GAPDH labeling served as loading control. Quantitative results and representative blots are from six independent experiments.

2.2.10. F-actin / G-actin in vivo assay

The ratio of F-actin versus G-actin in growth cones was analyzed using an F actin / G actin in vivo assay kit (Cytoskeleton, Inc.) based on the manufacturer's protocol. Briefly, equal protein content of wild-type and NCAM-deficient growth cones were lysed with a pre-warmed LAS buffer (supplemented with 1 mM ATP and 1x protease inhibitor cocktail) and homogenized by pipetting eight times with 200 µl fine pipette tips at 37°C. The samples were incubated at 37°C for 10 min total time after suspension in LAS, following centrifugation at 100,000 g for 1h at 37°C. The supernatants (G actin) were separated from the pellets (F actin) and were immediately placed on ice. The pellets were re-suspended to the same volume as the supernatants using ice cold water containing 1 µM cytochalasin D and were incubated on ice for 1 h with mixing by pipetting every 15 min to dissociate F-actin. Equal amount of proteins from each sample was subjected to SDS-PAGE and analyzed by Western blotting with an anti-actin antibody. Tubulin was also probed to serve as a control. The assays were performed three times in duplicate for accurate results.

2.2.11. Pak1 kinase assay

Pak1 kinase activity was analyzed by a HTScan Pak1 kinase assay kit (Cell Signaling Technology) with modifications. In brief, Pak1 was immunoprecipitated from wild-type and NCAM-deficient brain homogenates by polyclonal rabbit Pak1 antibodies immobilized on protein A-agarose beads as described in 2.2.7. The beads were washed four times with lysis buffer, twice with TBS, and mixed with kinase buffer. Pak1 kinase assays were initiated by adding 200 µM ATP and 1.5 µM tyrosine hydroxylase (Ser40) biotinylated peptide to the immunoprecipitation mixture. The assays were performed for 30 min at 30°C with constantly gentle agitation and stopped by adding Stop Buffer (50 mM EDTA, pH 8.0). After a brief centrifugation, 2 µl of the reaction supernatants were dotted onto a nitrocellulose transfer membrane and visualized by immunoblotting with an anti-phosphorylated tyrosine hydroxylase antibody (pSer40). The beads were boiled in 5x SDS-PAGE sample buffer and resolved on an 8 % SDS-PAGE gel to monitor the immunoprecipitation efficacy. Mock immunoprecipitation with non-specific IgG served as a control. The data shown are representative of five independent experiments.

To analyze Pak1 activity in growth cones, isolated wild-type growth cones were pre-incubated with polyclonal rabbit NCAM antibodies or non-specific rabbit IgG for 30 min at 37°C before lysis. Pak1 was immunoprecipitated and subjected to kinase assays as described above.

III.2.3. Cell culture of primary neurons

The experiments with primary cultures of hippocampal or cortical neurons were performed in cooperation with Dr. Leshchyns'ka and Dr. Sytnyk.

2.3.1. Coating of coverslips

Primary hippocampal or cortical neurons were grown on glass coverslips (15 mm, Carl Roth GmbH & Co. KG) coated with poly-D-lysine (PDL). The coating procedure required several incubation and washing steps which were performed with gentle shaking in a glass Erlenmeyer flask in solutions with a volume of 100 ml each. Coverslips were incubated for 30 min with 3 M HCl at room temperature. Afterwards they were washed twice for 10 min with sterile distilled water and incubated overnight with acetone at 4°C. This was followed by five washing steps for 10 min with sterile distilled water and two times for 10 min with absolute ethanol. To sterilize coverslips they were heated for 2 h at 200°C. After cooling down to room temperature coverslips were incubated overnight in sterile 0.01 % PDL in PBS at 4°C and afterwards washed three times with distilled water. Thereafter, coverslips were dried uncovered in the sterile laminar flow hood by exposing them to UV light for 30 min. The coated coverslips were stored in a sterile tube at room temperature until use.

2.3.2. Preparation and cultivation of hippocampal and cortical neurons

Cultures of hippocampal or cortical neurons were prepared from 1-3-day-old mice. Mice were decapitated and brains were removed from the skull. Hippocampi or cortices were extracted, placed in cold HBSS and cut into 1 mm thick pieces. Hippocampi or cortices were washed once with dissection solution and treated with the digestion solution containing papain and DNase I for 30 min at 30°C. The digestion solution was removed and hippocampi or cortices were suspended in dissection solution. Hippocampi or cortices were carefully dispersed into a homogeneous suspension by trituration with glass Pasteur pipettes having successively smaller diameters. The suspension was centrifuged at 80 g for 15 min at room temperature. The pelleted cells were resuspended in warmed culture medium. Cell number was estimated using a Neubauer counting cell chamber (Carl Roth GmbH & Co. KG). The cells were seeded on coverslips coated with 0.01 % PDL (see 2.3.1) and incubated at 37°C in a constant CO_2 atmosphere of 5 % and with 90 % relative humidity.

2.3.3. Transfection of primary cultured neurons

Cortical or hippocampal neurons were transfected 6 h after plating using Lipofectamine 2000 (GIBCO Invitrogen, Carlsbad, CA) according to the manufacturer's instructions. Briefly, DNA and transfection reagent were diluted with equal volume of Opti-MEM I reduced serum medium (without serum) before they were combined to form transfection complexes. Neurons were washed with PBS once and changed to fresh Opti-MEM I medium. Then, the transfection complexes were added drop-wisely onto the cells and mixed by gentle swirling the plate. Cells were incubated at 37°C in a CO_2 incubator for 24 h prior to further analysis.

2.3.4. Immunofluorescence labeling

Indirect immunofluorescence labeling was performed as described previously (Sytnyk et al., 2002). All steps were performed at room temperature. Neurons on glass coverslips were washed with PBS, and fixed in 4 % formaldehyde (PFA) in PBS for 15 min to crosslink and preserve proteins in their native conformation. Subsequently cells were washed three times with PBS and blocked in 1 % BSA in PBS for 20 min. Antibodies against NCAM (H28 1:1, in 1 % BSA in PBS) were applied to fixed but non-permeabilized cells for 1 h and detected with fluorochrome coupled secondary antibodies applied for 45 min. To detect the intracellular proteins Pak1, Cdc42 and PIX, cells were treated with detergent to permeabilize the cell membrane. The neurons were post-fixed for 5 min in 2 % PFA in PBS, washed with PBS, permeabilized with 0.25 % Triton X-100 in PBS for 5 min, blocked with 1 % BSA in PBS for 20 min. Antibodies were applied in 1 % BSA in PBS for 2 h and then detected with corresponding secondary antibodies applied for 45 min. Cells were further washed with PBS for 4 times and mounted.

2.3.5. Image acquisition and manipulation

Coverslips were embedded in Aqua-Poly / Mount (Polysciences Europe GmbH) and fixed on the microscope slide over night at room temperature. Immunofluorescence images were acquired at room temperature using a confocal laser scanning microscope LSM510, LSM510 software (version 3) and oil Plan-Neofluar 40x objective (numerical aperture 1.3) at 3x digital zoom (Zeiss, Jena, Germany). Contrast and brightness of the images were further adjusted in Corel Photo-Paint 9 (Corel Corporation, Ottawa, Ontario, Canada).

2.3.6. Quantification of neurite length (neurite outgrowth assay)

To assess the role of Pak1 on NCAM-dependent neurite outgrowth, 8 µg/ml NCAM-Fc or 8 µg/ml human Fc were applied to the cell culture media immediately after plating of neurons, together with or without 1 mM Pak1 inhibitor (PAK18) or the solvent DMSO.

In another approach, GFP, CA-Pak1 or DN-Pak1 transfected neurons were stimulated by NCAM antibodies to induce NCAM clustering on the cell surface. Polyclonal rabbit NCAM antibodies were applied to cells 6 h after transfection. Pre-immune serum was used in parallel as control.

After 24 h of NCAM stimulation, neurons were treated with 4 % PFA in PBS for 30 min at room temperature and washed twice with PBS. Coverslips were fixed on the microscope slide over night at room temperature. The cells were imaged using Axiophot 2 microscope equipped with Plan-Neofluar 40x objective (numerical aperture 0.75), AxioCam HRc digital camera and AxioVision software version 3.1 (Zeiss, Jena, Germany). Neurite length was measured with the image processing software ImageJ version 1.34s (open source, National Institutes of Health, USA). For each experimental value at least 3 coverslips for each group, and at least 100 neurons from one coverslip with neurites longer than half of the cell body diameter were measured. Results were statistically evaluated with *t*-test (two-tailed). Results are presented as mean ± SEM.

2.3.7. Live cell imaging

Recordings of live neurons were performed using a time-lapse function of the laser scanning microscope LSM510 (Zeiss, Jena, Germany). During recordings, neurons were maintained on the microscope stage in an incubator (Zeiss, Jena, Germany) at 37°C and 5 % CO_2. Images were acquired with a 1 s interval. Growth cone morphology was analyzed using ImageJ software (National Institute of Health).

IV. RESULTS

IV.1. PAK1 IS A NOVEL BINDING PARTNER OF NCAM

In order to search for new binding partners of NCAM, yeast two-hybrid screening was carried out within the mouse brain cDNA library. The NCAM140 intracellular domain or the specific fragment of NCAM180 intracellular domain was used as a bait. Among more than $2x10^6$ clones screened, 26 clones showed positive phenotypes.

A BLAST database search (http://www.ncbi.nlm.nih.gov/BLAST/) indicated that eight cDNAs (see table below) were in correct open reading frame (ORF) and coded likely binding partners. One clone, containing a 1.71 kb sequence, revealed an ORF of 164 amino acids. This sequence encodes the C-terminal kinase domain of Pak1 protein (NCBI accession No. NM_011035.2).

Tab. 1: Results of yeast two-hybrid screening

NCAM 180 only	Protein disulfide-isomerase precursor (PDI) (Prolyl 4-hydroxylase subunit β) (Cellular thyroid hormone-binding protein)
	Prostaglandin-H2 D-isomerase precursor (Lipocalin-type prostaglandin-D synthase) (Glutathione-independent PGD synthetase) (Prostaglandin-D2 synthase)
NCAM 140 / NCAM180	Serine / threonine protein kinase Pak1
	Alcohol dehydrogenase [NADP+]
	Myosin Vb
	FXYD domain-containing ion transport regulator 7
	Profilin 2
	60S ribosomal protein L29

To confirm the interaction between NCAM and Pak1, NCAM was immunoprecipitated from brain homogenates of 1-day-old wild-type mice using antibodies recognizing all NCAM isoforms. Western blot analysis of the immunoprecipitates showed that Pak1 co-immunoprecipitated with NCAM (Fig. 6). This result provided evidence for the physiological binding between NCAM and Pak1.

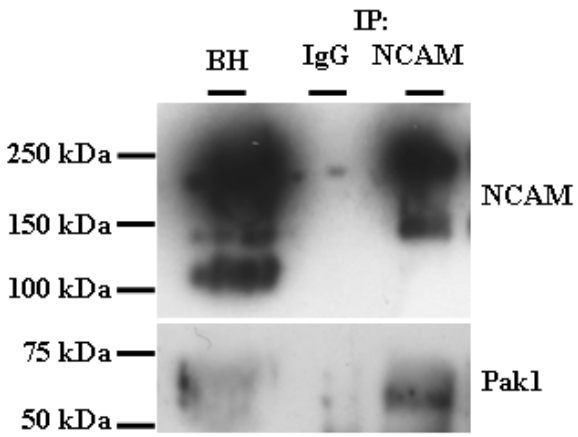

Fig. 6: **Pak1 co-immunoprecipitates with NCAM from brain homogenates of young mice.** NCAM immunoprecipitates from the brains of 1-day-old wild-type mice and input material used for immunoprecipitation (BH) were probed by Western blot with antibodies against NCAM and Pak1. Mock immunoprecipitation with non-specific immunoglobulins (IgG) served as control. Note that Pak1 co-immunoprecipitates with NCAM.

To validate the association between NCAM and Pak1 in neurons, indirect immunofluorescence experiments were performed. Co-labeling of 1-day-old cultured hippocampal neurons with antibodies against NCAM and Pak1 showed that both proteins were present at high levels and partially co-localized in growth cones of the growing neurites (Fig. 7). This observation suggested that NCAM and Pak1 might function together in growth cones.

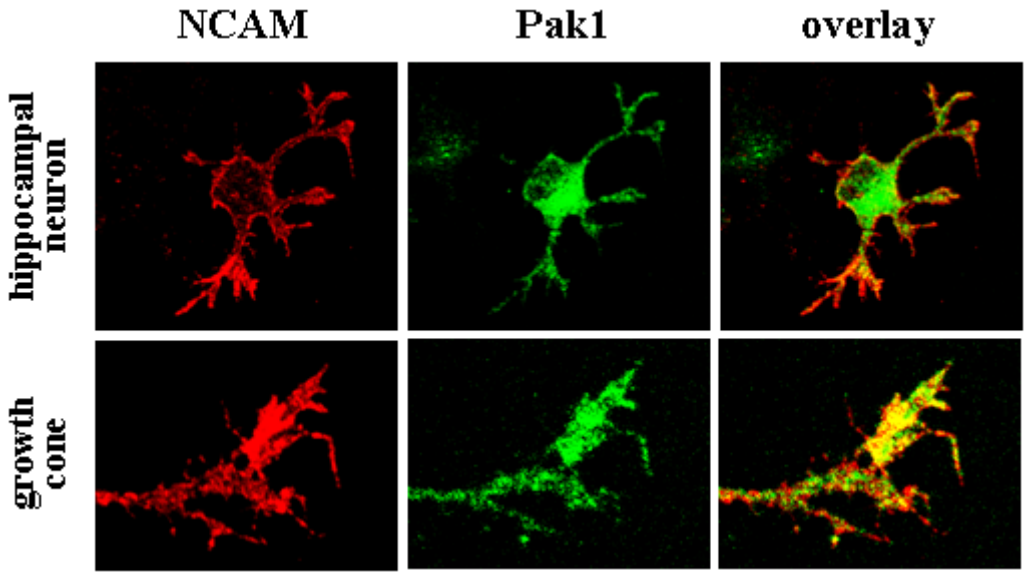

Fig. 7: **NCAM partially co-localizes with Pak1 in growth cones.** Cultured wild-type hippocampal neurons were co-labeled with antibodies against Pak1 and NCAM. Note that NCAM partially co-localizes with Pak1 with the most prominent overlap in growth cones.

To further elucidate whether NCAM and Pak1 associate physiologically in growth cones, co-immunoprecipitation assays were performed with growth cone fractions isolated from 1-3-day-old mouse brains. Western blot analysis of the immunoprecipitates showed that Pak1 co-immunoprecipitated with NCAM, and NCAM co-immunoprecipitated with Pak1 (Fig. 8).

PIX, a guanine nucleotide exchange factor for Rho GTPases Cdc42 and Rac, constitutively binds to Pak1 and it plays a role in the recruitment of Pak1 to the plasma membrane (Koh et al., 2001; Loo et al., 2004; Manser et al., 1998; Zhao et al., 2000a). I hypothesized that PIX might be included in NCAM-Pak1 complex. Co-immunoprecipitation assays carried out with growth cone fractions showed that PIX co-immunoprecipitated with both NCAM and Pak1. This result provided further proof for the interaction between NCAM and Pak1 in growth cones.

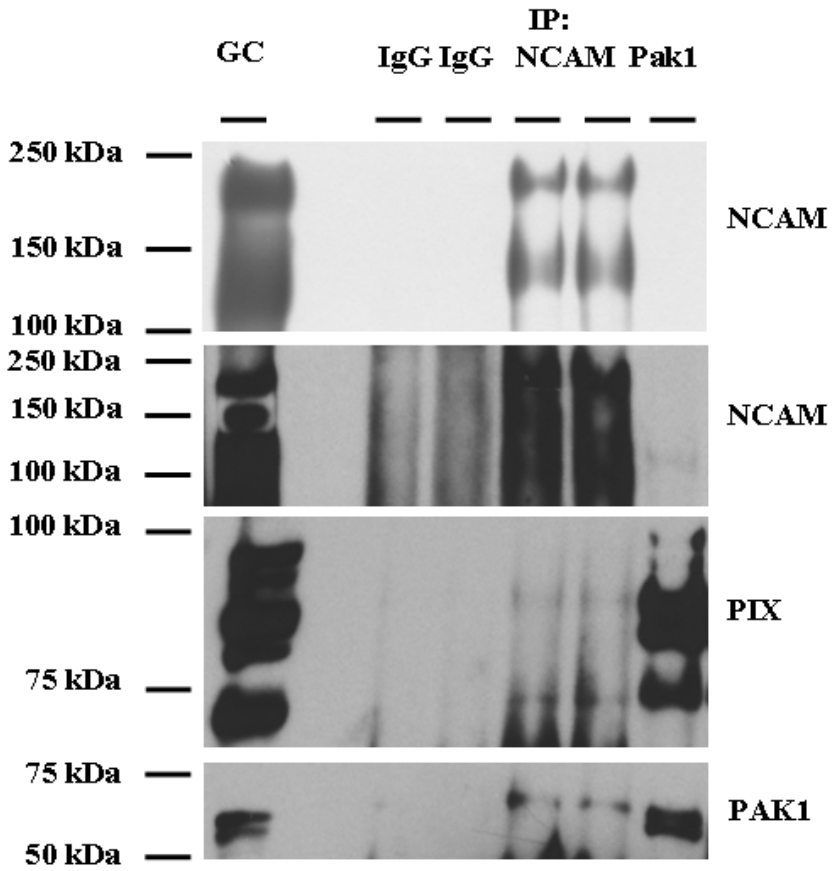

Fig. 8: **Pak1 and NCAM co-immunoprecipitate with each other in growth cones.** NCAM and Pak1 immunoprecipitates from the growth cones of wild-type mouse brains and input material (GC) used for immunoprecipitation were probed by Western blot with antibodies against NCAM (lower panel is of longer exposure time), PIX and Pak1. Mock immunoprecipitation with non-specific immunoglobulins (IgG) served as control. Note that Pak1 co-immunoprecipitates with NCAM and *vice versa*. PIX co-immunoprecipitates with both NCAM and Pak1.

IV.2. CLUSTERING OF NCAM INDUCES ACTIVATION OF PAK1 SIGNALING PATHWAY IN GROWTH CONES

The physiological binding between NCAM and Pak1 led to the following questions: what is the consequence of this interaction, whether NCAM plays a role in regulation of Pak1 activity. To answer these questions, biochemically isolated growth cones from 1-3-day-old wild-type mouse brains were treated with either control non-specific immunoglobulins or the antibodies against the extracellular domain of NCAM. This approach was regarded as NCAM stimulation and was widely used to induce the clustering of NCAM at the plasma membrane and the activation of its downstream signaling transduction (Bodrikov et al., 2005; Bodrikov et al., 2008; Leshchyns'ka et al., 2003).

Pak1 kinase activity is affected by its phosphorylation at several different sites (Bokoch, 2003). To examine the phosphorylation state of Pak1 after NCAM stimulation Western blot analysis was carried out. The results revealed that activation of NCAM enhanced the autophosphorylation of Pak1 at Ser199/204 and Thr423 within 5 min (Fig. 9). In contrast, phosphorylation of Thr212 in Pak1, which can be mediated by p35 / CDK5 and reduces Pak1 activity (Nikolic et al., 1998; Rashid et al., 2001), remained unchanged within 5 min after NCAM antibody application and slightly declined after 15 min and 30 min of NCAM antibody incubation (Fig. 9).

Since clustering of NCAM changes the phosphorylation pattern of Pak1, involving both excitory and inhibitory sites, it is necessary to verify whether clustering of NCAM influences the kinase activity of Pak1. Pak1 was immunoprecipitated from growth cones pre-treated with NCAM antibodies or control immunoglobulins for 30 min and subjected to the *in vitro* kinase assay using a peptide derived from tyrosine hydroxylase (TH) as a specific substrate for Pak1. Dot blot data showed that the ability of Pak1 to phosphorylate the TH peptide at Ser40 increased approximately five fold after stimulation of NCAM (Fig. 10). Thus, clustering of NCAM at growth cone membrane induces Pak1 activation.

The phosphorylation status of Pak1 effectors was also investigated after NCAM stimulation at growth cons. Phosphorylation of LIMK1 at Thr508, which is mediated by Pak1 (Edwards et al., 1999), increased within 5 min after NCAM antibody application (Fig. 9) indicating that this kinase was activated in response to NCAM clustering. LIMK1-mediated phosphorylation of cofilin at Ser3, an actin depolymerizing factor (Bamburg et al., 1999; Meberg et al., 1998), increased in response to NCAM clustering as well (Fig. 9). LIMK1-mediated phosphorylation and inactivation of cofilin could be observed only after 15 min of NCAM antibody application, indicating slower phosphorylation kinetics when compared to Pak1 and LIMK1.

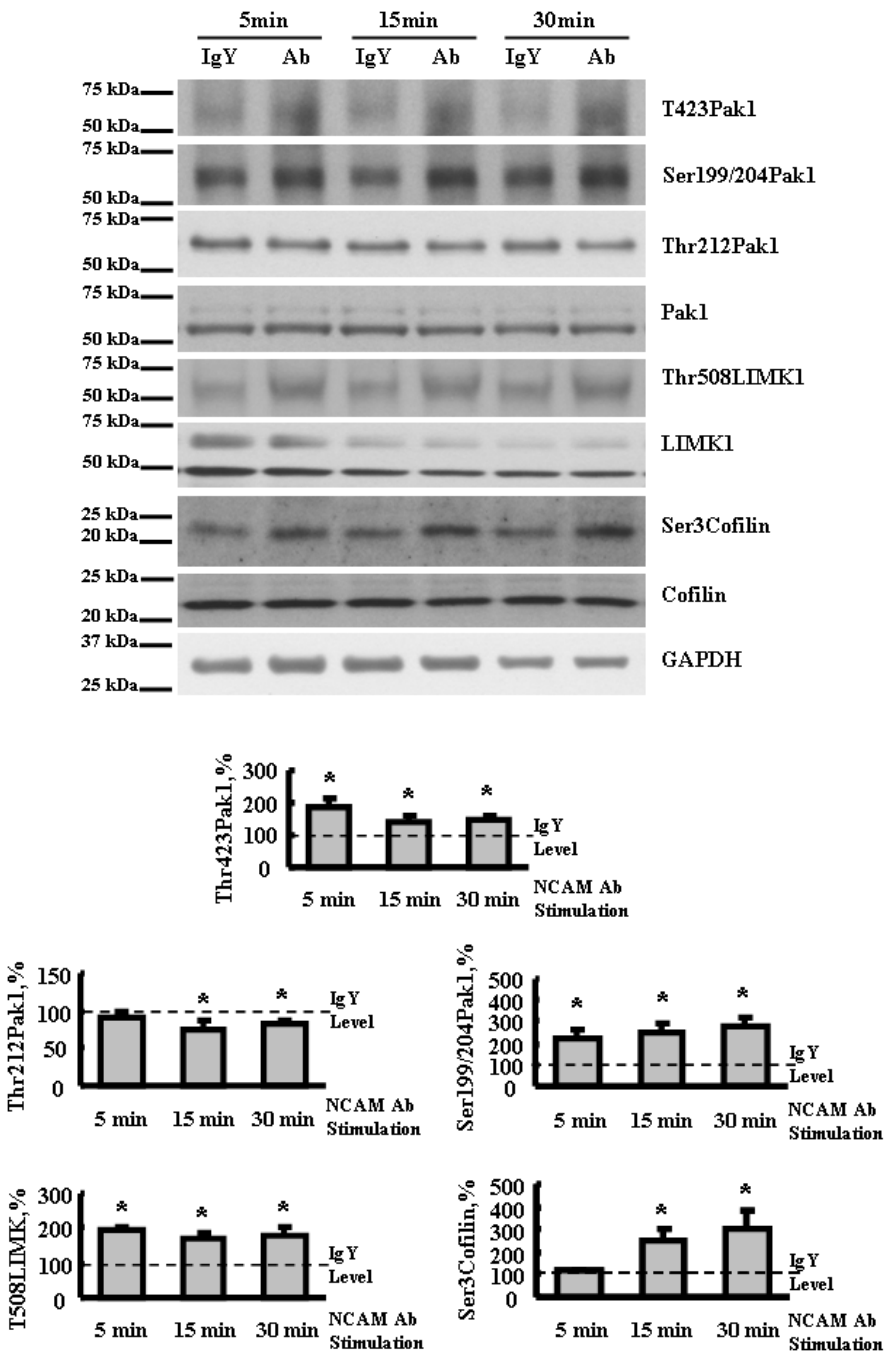

Fig. 9: **Clustering of NCAM on the growth cone membrane results in Pak1 pathway activation.** Growth cones isolated from wild-type mouse brains were incubated with polyclonal chicken antibodies against the extracellular domain of NCAM for 5, 15 or 30 min to induce NCAM clustering at the surface of growth cones. Growth cones treated with non-specific chicken immunoglobulin (IgY) served as control. Lysates of the growth cones were then probed by Western blot with the indicated antibodies. Graphs show optical densities of the protein bands in probes from NCAM antibody-treated growth cones normalized to the signals in probes from IgY-treated growth cones set to 100 %. Mean values ± SEM (n=5) are shown. Note that clustering of NCAM results in enhanced phosphorylation of Pak1 at Ser199/204 and Thr423, LIMK1 at Thr508 and cofilin at Ser3, while phosphorylation of Pak1 at Thr212 is reduced. *$p<0.05$ (paired t-test, compared to corresponding probes from IgY-treated growth cones).

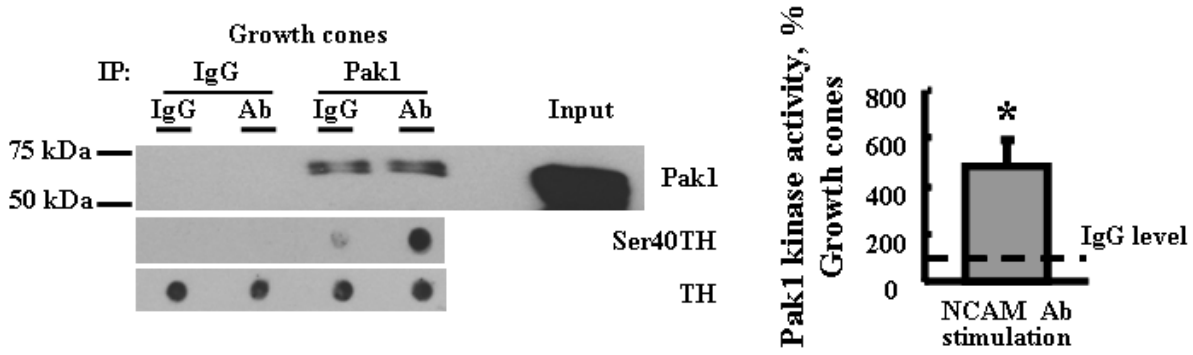

Fig. 10: **Clustering of NCAM at the growth cone membrane enhances Pak1 kinase activity.** Pak1 was immunoprecipitated from growth cones pre-incubated with NCAM antibodies or non-specific immunoglobulin (IgG) and subjected to *in vitro* kinase assay using a peptide derived from tyrosine hydroxylase (TH) as a specific substrate for Pak1. Total levels of TH peptide and levels of TH peptide phosphorylated by Pak1 at Ser40 were analyzed by dot blot. Western blots with Pak1 antibodies shows that Pak1 was immunoprecipitated with the same efficacy. Graph shows mean ± SEM of phosphorylation levels of TH peptide incubated with Pak1 from NCAM antibody-treated growth cones normalized to the phosphorylation levels of TH peptide obtained by Pak1 from IgG-treated growth cones (dashed line). Note that the kinase activity of Pak1 from NCAM antibody-treated growth cones is enhanced. *$p<0.05$, paired t-test.

IV.3. NCAM DEFICIENCY RESULTS IN IMPAIRED MEMBRANE ASSOCIATION AND REDUCED ACTIVITY OF PAK1

Stimulation of NCAM at growth cones resulted in modulation of Pak1 phosphorylation and activation of the kinase (Fig. 10), indicating that NCAM is a regulator of Pak1 activity. To verify this notion, an investigation on how NCAM deficiency influences Pak1 activity might provide useful information. So, the phosphorylation and subcellular distribution of Pak1 were examined in mice constitutively deficient in NCAM. Western blot analysis of the total brain homogenates from wild-type (NCAM+/+) and NCAM-deficient (NCAM-/-) mice showed that the overall levels of Pak1 were not changed in NCAM-/- brains as compared to NCAM+/+ brains (Fig. 11). However, levels of Pak1, that could be co-isolated with growth cones or other non-growth cone membranes (other membranes), were reduced by approximately 40 % in NCAM-/- mice when compared to NCAM+/+ mice (Fig. 11). This observation suggested that NCAM plays a role in recruitment of Pak1 to the membranes.

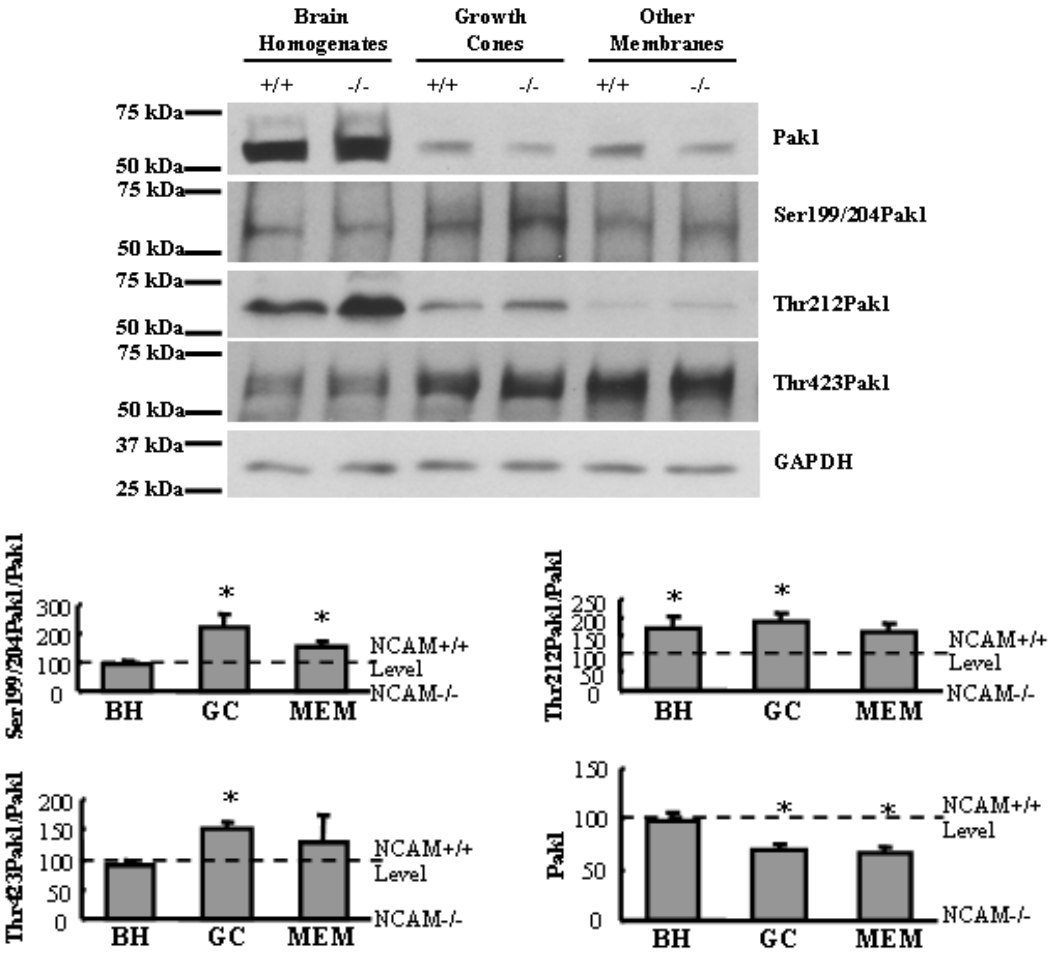

Fig. 11: **Pak1 is abnormally phosphorylated and its membrane association is reduced in NCAM-deficient brains.** Brain homogenates (BH), growth cones (GC) and other membranes (MEM) from wild-type (NCAM+/+) and NCAM-deficient (NCAM-/-) mouse brains were probed by Western blot with antibodies against total Pak1 or Pak1 phosphorylated at Ser199/204, Thr212 or Thr423. Labeling for GAPDH was included as loading control. Diagrams show optical densities of the protein bands in NCAM-/- probes normalized to NCAM+/+ levels set to 100 % (dashed lines). Mean values ± SEM are shown (n=6). *$p<0.05$, (paired t-test, compared to corresponding NCAM+/+ values).

Phosphorylation of Pak1 at Ser199/204, Thr423 and Thr212 was increased in NCAM-/- brains if the absolute phosphorylation levels were normalized to the reduced total Pak1 levels on membranes (Fig. 11). The autophosphorylation of Pak1 at Thr423 was suggested to enhance its kinase activity (Yu et al., 1998; Zenke et al., 1999). However, the *in vitro* kinase assay showed that the kinase activity of Pak1 was strongly reduced in NCAM-/- brain homogenates when compared to that in NCAM+/+ brain homogenates (Fig. 12). These observations suggested that the abnormalities in the recruitment of Pak1 to the membranes and hyperphosphorylation of Pak1 at Thr212 could not be fully compensated by increased phosphorylation of Pak1 at Thr423 and Ser199/204 and resulted in a reduced kinase activity of Pak1 in NCAM-/- brains.

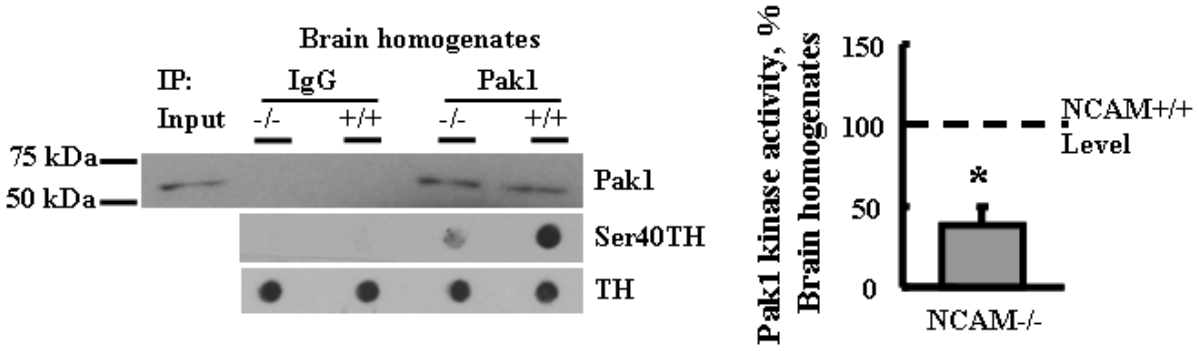

Fig. 12: **Pak1 kinase activity is reduced in NCAM-deficient mouse brains.** Pak1 was immunoprecipitated from wild-type (NCAM+/+) and NCAM-deficient (NCAM-/-) mouse brains and subjected to the *in vitro* kinase assay using a peptide derived from tyrosine hydroxylase (TH) as a specific substrate for Pak1. Total levels of TH peptide and levels of TH peptide phosphorylated by Pak1 at Ser40 were analyzed by dot blot. Western blot analysis with Pak1 antibodies shows that Pak1 was immunoprecipitated with the same efficacy. Graph shows mean phosphorylation levels of this peptide (Ser40TH) ± SEM (n=5) following incubation with Pak1 from NCAM-/- brains normalized to the phosphorylation levels obtained with Pak1 from NCAM+/+ brains (dashed line). Note that the kinase activity of Pak1 from NCAM-/- brains is reduced. *$p<0.05$, paired t-test.

IV.4. PAK1 SIGNALING IS AFFECTED IN NCAM-DEFICIENT GROWTH CONES

To confirm the *in vitro* kinase assay data, the downstream molecules of Pak1 signaling pathway, LIMK1 and cofilin were examined in the total brain homogenates, growth cones and other membranes from NCAM+/+ and NCAM-/- brains by Western blot analysis. As shown in Fig. 13, it was revealed that NCAM deficiency led to the decreased Pak1 activity correlated with the reduced phosphorylation of LIMK1 at Thr508 in growth cones (Fig. 13). On the contrary, total LIMK1 levels were slightly increased in NCAM-/- brain homogenates and growth cones. Phosphorylation of cofilin at Ser3 was consequently reduced by approximately 50 % in NCAM-/- brain homogenates and growth cones, while the total cofilin levels were significantly upregulated in both fractions (Fig. 13). These data showed that decreased Pak1 activity due to NCAM deficiency in turn downregulated LIMK1 and cofilin phosphorylation. However, the overall levels of LIMK1 and cofilin were increased which indicated a compensatory mechanism. Notably, there was no dysregulation of LIMK1 or cofilin observed in other membrane fractions of NCAM-/- brains which suggested that the modulation of NCAM on Pak1 pathway has cell compartment specificity which happens particularly in grwth cones (Fig. 13).

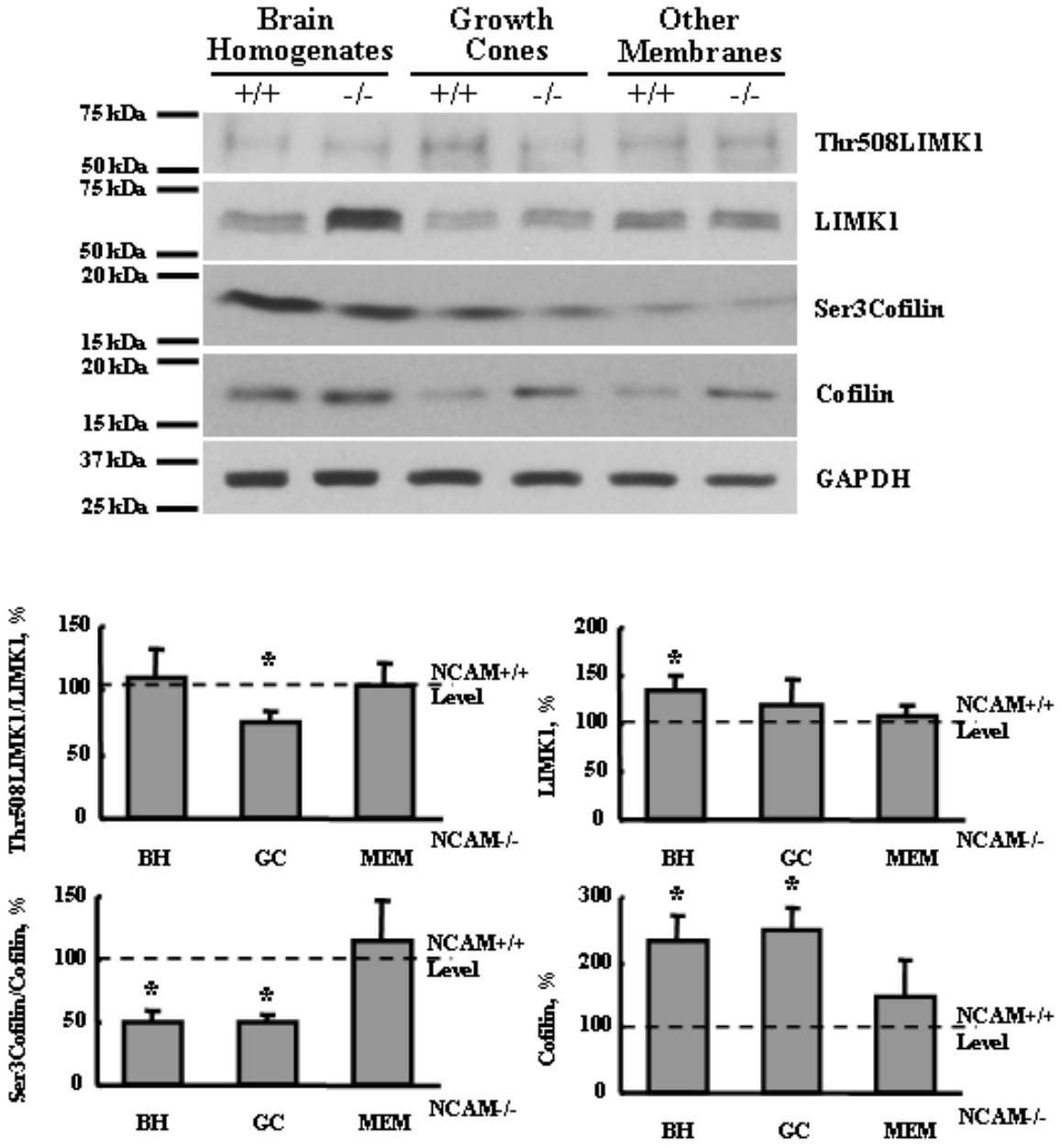

Fig. 13: **Phosphorylation of LIMK1 and cofilin is reduced in NCAM-/- growth cones.** Brain homogenates (BH), growth cones (GC) and other membranes (MEM) isolated from wild-type (NCAM+/+) and NCAM-deficient (NCAM-/-) mouse brains were probed by Western blot with antibodies against Thr508 phosphorylated LIMK1, Ser3 phosphorylated cofilin, total LIMK1 or total cofilin. Labeling for GAPDH was included as loading control. Diagrams show optical densities of NCAM-/- bands normalized to NCAM+/+ levels set to 100 % (dashed lines). Mean values ± SEM are shown (n=6). *p<0.05 (paired t-test, compared to the corresponding NCAM+/+ probes).

IV.5. ACTIN POLYMERIZATION IS REDUCED IN NCAM-DEFICIENT GROWTH CONES

LIMK-mediated phosphorylation of cofilin at Ser3 results in its dissociation from actin filaments and inhibition of its actin depolymerizing activity (Bamburg et al., 1999; Meberg et al., 1998). Since the levels of phosphorylated cofilin were decreased in NCAM-/- brains, we analyzed how NCAM deficiency could affect the ratio of filamentous actin to monomeric actin in the growth cones. Growth cones isolated from NCAM+/+ and NCAM-/- brains were treated with LAS buffer to separate monomeric actin from filamentous actin. After centrifugation at 100,000 g for 1 h, the supernatants, containing monomeric actin, and the pellets, containing filamentous actin, were analyzed by Western blot. The result of this analysis showed that levels of the monomeric actin were approximately two times higher in NCAM-/- growth cones when compared to NCAM+/+ growth cones (Fig. 14). Proportionally, levels of filamentous actin in NCAM-/- growth cones were just about half of those in NCAM+/+ growth cones (Fig. 14). Total levels of actin were not different in growth cones, brain homogenates and other membranes between NCAM+/+ and NCAM-/- mice (Fig. 15). Polymerization of tubulin, analyzed for comparison, was not altered in NCAM-/- growth cones (Fig. 14) indicating that the depolymerizing defect is specific for the actin cytoskeleton.

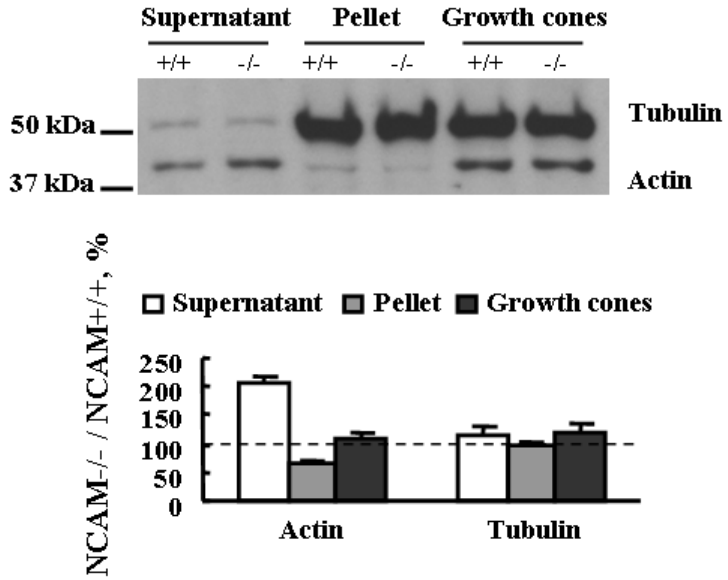

Fig. 14: **Actin polymerization is reduced in NCAM-deficient growth cones.** Growth cones isolated from 1-3-day-old wild -type (NCAM+/+) and NCAM-deficient (NCAM-/-) mouse brains were centrifuged in LAS buffer at 37°C for 1 h. The supernatant, containing monomeric actin, and the pellet, containing filamentous actin, as well as input growth cones were analyzed by Western blot. Graph shows optical densities of NCAM-/- bands normalized to NCAM+/+ levels set to 100 % (dashed lines). Mean values ± SEM are shown (n=6). *$p<0.05$ (paired t-test). Note that the levels of monomeric actin are higher and the levels of filamentous actin are lower in NCAM-/- growth cones. Tubulin polymerization is not different between genotypes.

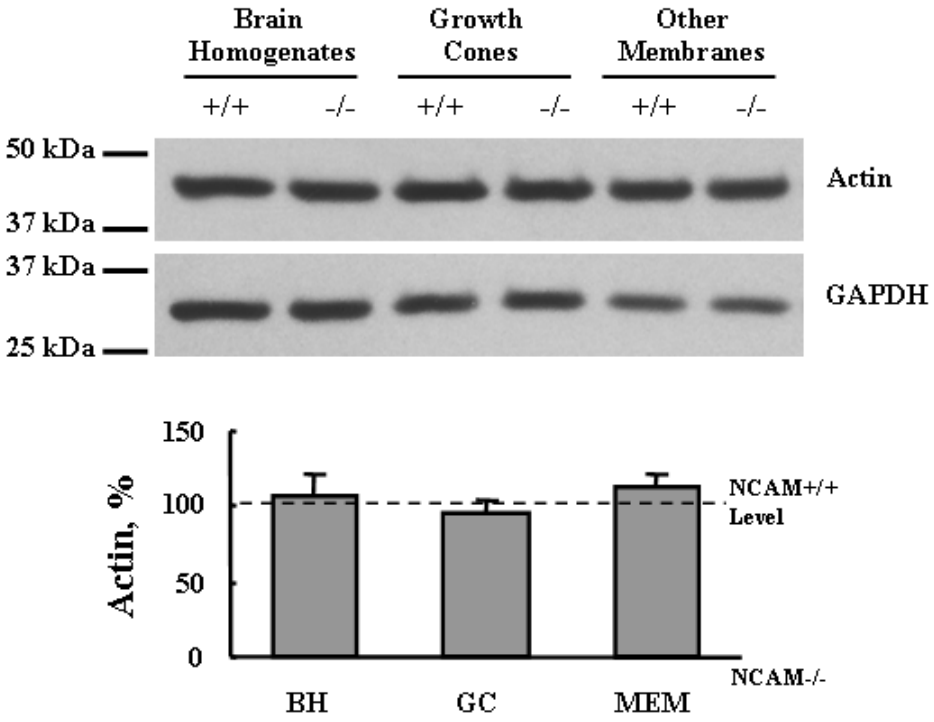

Fig. 15: **Actin expression is not changed between wild-type and NCAM-deficient brains.** Brain homogenates (BH), growth cones (GC) and other membranes (MEM) from wild-type (NCAM+/+) and NCAM-deficient (NCAM-/-) mouse brains were probed by Western blot with antibodies against actin. Labeling for GAPDH was included as loading control. Graph show optical densities of the protein bands in NCAM-/- probes normalized to NCAM+/+ levels set to 100 % (dashed lines). Mean values ± SEM are shown (n=6). *P<0.05 (paired t-test, compared to corresponding NCAM+/+ probes).

Since polymerization of actin plays a pivotal role in the formation of filopodia in growth cones (Lewis and Bridgman, 1992), the behavior of growth cones in cultured hippocampal neurons from NCAM+/+ and NCAM-/- mice was compared. Imaging of the growth cones with 1 second interval between frames showed that growth cones of NCAM-/- neurons were less mobile than growth cones of NCAM+/+ neurons (Fig. 16A). This defect was due to the reduced formation of filopodia. Quantification of the live cell imaging showed that the number of filopodia per growth cone area, the number of filopodia that were moving during the recording time and the length of filopodia were reduced in growth cones of NCAM-/- neurons when compared to NCAM+/+ neurons (Fig. 16B). In combination with the biochemical data, these observations strongly suggest that NCAM deficiency causes impairment in actin polymerization in growth cones. This can be linked to enhanced actin filament severing and depolymerizing activity of cofilin NCAM-/- growth cones.

A

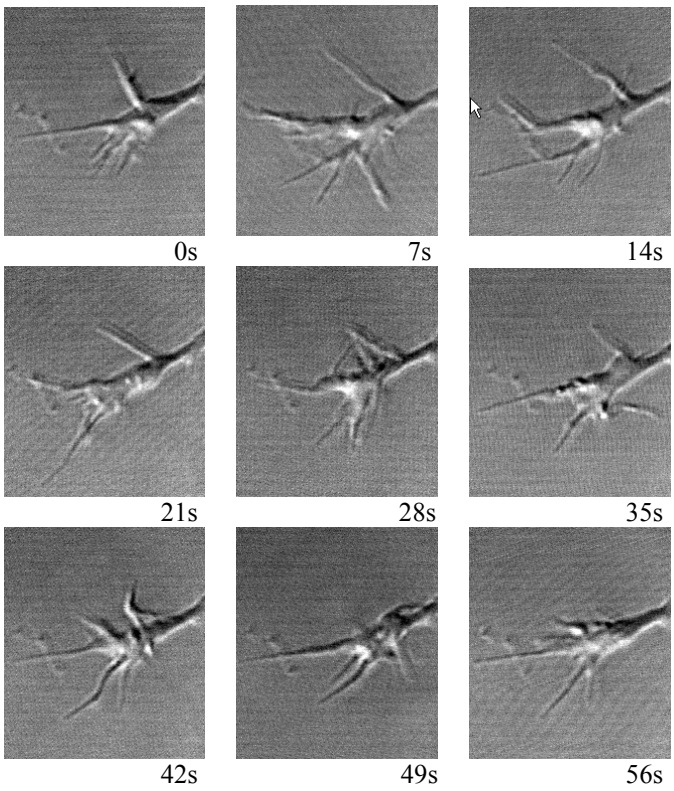
0s
7s
14s
21s
28s
35s
42s
49s
56s

NCAM +/+

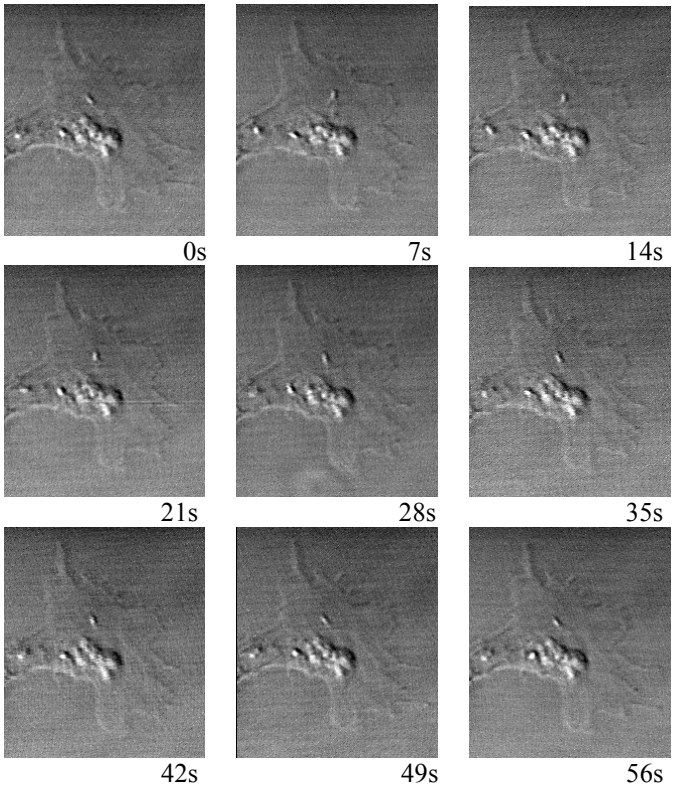
0s
7s
14s
21s
28s
35s
42s
49s
56s

NCAM -/-

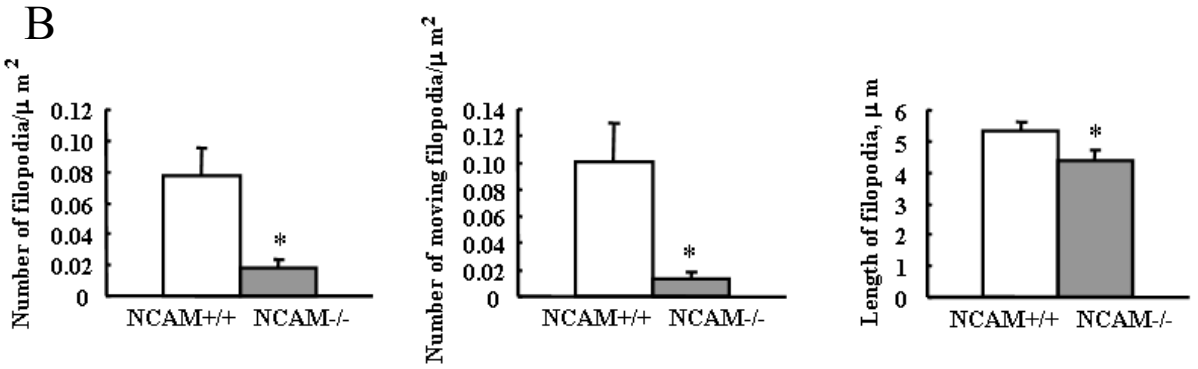

Fig. 16: **Formation and mobility of filopodia are reduced in NCAM-deficient growth cones.** Growth cones of live 1-day-old cultured hippocampal neurons from wild-type (NCAM+/+) and NCAM-deficient (NCAM-/-) mouse brains were imaged with 1s interval between individual frames and the number of filopodia, their mobility and length were analyzed. (A) Two representative growth cones from wild-type (NCAM+/+) and NCAM-deficient (NCAM-/-) hippocampal neurons are shown. (B) Diagrams show the number of filopodia, number of moving filopodia per growth cone area and the length of filopodia in wild-type (NCAM+/+) and NCAM-deficient (NCAM-/-) growth cones. Mean values ± SEM are shown. Note that the number of filopodia per growth cone area, filopodia mobility and length are reduced in NCAM-/- growth cones. *$p<0.05$, t-test.

IV.6. PAK1 ACTIVITY IS REQUIRED FOR NCAM-DEPENDENT NEURITE OUTGROWTH

Clustering of NCAM at the neuronal cell surface with either NCAM antibodies or soluble dimeric fragments of the extracellular domain of NCAM fused to the Fc portion of human IgG (NCAM Fc) has a neurite outgrowth promoting effect on developing neurons (Bodrikov et al., 2005, 2008; Santuccieone et al., 2005). Since growth cones provide a major driving force for the neurites to elongate (Bray, 1984; Lamoureux et al., 1989) and reduced Pak1 activity in NCAM-deficient brains led to impaired filopodia dynamics, whether Pak1 activation is necessary for NCAM-dependent neurite outgrowth was analyzed. Cultured wild-type hippocampal neurons were treated with either NCAM Fc or Fc in the presence of Pak1 inhibtor (PAK18) or the solvent DMSO.

In agreement with previous reports, the application of NCAM-Fc enhanced neurite outgrowth by approximately 25 % when compared to Fc treated neurons (Fig. 17). This neurite outgrowth promoting effect of NCAM was completely blocked by PAK18 that inhibits Pak1 activation by disrupting the association between Pak1 and PIX, a well established activator of Pak1 (Ku et al., 2001; Manser et al., 1998), indicating that NCAM-dependent neurite outgrowth requires the activation of Pak1.

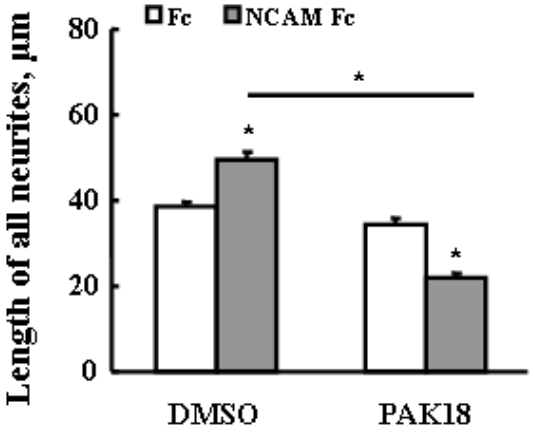

Fig. 17: **NCAM-dependent neurite outgrowth is inhibited by Pak1 inhibitor.** Cultured hippocampal neurons from wild-type mice were treated with Fc or NCAM-Fc in the presence or absence of Pak1 inhibitor peptide PAK18. Graph shows mean lengths ± SEM of all neurites per neuron (n=300 neurons were analyzed in each group). Note increased neurite lengths in NCAM-Fc treated neurons and reduced neurite lengths in neurons treated with Pak1 inhibitor PAK18. *$p<0.05$ (t-test).

To corroborate these data, cultured wild-type cortical neurons were transfected with either catalytically active Pak1, dominant negative Pak1 or the empty vector as a control. Neurons were then treated with NCAM antibodies or control pre-immune serum for 24 hours. A quantification of neurite lengths showed that in neurons transfected with the empty vector, application of NCAM antibodies increased neurite lengths by approximately 30 % when compared to neurons treated with pre-immune serum (Fig. 18). This neurite outgrowth promoting effect of NCAM could be observed when either the lengths of all neurites, or only the lengths of the longest neurites (considered as putative axons) were measured (Fig. 18). Transfection of neurons with catalytically active Pak1 only slightly increased basal neurite outgrowth levels in control pre-immune serum treated neurons when compared to the empty vector transfected neurons also treated with the pre-immune serum (Fig. 18). However, the increased neurite outgrowth rates triggered by NCAM antibodies were strongly further enhanced in neurons transfected with the catalytically active Pak1, suggesting a synergistic effect (Fig. 18). In contrast, NCAM antibody-induced neurite elongation was completely blocked in neurons transfected with the dominant negative Pak1 (Fig. 18). Dominant negative Pak1 did not show effect on the basal neurite outgrowth rates (Fig. 18). Similar results were obtained when cultured hippocampal neurons were analyzed (data not shown). Thus, these observations indicate that Pak1 activity is required for NCAM-dependent neurite outgrowth.

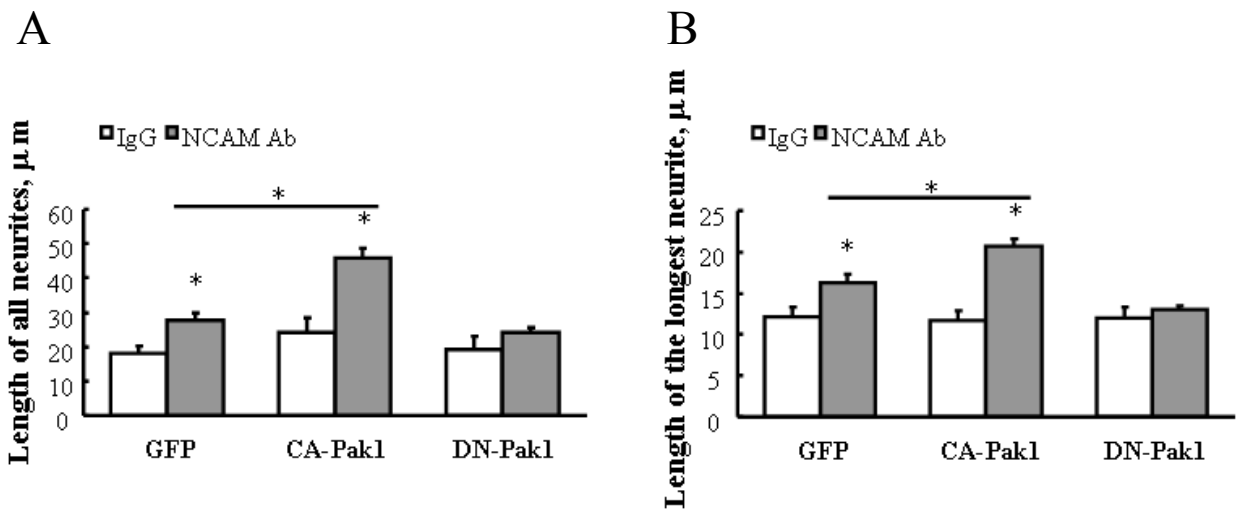

Fig. 18: **NCAM-dependent neurite outgrowth is enhanced by catalytically active Pak1 and inhibited by dominant negative Pak1.** Cultured cortical neurons from wild-type mice were transfected with the empty vector (GFP), catalytically active Pak1 (CA-Pak1) or dominant negative Pak1 (DN-Pak1). Neurons were then treated with NCAM antibodies or pre-immune serum for 24 h. Diagram shows mean lengths ± SEM of all neurites (A) or the longest neurite (B) per neuron (n=100 neurons were analyzed in each group). Note increased response to NCAM antibodies in CA-Pak1 transfected neurons and blocked NCAM-dependent neurite outgrowth in neurons transfected with DN-Pak1. * $p<0.05$ (t-test).

IV.7. NCAM PROMOTES FORMATION OF PAK1-PIX-CDC42 COMPLEX

The observations that PIX co-immunoprecipitates with NCAM and the disruption of Pak1-PIX complex inhibits NCAM-dependent neurite outgrowth, prompted me to investigate whether NCAM has a role on regulation of the expression and subcellular distribution of PIX. The levels of PIX were slightly increased in NCAM-/- brain homogenates when compared to NCAM+/+ brain homogenates (Fig. 19), suggesting a compensatory reaction to its abnormal function. Although the absolute levels of PIX were similar between NCAM+/+ and NCAM-/- growth cones and other membranes, the relative accumulation of PIX in growth cones and other membranes defined as the ratio of PIX levels in these two fractions to the levels of PIX in brain homogenates was reduced in NCAM-/- brains (Fig. 19). This phenomenon suggests that NCAM regulates targeting of PIX to membrane fractions.

Another Pak1 activator, Rho GTPase Cdc42, was also taken into investigation because it is crucial for filopodia formation (Nobes and Hall, 1995; Shin et al., 2002), which is abnormal in NCAM-/- growth cones (Fig. 16). Cdc42 levels were slightly increased in NCAM-/- growth cones probably reflecting an overall increased expression level (Fig. 19). In contrast to PIX, relative accumulation of Cdc42 at membranes was not affected by NCAM deficiency (Fig. 19).

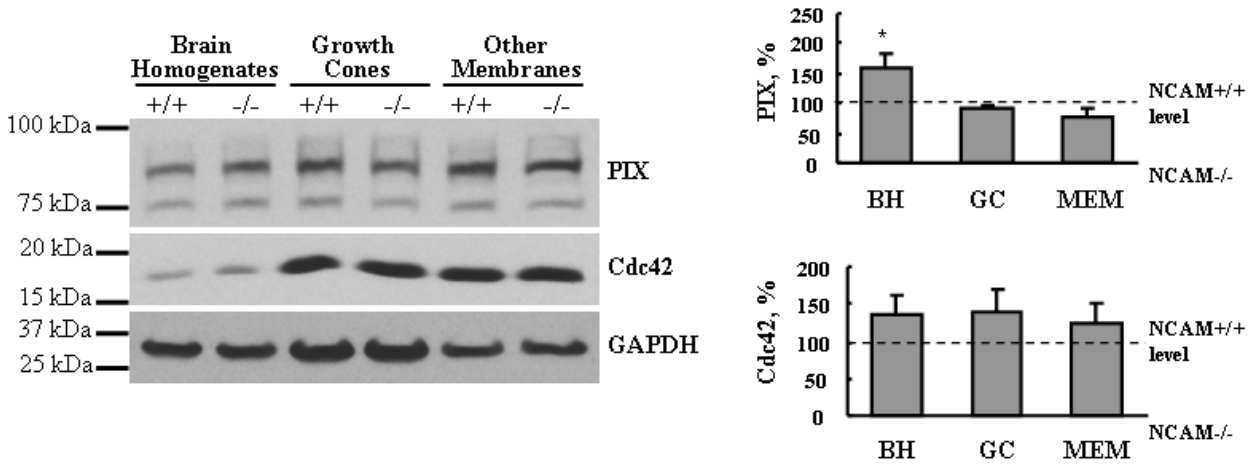

Fig. 19: **PIX expression and membrane-association are abnormal in NCAM-deficient brains.** Brain homogenates (BH) growth cones (GC) and other membranes (MEM) isolated from wild-type (NCAM+/+) and NCAM-deficient (NCAM-/-) mouse brains were probed by Western blot with antibodies against PIX or Cdc42. Labeling for GAPDH was included as loading control. Diagrams show optical densities of NCAM-/- protein bands normalized to NCAM+/+ levels set to 100 % (dashed lines). Mean values ± SEM are shown (n=6). *p<0.05 (paired t-test, compared to corresponding NCAM+/+ probes). Note that PIX expression is upregulated and its relative targeting to growth cones and other membrane fractions is reduced in NCAM-/- brains.

Furthermore, the Pak1-PIX-Cdc42 complex formation was examined by analyzing the efficiency of the co-immunoprecipitation of the complex components from NCAM+/+ and NCAM-/- brain homogenates. It was found that the levels of Pak1 and PIX co-immunoprecipitated with Cdc42 from NCAM-/- brain homogenates were reduced when compared to NCAM+/+ brain homogenates (Fig. 20). This observation thus suggests that NCAM plays a role in the regulation of Pak1-PIX-Cdc42 complex formation.

In addition, NCAM could be immunoprecipitated by Cdc42 antibodies (Fig. 20). Since NCAM140 co-immunoprecipitates with Pak1 and PIX co-immunoprecipitates with NCAM (Fig. 8), our data thus suggest that NCAM associates with the whole Pak1-PIX-Cdc42 complex. In other to support this biochemical result, indirect immunofluorescence experiments were carried out. And indeed clusters of NCAM co-localized with accumulations of Cdc42 or PIX with the most prominent overlap in growth cones of cultured wild-type hippocampal neurons (Fig. 21).

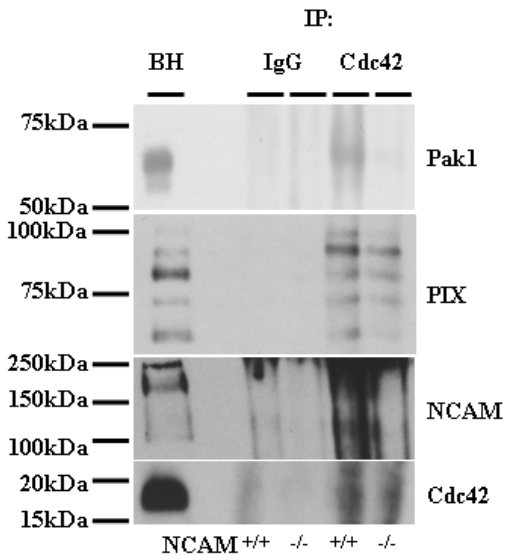

Fig. 20: **Cdc42-Pak1-PIX complex formation is inhibited in NCAM-deficient brains.** Cdc42 immunoprecipitates from 1-3-day-old wild-type (NCAM+/+) and NCAM-deficient (NCAM-/-) mouse brains were probed with antibodies against Pak1, PIX, NCAM and Cdc42 by Western blot. Mock immunoprecipitation with non-specific immunoglobulin (IgG) served as control. Note reduced co-immunoprecipitation of Pak1 and PIX with Cdc42 from NCAM-/- brains.

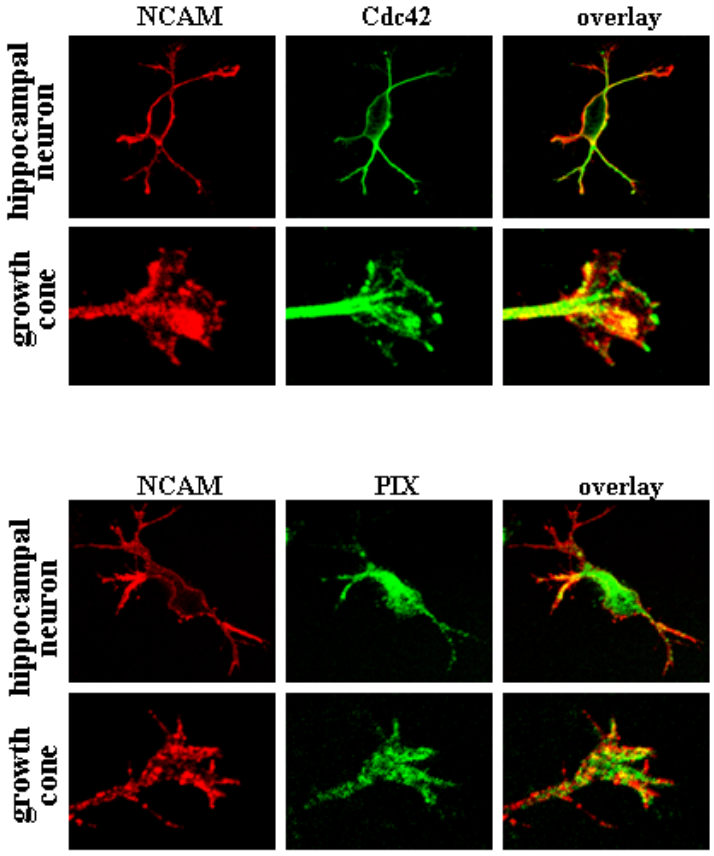

Fig. 21: **PIX and Cdc42 co-localize with NCAM in growth cones.** Primary cultured wild-type hippocampal neurons were co-labeled with antibodies against NCAM and Cdc42 or PIX. Note that clusters of NCAM partially overlap with accumulations of Cdc42 and PIX in growth cones.

IV.8. LIPID RAFTS ARE INDISPENSABLE FOR NCAM-DEPENDENT PAK1 CASCADE ACTIVATION

Downstream effectors in NCAM signaling pathways are often segregated from NCAM and NCAM-associated upstream molecules by accumulating at lipid rafts. NCAM then acts as a shuttle that carries NCAM-associated upstream activators to lipid rafts in response to NCAM stimulation (Bodrikov et al., 2005, 2008; Leshchyns'ka et al., 2003; Santuccione et al., 2005). To investigate whether lipid rafts play a role in Pak1 pathway activation, firstly, the distribution of Pak1 and its activators PIX and Cdc42 was analyzed between total membranes, lipid rafts and cytosolic fractions isolated from the brains of NCAM+/+ and NCAM-/- brains.

Western blot analysis of these fractions showed that Pak1 was enriched in the cytosol and total membranes, with only low levels of this enzyme detectable at lipid rafts (Fig. 22). Cdc42 was highly enriched at total membranes, but similarly to Pak1, it was present only at low levels in lipid raft fractions (Fig. 22). In contrast to Cdc42 and Pak1, PIX was concentrated at lipid rafts when compared to other fractions analyzed (Fig. 22). These observations indicate that Pak1 is normally segregated from its activator PIX to distinct cell compartments. And Pak1 activation probably requires redistribution of Pak1 and Cdc42 to PIX-enriched lipid rafts to form a functional complex together with NCAM. Levels of PIX were reduced by approximately 40 % at NCAM-/- lipid rafts as compared to those at NCAM+/+ rafts, suggesting that NCAM plays a role in the recruitment of PIX to lipid rafts (Fig. 22).

Phosphorylation of Pak1 at Ser199/204 abnormally aggregated at NCAM-/- membranes and lipid rafts, which indicated a dysregulated Pak1 function at these places. Thr212 phosphorylated Pak1 was nearly not detectable at total membranes and lipid rafts, and it was increased in NCAM-/- brain homogenates and cytosolic fractions (Fig. 22), as in consistent with previous data (Fig. 11). Net phosphorylation of Pak1 at Thr423 was not altered in NCAM-/- brains. Pak1 phosphorylated at Thr423, Ser199/204 and Thr212 was highly enriched in the cytosol correlating with the report showing that Pak1 only transiently associates with PIX at membranes, after it gets activated it is rapidly released back to the cytosol to phosphorylates its substrates (Zhao et al., 2000a). In support of this notion, Pak1-activated Thr508-phosphorylated LIMK1 and LIMK1-inactivated Ser3-phosphorylated cofilin both accumulated in the cytosol (Fig. 22). Similar to data shown in Fig. 13, phosphorylation of cofilin was decreased in both NCAM-/- brain homogenates and cytosol while total cofilin levels were increased in both fractions (Fig. 22).

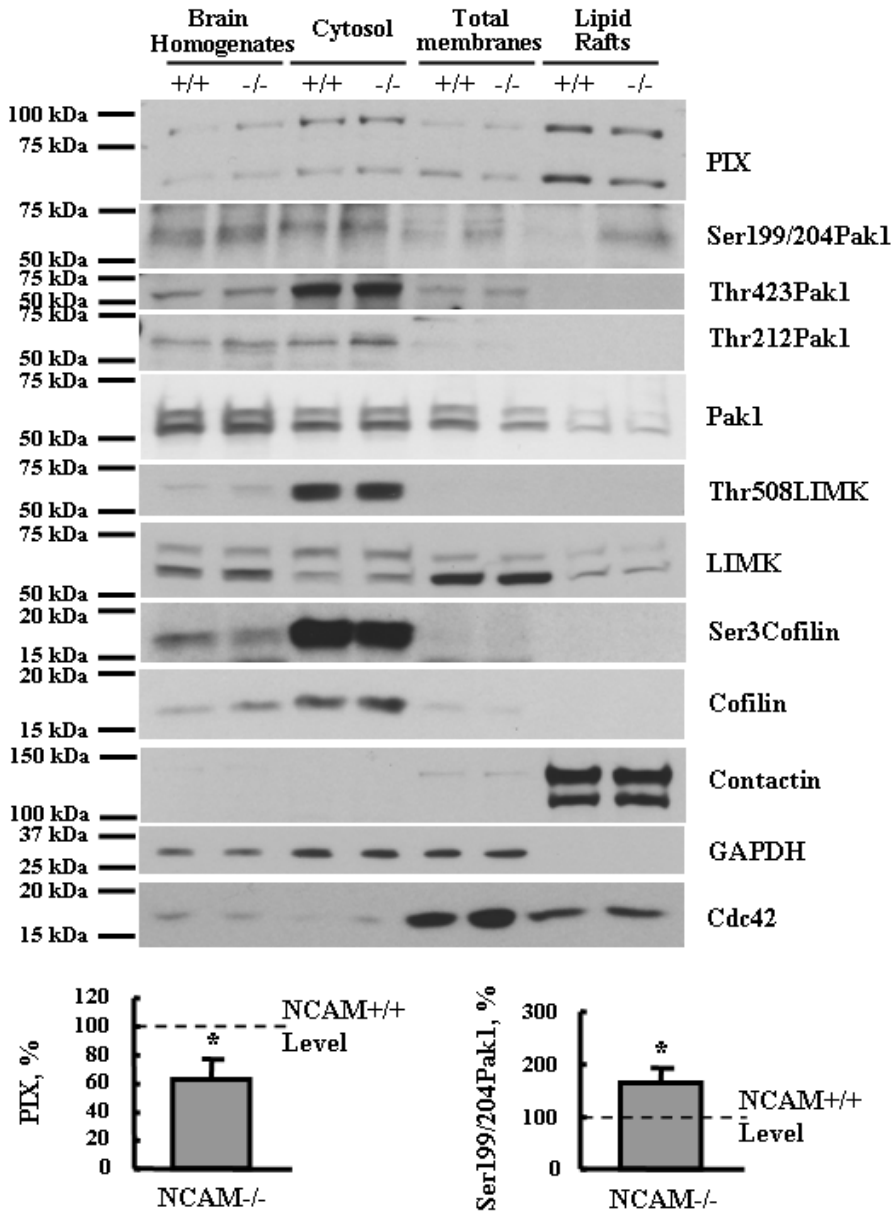

Fig. 22: **Lipid raft enriched PIX is segregated from non-lipid raft localized Pak1 and Cdc42, and PIX targeting to lipid rafts is reduced in NCAM-/- brains.** Brain homogenates, cytosol, total membranes and lipid rafts from wild-type (NCAM+/+) and NCAM-deficient (NCAM-/-) mouse brains were probed by Western blot with indicated antibodies. Labeling for contactin and GAPDH was included as loading control. Diagrams show optical densities of the protein bands in NCAM-/- probes normalized to NCAM+/+ levels set to 100 % (dashed lines). Mean values ± SEM are shown (n=6). Note that Pak1 is hyperphosphorylated at Ser199/204 in NCAM-/- lipid rafts while levels of PIX are reduced in NCAM-/- lipid rafts. *$p<0.05$ (paired t-test, compared to corresponding NCAM+/+ probes).

Since the regulation of Pak1 pathway by NCAM has growth cone specificity (conclusion from Fig. 13) and at NCAM-/- lipid rafts there are defects in Pak1 phosphorylation, meanwhile, targeting of Pak1 activator PIX to lipid rafts is reduced in NCAM-/- brains, it is reasonable to hypothesize that NCAM might modulate Pak1 pathway activity at growth cone

lipid rafts. So, the raft-association of NCAM and Pak1 pathway molecules on growth cone lipid rafts and rafts isolated from other membranes were examined. In agreement with the hypothesis, levels of NCAM were several fold higher in lipid rafts from growth cones when compared to lipid rafts from other membranes (Fig. 23). Pak1 and Cdc42 were also enriched in lipid rafts from growth cones when compared to lipid rafts from other membranes (Fig. 23). Thus, enhanced accumulation of Pak1 and Cdc42 at growth cone lipid rafts suggested an enhanced Pak1-Cdc42-PIX complex formation and Pak1 activation (Fig. 23). Similar to the total pool of lipid rafts (Fig. 22), only very low levels of phosphorylated Pak1, its substrate LIMK1, and LIMK1 substrate cofilin were detectable in lipid rafts (Fig. 23). Once more, these data suported the published data showing that Pak1 resides only transiently in the complex with PIX and Cdc42, it rapidly redistributes to the cytosol after its activation (Zhao et al., 2000a).

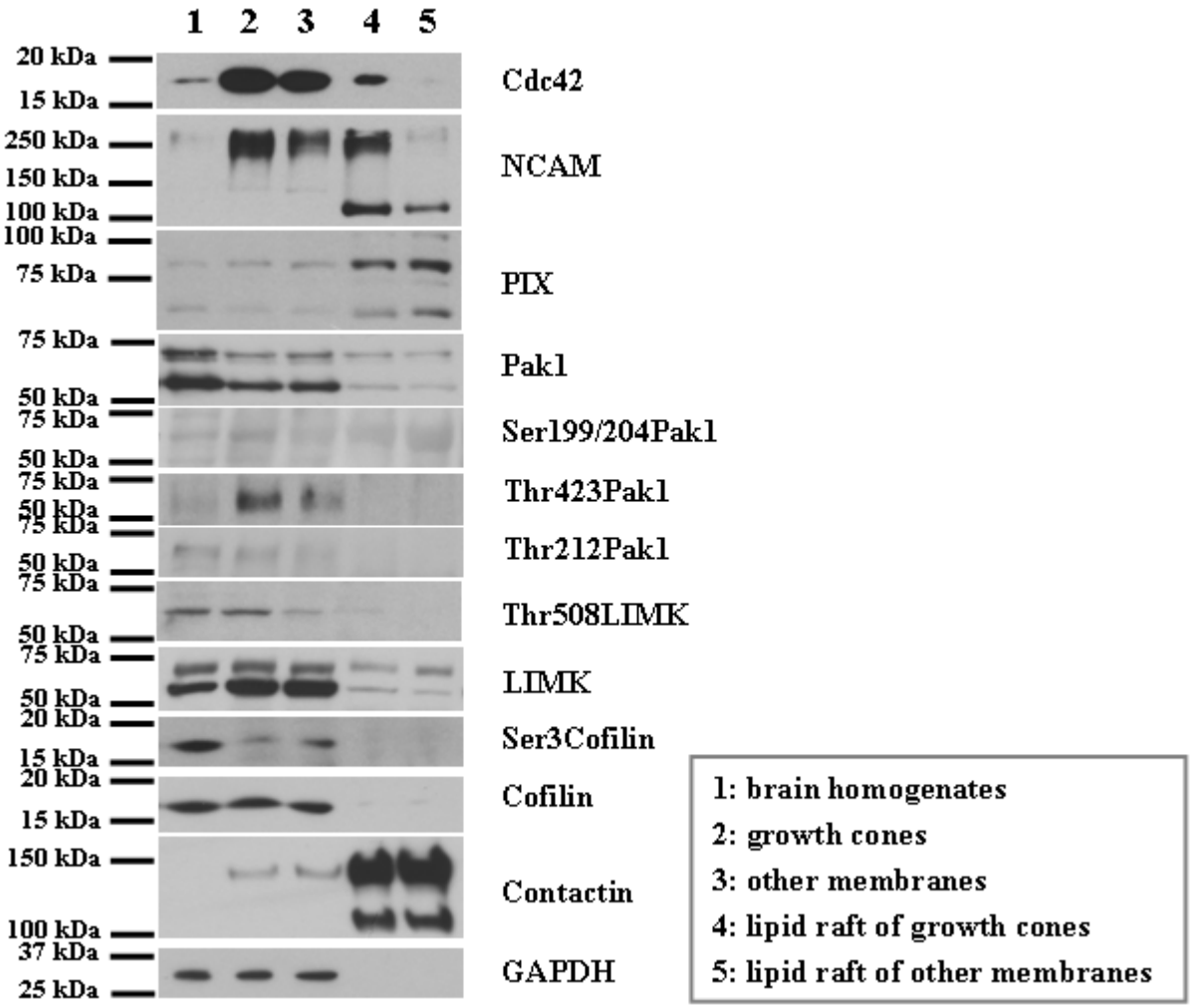

Fig. 23: **Cdc42, Pak1 and NCAM are enriched at growth cone lipid rafts.** Lipid rafts were isolated either from growth cones or growth cone-free other membrane fractions from 1-3-day-old wild-type mouse brains. Probes were analyzed by Western blot with indicated antibodies.

To verify the role of lipid rafts in Pak1 pathway activation in a more direct manner, I analyzed NCAM-dependent Pak1 activation under conditions when lipid rafts were acutely disrupted by methyl-β-cyclodextrin (MCD), an agent which extracts cholesterol from plasma membranes. NCAM antibody-induced hyperphosphorylation of Pak1 at Thr423 and Ser199/204, downstream activation of LIMK and inactivation of cofilin were totally blocked in growth cones pre-treated with MCD (Fig. 24). Thus, we conclude that lipid raft integrity is required for NCAM-dependent Pak1 activation.

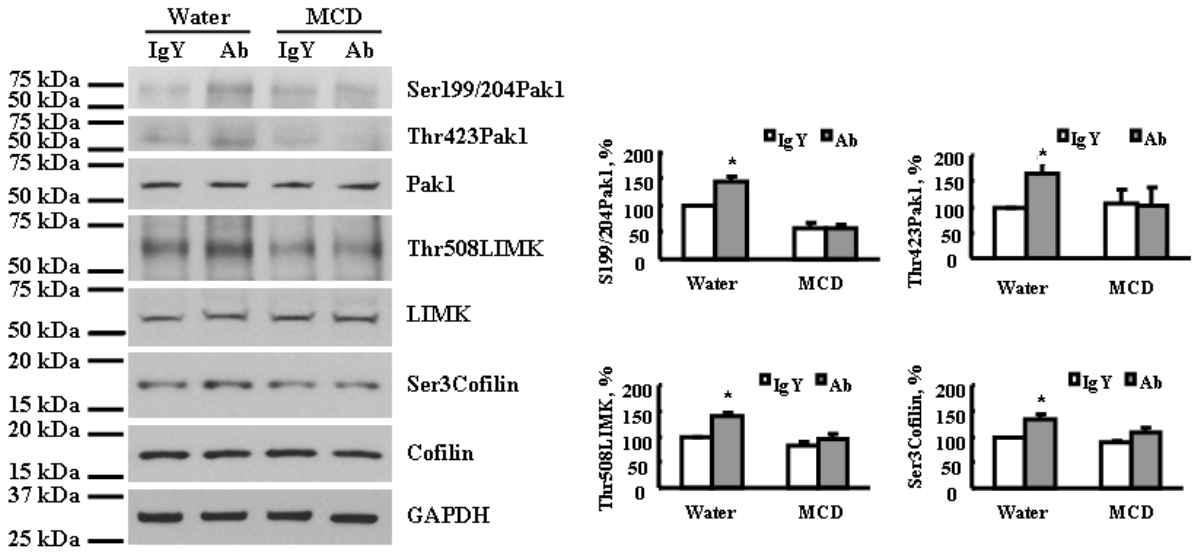

Fig. 24: **Lipid rafts are indispensible for Pak1 pathway activation.** Growth cones isolated from wild-type (NCAM+/+) mouse brains were pre-incubated with 5 mM MCD for 20 min on ice. Control and MCD treated growth cones were then treated with polyclonal chicken antibodies against NCAM for 30 min at 37°C to induce NCAM clustering at the surface of the growth cones. Growth cones treated with non-specific chicken immunoglobulin (IgY) served as control. Lysates of the growth cones were then probed by Western blot with the indicated antibodies. Graphs show optical densities of the protein bands. Mean values ± SEM (n=5) are shown. Note that MCD inhibits NCAM-dependent phosphorylation of Pak1 at Ser199/204 and Thr423, LIMK1 at Thr508 and cofilin at Ser3. *$p<0.05$ (paired t-test, compared to corresponding probes from IgY treated growth cones).

V. DISCUSSION

V.1. NCAM SIGNALS THROUGH PAK1 TO REGULATE ACTIN DYNAMICS IN GROWTH CONES TO PROMOTE NEURITE OUTGROWTH

NCAM, a member of the immunoglobulin superfamily of cell adhesion molecules, is involved in neuronal migration, differentiation, axon outgrowth and fasciculation, as well as synaptic plasticity (Maness and Schachner, 2007). In this study, we identify serine / threonine protein kinase Pak1 as a novel binding partner of the intracellular domain of NCAM. NCAM affects the membrane association and phosphorylation of Pak1, thus, the kinase activity of Pak1. Pak1, together with its activators, Cdc42 and PIX, co-localizes with NCAM clusters most prominently in neuronal growth cones where it controls the dynamic rearrangement of actin cytoskeleton via sequential phosphorylation and modification of LIMK1 and cofilin activity. Further investigations with the aid of Pak inhibitor or mutant Pak1 constructs reveal that Pak1 activity is essential for NCAM-mediated neurite outgrowth.

Most of the previously reported signaling cascades downstream of NCAM in promotion of neurite outgrowth terminate in MAPK pathway activation and the alteration of related gene expression (Bodrikov et al., 2005; Bodrikov et al., 2008; Leshchyns'ka et al., 2003; Niethammer et al., 2002). In contrast, in the present study a novel signaling pathway is demonstrated, which could function in a more direct and local manner and account for the need of rapid changes of growth cone function. The results also add up the complexity of NCAM induced signal transduction. To realize its neurite elongation promoting effect, NCAM could utilize distinct approaches at various levels, ranging from regional regulation to global adjustment. It is not difficult to deduce that these strategies might act in compensatory or competitive ways. Under different circumstances, NCAM could switch from one or several dominant pathways to other ones.

V.2. THE MECHANISM OF PAK1 ACTIVATION

The activity of Pak1 is tightly controlled at several different levels, including dimerization, phosphorylation, localization and binding of active Rho GTPases (Bokoch, 2003). The majority of Pak1 exists in the cytosol as a homodimer adopting a *trans*-inhibited conformation with the KI region of one Pak1 molecule packed against the catalytic domain of the other (Lei et al.,

2000; Parrini et al., 2002; Zhao et al., 1998). GTPase binding disrupts dimerization and leads to a series of conformational changes that destabilize the folded structure and rearrange the kinase into a catalytically competent state (Bokoch, 2003; Zhao and Manser, 2005). Although primarily regarded as Rho GTPases effectors, Pak1 can also be activated through mechanisms that do not need GTPases. Pak1 can be recruited to the plasma membrane in a similar manner by adaptor proteins Nck (Bokoch et al., 1996; Lu et al., 1997), Grb2 (Puto et al., 2003) or PIX (Manser et al., 1998), where Pak1 can be activated by lipids (Bokoch et al., 1998) or 3-phosphoinositide-dependent kinase-1 (PDK1) (King et al., 2000a).

Pak1 has multiple phosphorylation sites that are shown to be related to regulation of its kinase activity. Among them, Thr423 lies in the activation loop of Pak1 catalytic domain and phosphorylation at this site is important for both maintaining relief from autoinhibition and for overall enzymatic function (Gatti et al., 1999; Yu et al., 1998; Zenke et al., 1999). Phosphorylation of Pak1 at Thr212 is believed to be a negative regulatory mechanism for Pak1 kinase activity (Nikolic et al., 1998; Rashid et al., 2001). Nuclear magnetic resonance (NMR) data show that Ser199 of Pak1 is in close contact with SH3 domain of PIX and phosphorylation at Ser199 decreases the affinity between PIX-SH3 and Pak peptide 6 fold. Residues 195-198 are necessary for the high-affinity binding between PIX and Pak1 peptides as mutations of His196 or Thr197 or removal of residues 198-204 decreases the interaction to 30-40 % of the wild-type level. Residues 200-204 are highly flexible and they do not make any interactions with the PIX SH3 domain (Mott et al., 2005).

The phosphorylation of Paks is also subject to temporal and spatial regulation by multiple kinases and phosphatases. While PDK1 phosphorylates Pak1 at the critical Thr423 residue and activates the kinase (King et al., 2000a), PKA negatively regulates Pak1 in anchorage-dependent signaling. Akt / PKB phosphorylates Pak1 at Ser21, and this modification decreases binding of Nck to the N-terminus of Pak1 while increasing kinase activity (Tang et al., 2000). PI3K activates Pak through protein-protein interaction (Tsakiridis et al., 1996). Two closely related human protein phosphatases POPX1 (partner of PIX 1) and POPX2 have been identified that efficiently dephosphorylate Pak1, including at Thr423 (Koh et al., 2002). They bind to various forms of PIX and form multimeric cellular complexes containing Pak. Overexpression of either of these phosphatases antagonizes the cellular effects of active Pak1 (Koh et al., 2002). The presence of such negative regulators in complex with the activating kinases explains the rapid activation / inactivation cycle of Pak (Zhan et al., 2003).

Activated Pak redistributes to the nucleus and also to the leading edges of motile cells, activates its substrates by phosphorylating them at specific serine or threonine residues or through protein–protein interaction.

In the current study, in spite of the fact that total Pak1 expression levels are not changed between wild-type and NCAM-deficient brain homogenates, we find that Pak1 targeting to growth cones and other membranes is significantly reduced in NCAM-deficient brains. This might result from the decreased membrane-associated PIX because of NCAM deficiency, as PIX is regarded to be crucial for recruitment of PAK1 to plasma membrane and activation (Chan et al., 2008; Koh et al., 2001; Loo et al., 2004; Manser et al., 1998). Decreased PIX levels on NCAM-deficient membranes correlates with our observation that phosphorylation of Pak1 at Ser199/204 is upregulated both in NCAM-deficient growth cones and other membranes, as phosphorylation at these residues serves to break Pak-PIX interaction (Mott et al., 2005). Phosphorylation of Pak1 at Thr212 is enhanced in NCAM-deficient brain homogenates which is in coincident with the reduced kinase activity of Pak1. Moreover, upon NCAM clustering on growth cone membranes, Thr212 phosphorylation is inhibited accompanying an increased Pak1 activity.

In contrast to the fact that Pak1 kinase activity is reduced in NCAM-deficient brain homogenates and Pak1 activity is upregulated in response to NCAM stimulation on growth cone membranes, the net phosphorylation of Pak1 at Thr423 is at the same levels in brain homogenates and growth cones between wild-type and NCAM-deficient mice. Furthermore, phosphorylation of Pak1 at Ser199/204 increases in NCAM-deficient growth cones, which is opposite to the result that these residues are hyperphosphorylated after activation of NCAM in growth cones. These seemingly contradictory data indicate that NCAM modulates Pak1 kinase activity in a sophisticated manner. It is not accurate to evaluate Pak1 activity by its phosphorylation at any single position. Rather, the various combinations of phosphorylation at different sites determine the absolute kinase activity. For instance, upon clustering of NCAM on growth cone membranes, Pak1 is hyperphosphorylated at both Thr423 and Ser199/204, but is dephosphorylated at Thr212, and the summation of these changes yields reduced Pak1 kinase activity.

V.3. PAK1 DYSFUNCTION COULD EXPLAIN THE ABNORMALITIES OBSERVED IN NCAM-DEFICIENT MICE

V.3.1. The role of Pak1 in neuronal development

The examination of Pak1 localization reveals that Pak1 is enriched in the central nervous system throughout development and persists in adulthood (Burbelo et al., 1999; Hayashi et al., 2002; Manser et al., 1994; Teo et al., 1995; Zhong et al., 2003). In the developing forebrain the highest level of Pak1 expression is observed in the cortical plate, hippocampus and major axonal tracts, including the thalamo-cortical and cortico-thalamic projection, corpus callosum, lateral olfactory tract and anterior commissures (Ong et al., 2002b; Zhong et al., 2003). Electron microscopy investigation indicates that Pak1 is concentrated in axon terminals and dendrites of primate forebrains (Ong et al., 2002b). In addition, Ser199/204 phosphorylated Pak1 is seen to accumulate in the cortical plate and axonal tracts of the developing mouse forebrain (Jacobs et al., 2007). While Thr423 phosphorylated Pak1 seems to be enriched in the tips of dendrites (Hayashi et al., 2002), Thr212 phosphorylated Pak1 is evident throughout axonal growth cones (Banerjee et al., 2002). It is worth mentioning that this residue is unique for Pak1 and not conserved in other group I Paks, and phosphorylation of Pak1 at Thr212 is developmental specific since it is undetectable in all adult tissues (Zhong et al., 2003). This preferential expression and phosphorylation pattern implies an important role Pak1 may play in the nervous system.

In agreement with NCAM function, Pak1 is a critical regulator of axon guidance, which is well exemplified in the model organism *Drosophila* where Pak1 kinase activity is indispensible for proper axon path finding of photoreceptor cells (Hing et al., 1999; Newsome et al., 2000). In the olfactory system, Pak, LIMK and cofilin signal in a linear manner to regulate the normal glomerular development in the antennal lobe (Ang et al., 2006). Furthermore, signaling pathways that cause growth cone collapse, such as stimulation of the plexin-B1 receptor by Semaphorin 4D can inhibit Rac-induced Pak1 activation (Vikis et al., 2002). Interestingly, Pak1 is reported to be essential for Roundabout (Robo) receptor induced growth cone repulsion at the midline, which suggests that Pak1 can function in both attractive and repulsive axon guidance (Fan et al., 2003).

Pak1 perturbations have also been shown to affect neuronal polarity and morphology. Hyperactivation of Pak1 at the membrane of all neurites, or loss of Pak1 expression disrupts

both neuronal morphology and the distinction between an axon and dendrites (Jacobs et al., 2007). The role of Pak1 in neuronal morphogenesis is further supported by the findings showing that expression of catalytically active Pak or dominant-negative Pak changes the spine shape and density (Boda et al., 2008; Hayashi et al., 2007; Hayashi et al., 2002; Hayashi et al., 2004). While constitutively active Pak1 effectively rescues the down regulation of spine formation induced by GIT1 knockdown (Zhang et al., 2005), inhibition of Pak1 in hippocampal neurons eliminates trans-synaptic ephrinB-EphB receptor signaling in promoting morphogenesis and maturation of dendritic spines (Penzes et al., 2003). However, in Pak1-deficient mice no apparent abnormality in the gross anatomy of the central nervous system could be observed which might result from a developmentally compensatory mechanism (Asrar et al., 2009).

The involvement of Pak kinase in neuronal migration was recently demonstrated (Causeret et al., 2008; Sakakibara and Horwitz, 2006). Alteration of Pak kinase activity by *in utero* electroporation of neuronal progenitors in the ventricular and subventricular zones of E14.5 mouse embryo cortices affects radial migration and morphology of projection neurons. Overexpression of hyperactivated Pak1 predominantly causes neurons to arrest in the intermediate zone (IZ) with apparently misoriented and disorganized leading projections. Loss of Pak1 disrupts the morphology of migrating neurons which accumulate in the IZ and deep cortical layers. In addition, a significant number of neurons with suppressed Pak1 expression aberrantly entered into the normally cell-sparse marginal zone, suggesting their inability to respond to local stop signals or dissociate from guiding radial glia (Causeret et al., 2008). During rhombic lip cell migration in the developing chicken cerebellum, introducing a kinase-dead mutant of Pak disturbs the coordinated spreading of the tips of the leading neuronal precursor processes and frequently branching of tips was observed. In contrast, overexpression of wild-type Pak produces a large, relatively stable tip of the migratory process and inhibited extension of the process (Sakakibara and Horwitz, 2006). These findings underline the *in vivo* importance of temporal and spatial regulation of Pak1 kinase during key stages of brain development

V.3.2. The role of NCAM in neuronal development

3.2.1. Anatomic abnormalities in NCAM-deficient brains

Investigations on constitutive and conditional NCAM-deficient mice reveal that NCAM is indispensible for normal neuronal development (Bukalo et al., 2004; Cremer et al., 1994;

Holst et al., 1998; Stork et al., 2000; Tomasiewicz et al., 1993). Mice with a constitutive ablation of all NCAM isoforms (Cremer et al., 1994) or null mutation of NCAM180 (Tomasiewicz et al., 1993) show a 10 % decrease in brain size and develop a dramatically smaller olfactory bulb. This phenotype was traced to disturbed cell migration of the neuronal precursor cells (Chazal et al., 2000; Tomasiewicz et al., 1993). The subventricular zone-derived olfactory precursors normally migrate along the rostral migratory pathway into the olfactory bulb where they differentiate into interneurons. In the absence of NCAM, the migration is disturbed and the precursor cells remain at their origin or accumulate along the pathway.

NCAM is also heavily implicated in the complex regulation of axonal growth, path finding and axonal fasciculation. NCAM-deficient mice show an altered cytoarchitecture of the hippocampus (Cremer et al., 1998; Cremer et al., 1997; Tomasiewicz et al., 1993). In the wild-type mouse mossy fibers are organized in a laminated pattern (Amaral and Witter, 1989) and a clear distinction between the pyramidal cell layer and the stratum lucidum is obvious. But in the NCAM-deficient mutant the laminated expression of NCAM in the stratum lucidum disappears, and the clear distinction between the pyramidal cell layer and the stratum lucidum no longer exists. Mossy fiber terminals, that are normally restricted to the stratum lucidum, are also found in the pyramidal cell layer in the mutant. Moreover, axonal growth is impaired and axon fasciculation of mossy fibers in the hippocampus is reduced. These studies underscore the importance of NCAM in the complex regulation of cell migration and axonal growth, which could be contributed by Pak1 function downstream of it.

3.2.2. Altered growth cone morphology in NCAM-deficient brains

Filopodia are highly dynamic structures that continuously go through rapid cycles of extension, lateral movement, and shortening. These extension and retraction are irregular and unpredictable, exploring the environment for guidance cues to mediate adhesion and motility (Bray and Chapman, 1985; Goldberg and Burmeister, 1986; Lamoureux et al., 1989). Our live image data reveal striking morphological changes of NCAM-deficient hippocampal growth cones. They are abnormally enlarged (Chernyshova et al, unpublished result) and develop much less and shorter filopodia as compared to wild-type growth cones. These rare filopodia are barely mobile, they protrude and retract very slowly, as if being frozen. The morphological defect in NCAM-deficient growth cones could be the cellular basis for the impaired neurite outgrowth and pathway finding exhibit in NCAM-deficient brains.

At the core of each filopodium is a dense, cross-linked bundle of actin filaments that extends into the lamellipodium (Lewis and Bridgman, 1992), thus the tightly control of actin polymerization lies in the center of filopodia dynamics. In this study, NCAM deficiency decreases Pak1 kinase activity which in turn reduces LIMK activity and promotes cofilin binding to actin filaments where hyperactive cofilin excessively severs and depolymerizes F-actin into G-actin. The destabilization of actin cytoskeleton in NCAM-deficient growth cones is proved by our biochemical analysis. While the expression of actin is not altered in NCAM-deficient brains, the actin polymerization is significantly repressed. There is about two times more monomeric actin in NCAM-deficient growth cones as compared to the wild-type level. Accordingly, filamentous actin level is just half of that in wild-type growth cones.

The role of NCAM in regulation of the actin cytoskeleton has been the subject of numerous studies. An early investigation shows that crosslinking of apCAM (*Aplysia* homologue of NCAM) by antibodies triggers localized actin assembly accompanied by formation of tail-like actin structures (Thompson et al., 1996). Some studies have focused on the role of GAP-43 as a linker between NCAM and the dynamic changes of actin cytoskeleton during cell morphogenesis (Korshunova et al., 2007; Meiri et al., 1998). GAP-43 binds to and modifies filamentous actin, thereby participating in cytoskeletal dynamics involved in growth cone motility (Frey et al., 2000; He et al., 1997; Oestreicher et al., 1997). NCAM is also connected to actin cytoskeleton through spectrin, which is a well studied binding partner of the intracellular domain of NCAM (Pollerberg et al., 1986, 1987), and is important for NCAM signaling on lipid rafts in promoting neurite outgrowth (Bodrikov et al., 2005; Leshchyns'ka et al., 2003). The results of this thesis work revealed a direct relationship between NCAM and the regulation of actin cytoskeletal dynamics.

V.4. THE ROLE OF LIPID RAFTS IN NCAM-MEDIATED SIGNAL TRANSDUCTION

The importance of lipid rafts in NCAM-mediated signaling transduction is once again emphasized in the present study. It has been demonstrated that NCAM partially overlaps with the lipid raft marker GM1 along neurites in hippocampal neurons and all three major NCAM isoforms can be detected in lipid rafts biochemically isolated from both mouse brain homogenates and neuroblastoma cells (Niethammer et al., 2002). The co-localization of NCAM with caveolin has also been reported (He and Meiri, 2002). Recently, NCAM is

observed in rafts prepared from forebrain synaptosomes, and the NCAM180 isoform is found to be enriched in GAP-43 containing rafts (Korshunova et al., 2007). The presence of NCAM in growth cone lipid rafts (He and Meiri, 2002) was further confirmed in this thesis work and it was further discovered here that the existence of NCAM in growth cone lipid rafts is more prominent than in lipid rafts isolated from other membrane fractions, which supports the notion that NCAM plays fundamental roles in growth cone.

By means of cold 1 % Triton X-100 extraction, I found that PIX accumulates at lipid rafts, and its raft-association decreases significantly in NCAM-deficient mouse brains, suggesting that NCAM may play a role in the recruitment of PIX to lipid rafts. Cdc42 is also seen to be present at neuronal lipid rafts and like NCAM, it preferentially localizes to growth cone lipid rafts as compare to raft fractions isolated from other membranes. In consideration that PIX and Pak1 can be co-immunoprecipitated by NCAM antibodies from both brain homogenates and growth cones, while NCAM, PIX, Pak1 co-immunoprecipitate with Cdc42, it is reasonable to hypothesize that NCAM, PIX, Cdc42 and Pak1 form a protein complex on neuronal growth cone lipid rafts. LIMK1, the further downstream signaling molecule of this pathway, shows very low level of raft-association and its active form, Thr508 phosphorylated LIMK1, is highly enriched in the cytosol. Both cofilin and Ser3-phosphorylated cofilin predominantly situate in the cytosolic fraction where they carry out their specific function.

In agreement with previous findings Pak1 and its phosphorylated forms concentrate in cytosolic fractions, but there is a certain amount of Pak1 that is raft-associated and it also displays the same preference to growth cone lipid rafts like NCAM and Cdc42. In addition, phosphorylation of Pak1 at Ser199/204 is abnormally increased in NCAM-deficient lipid raft implying a dysregulated Pak1 kinase activity at this place. To find out whether lipid rafts may play a role in the regulation of Pak1 activity downstream of NCAM stimulation, a widely used cholesterol depletion agent, MCD was applied to induce lipid raft disassembly in isolated growth cones. The hyperphosphorylation of Pak1 at Thr423 and Ser199/204 upon NCAM clustering on growth cone membranes was completely abolished after the disruption of lipid rafts. Consequently, activation of LIMK and inhibition of cofilin activity are also attenuated upon lipid raft disassembly, which highlight the importance of lipid rafts integrity in Pak1 pathway activation downstream of NCAM.

V.5. THE ROLE OF PIX IN PAK1 ACTIVATION AND PAK1-DEPENDENT NEURITE OUTGROWTH

PIX is a widely expressed focal complex protein and PIX binding is required for Pak localization to lamellipodia and focal complexes (Koh et al., 2001; Loo et al., 2004; Manser et al., 1998). β-PIX is reported to function either as a scaffold or a GEF or both to coordinate the activation of Cdc42 and Rac (Jones and Katan, 2007; Koh et al., 2001; Manser et al., 1998). It was shown in this study that PIX is highly enriched at lipid rafts, where it meets active NCAM, which translocates there. NCAM and PIX further recruit Cdc42 and Pak1 to form a functional complex that is capable of regulating actin cytoskeleton. Because Ser199 and Ser204 autophosphorylated Pak dissociates from PIX (Mott et al., 2005; Zhao et al., 2000a), Pak only transiently forms complexes with PIX at the membrane owing to the presence of kinase activators at this site, cycling back to the cytoplasm immediately after autophosphorylation (Zhao et al., 2000a).

In support of the current data, the role of PIX in regulation of actin dynamics was also reported by several studies. PIX was shown to localize to the cell periphery via its C-terminal region to drive the formation of membrane ruffles and microvillus-like structures, and Pak binding was indispensable for this effect (Kim et al., 2001; Koh et al., 2001; Manser et al., 1998). Dependent on its GEF activity, β-PIX overexpression induces vigorous membrane ruffling and potentiates Pak1 activation by Cdc42 (Manser et al., 1998). In NGF-stimulated PC12 cells, Pak and β-PIX act upstream to promote activation of Rac, which is essential for lamellipodia formation (Obermeier et al., 1998). In response to basic fibroblast growth factor (b-FGF), β-PIX translocates to the lamellipodia at neuronal growth cones, and β-PIX promotes neurite formation at ~2 fold greater efficiency than does a GFP control. Phosphorylation of β-PIX (p85 isoform) via the Ras / ERK / Pak2 pathway is required for b-FGF-induced neurite outgrowth (Shin et al., 2002). Mutated β1-PIX, which lacks GEF activity, or lacks the ability to bind to Pak, decreased endothelin-1-induced Cdc42 activation (Chahdi et al., 2005).

In the case of T-cell receptor activation, the PIX-Pak interaction is required for GTPase mediated kinase activation (Ku et al., 2001). A regulated interaction of Pak with β-PIX is necessary for directional cell migration (Zegers et al., 2003). In the scratch-induced wound healing system, knockdown of β-PIX expression significantly reduces the protrusion formation, elongation of the microtubule network, and polarization of the actin cytoskeleton. Furthermore,

expression of wild-type β-PIX in leading edge cells induces dyslocalized protrusions all around the cell periphery (Cau and Hall, 2005; Osmani et al., 2006). In fibroblasts, a Cdc42 / Pak / β-PIX signaling cascade has been proposed to restrict Rac-dependent protrusion formation to the leading edge of the migrating cells (Cau and Hall, 2005). In astrocytes Scrib targets β-PIX to membrane protrusions at the wound edge, which elicits activation of Cdc42 and results in polarization of the cytoskeleton and secretory apparatus permissive for directional cell migration (Osmani et al., 2006).

V.6. PAK1 IS A COMMON SIGNALING MOLECULE DOWNSTREAM OF CAMS

The Down syndrome cell adhesion molecule (DSCAM), a member of the immunoglobulin superfamily, plays a pivotal role in neuronal axon guidance and axon bifurcation (Hummel et al., 2003; Schmucker et al., 2000; Wang et al., 2002). While in *Drosophila* Pak1 is recruited to the Dscam signaling complex through adaptor protein Dock (mammalian Nck homolog) (Worby et al., 2001), human DSCAM directly binds to Pak1 and stimulates Pak1 phosphorylation and activation (Li and Guan, 2004). These observations suggest that DSCAM may signal through Pak1 in axon guidance. Pak1 is also reported to lie downstream of another important IgSF CAM, L1. A signaling pathway is proposed from L1 through GEF Vav2, Rac1, Pak1 and ERK that may be important for L1-mediated neuronal cell migration (Schmid et al., 2004). Being a crucial focal complex protein, Pak1 participates in the signaling elicited by integrin which induces activation of MAPK cascades and cell migration (Juliano et al., 2004; Rosenberger and Kutsche, 2006). Furthermore, Pak1 is postulated to be a convergent point of L1 and integrin signaling pathway, which culminates in MAPK activation (Schmid and Maness, 2008). Thus, these neuritogenic adhesion molecules appear to employ shared intracellular signaling molecules to execute their cellular function.

In the current study, I discover that Pak1 phosphorylates LIMK and inactivates cofilin to relay NCAM stimulation to modulate the actin cytoskeleton. Although activation of MAPK pathway is involved in the induction of neurite outgrowth aroused by NCAM, it is still an open question whether Pak1 could work downstream of NCAM to trigger MAPK activation, like it does to convey L1 and integrin signaling. Being a homologue to the yeast Ste20, a known regulator of MAPK signaling (Dan et al., 2001b), the role of Pak1 in mammalian MAPK signaling has been widely studied. Paks activate MEK1 (MAPK/ERK (extracellular-signal-regulated kinase) kinase 1) as well as Raf1 by phosphorylating them on

Ser298 and Ser338, respectively (Eblen et al., 2002; Slack-Davis et al., 2003). It is also reported that the Rac / Cdc42-Pak cascade contributes to the activation of MAPK including ERK (Tang et al., 1997), p38 MAPK (Zhang et al., 1995) and JNK (Bagrodia et al., 1995; Brown et al., 1996; Frost et al., 1996; Polverino et al., 1995; Teramoto et al., 1996). Interestingly, the inhibition of group I Paks function by using either the Pak inhibitor domain (Zhao et al., 1998) or siRNA (small interfering RNA), blocks activation of MAPK by platelet-derived growth factor (PDGF), but not by epidermal growth factor (EGF), implying that similar growth factors can achieve MAPK activation by distinct mechanisms (Beeser et al., 2005). Finally, both group I and group II Paks may, in some cases, also act downstream of MAPKs. For example, it is reported that ERK2 phosphorylates Pak1 at Thr212, and that expression of a constitutively phosphorylated (Glu212) Pak1 mutant attenuates ERK activity (Sundberg-Smith et al., 2005).

V.7. THE ROLE OF PAK1 IN MODULATION OF THE ACTIN CYTOSKELETON

Sequential phosphorylation of LIMK and cofilin downstream of Pak1 and its effects on dynamic organization of acin cytoskeleton have been implicated in multiple stages of central nervous system development. These include cell migration along diverse pathways from their origin of birth to their final destination in the brain (Causeret et al., 2008; Sakakibara and Horwitz, 2006), the specification of a single axon and neuronal polarization formation (Jacobs et al., 2007), the promotion of neurite outgrowth and thus morphological maturation (Jacobs et al., 2007), the ability of axons to navigate over long distances following guidance cues and forming precise circuitry (Ang et al., 2006); the formation and decoration of dendritic spines and thus the functionality of synapses (Hayashi et al., 2007; Hayashi et al., 2002).

Besides LIMK (Edwards et al., 1999), Pak1 is also reported to be capable of regulating actin reorganization through p41 / Arc and filamin. Pak1 is a direct activator of actin nucleation and branching through the phosphorylation of p41 / Arc, which stimulates assembly of the Arp2/3 complex (Vadlamudi et al., 2004). Along with Arp2/3 complex proteins, another Pak1 substrate, filamin A, mediates the dynamic actin changes and stabilization of membrane ruffling that occurs at the leading edge of the motile cells (Vadlamudi et al., 2002). Interestingly, filamin A also stimulates Pak1 activity, which indicates that the interaction is important for the local activation of Pak (Vadlamudi et al., 2002). Through these multiple interacting partners and kinase substrates, Pak family kinases probably function as signaling nodes for the cytoskeleton, coordinating upstream signaling with multiple effectors.

V.8. MODEL

At last, I would like to propose following model. At rest, only a small portion of NCAM locates in lipid rafts, while the majority of NCAM resides in lipid raft free areas of membranes (Niethammer et al., 2002). Upon stimulation, NCAM transits to lipid rafts and binds to adaptor protein PIX, which predominantly situates there. The NCAM-PIX complex further recruits Cdc42 and Pak1 to lipid rafts to form a functional complex. Pak1 gets activated at lipid rafts, then goes back to the cytosol and phosphorylates its substrates LIMK. Activated LIMK phosphorylates cofilin, an actin depolymerizing protein, and inactives it, which leads to more stationary actin filaments and sustains normal growth cone morphology and motility. In NCAM-deficient growth cones, PIX-Cdc42-Pak1 complex formation is reduced. There is less active Pak1, less active LIM kinase and more active cofilin, which excessively depolymerizes and serves actin filaments. Normal growth cone morphology cannot be maintained as exemplified by enlarged growth cones and impaired filopodia formation and motility, which further leads to the hindered neurite outgrowth (Fig. 25).

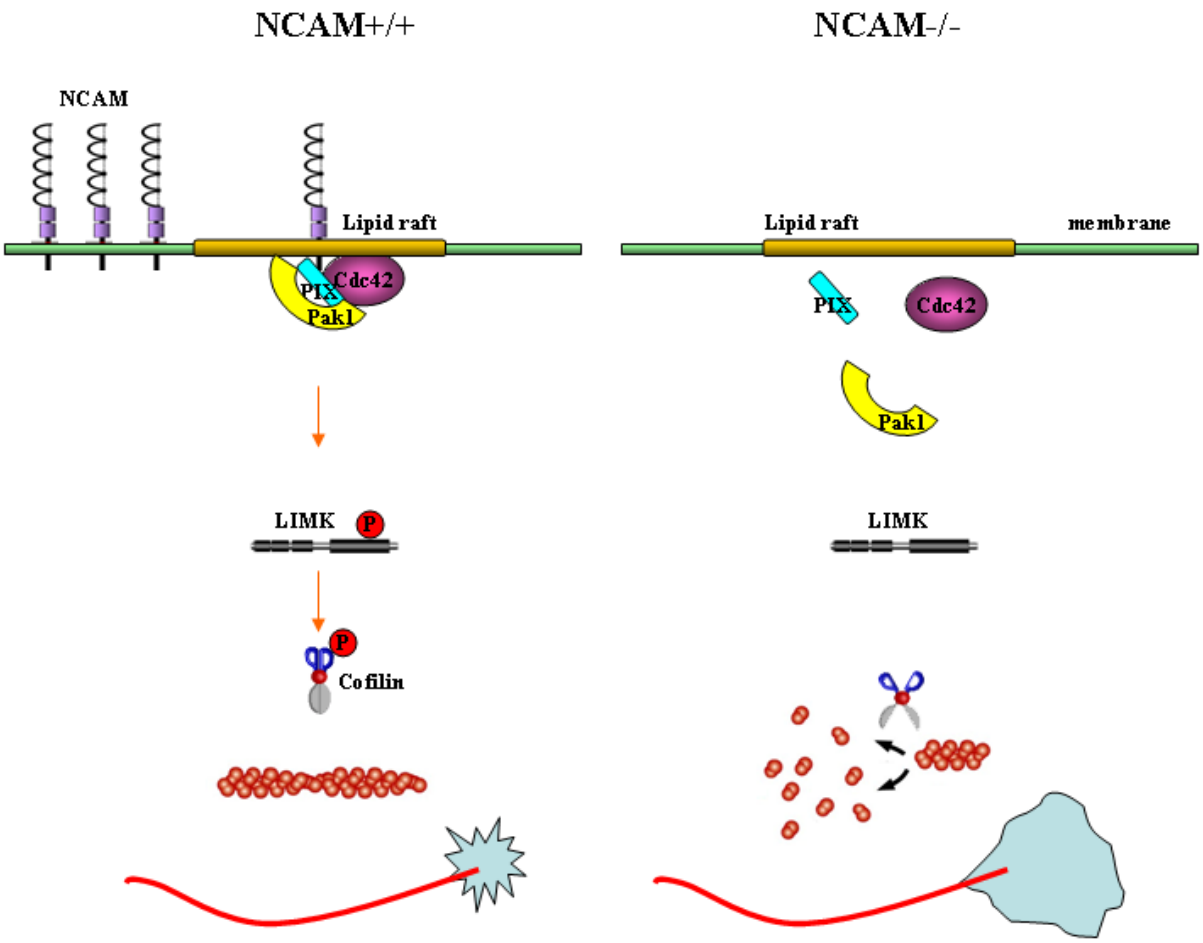

Fig. 25: **A model for Pak1 signaling downstream of NCAM in promotion of neurite outgrowth.** Stimulation of NCAM on the plasma membrane induces its translocation to lipid rafts, where it recruits PIX and further assembles Cdc42 and Pak1. Pak1 gets activated in NCAM-PIX-Cdc42-Pak1 complex on lipid rafts, and rapidly released back to cytosol to phosphorylate and activate its target LIMK. LIMK further phosphorylates cofilin and inhibits its F-actin severing and depolymerization property to maintain normal growth cone morphology. In NCAM-deficient growth cones, PIX-Cdc42-Pak1 complex formation is reduced, which results in less activated Pak1, less activated LIMK and hyperactivated cofilin. Cofilin binds to actin filaments and inhibits actin polymerization leading to reduced filopodia formation and mobility and enlargement of the growth cones.

VI. ABBREVIATION

AD	Activation domain
ADF	Actin-depolymerizing factor
approx.	approximately
3-AT	3-aminotriazole
ATP	Adenosine triphosphate
b-FGF	Basic fibroblast growth factor
BAD	Bcl-2 / Bcl-X_L-antagonist, causing cell death
BCA	Bicinchoninic acid
BDNF	Brain derived neurotrophic factor
BSA	Bovine serum albumine
CA	Catalytically active
CAM	Cell adhesion molecule
CaMKII	Calcium/calmodulin dependent protein kinase II
CDK5	Cyclin-dependent kinase 5
CHO cells	Chinese hamster ovary cells
Co.	Compagnie
Cofilin	Co-filamentous with actin
Corp.	Corporation
CREB	cAMP response element binding protein
CRIB	Cdc42 and Rac interactive binding domain
CSF	Cerebrospinal fluid
DAG	Diacylglycerol
DB	DNA binding domain
DH	Dbl homology
ddH_2O	Bi-distilled water
DMSO	Dimethyl sulfoxide
DN	Dominant-negative
DNA	Deoxyribonucleic acid
DSCAM	Down syndrome cell adhesion molecule
ECL	Enhanced chemiluminescence
EDTA	Ethylenediaminetetraacetic acid
EGF	Epidermal growth factor
ERK	Extracellular signal regulated kinase
et al.	*Et alii* (and others)
F-actin	Filamentous actin
FAK	Focal adhesion kinase
Fc	Fragment crystallizable
FCS	Fetal calf serum

FGF	Fibroblast growth factor
FGFR	Fibroblast growth factor receptor
FRS2	FGFR substrate 2
Fig.	Figure
FNIII	fibronectin type 3 like domain
g	G-force
G-actin	globular actin (monomeric)
GAP	GTPase-activating protein
GAP-43	Growth-associated protein-43
GAPDH	Glyceraldehyde-3-phosphate dehydrogenase
GDI	GDP dissociation inhibitor
GDNF	Glial cell derived neurotrophic factor
GEF	Guanine nucleotide exchange factor
GFRα	GDNF family receptor α
GIT	G-protein-coupled receptor kinase-interacting targets
GPI	Glycosylphosphatidylinositol
Grb2	Growth factor receptor bound protein 2
HEPES	4-(2-Hydroxyethyl)-1-piperazine ethanesulfonic acid
HRP	Horse radish peroxidase
ICD	Intracellular domain
ICE	Interleukin-1β converting enzyme
Ig	Immunoglobulin
IgSF	Immunoglobulin superfamily
IZ	Intermediate zone
IP_3	Inositol 1,4,5-trisphosphate
KI	Kinase inhibitory
LB	Luria Bertani
LAS	Cell lysis and F-actin stabilization
LIMK	LIM domain kinase
MAPK	Mitogen activated protein kinase
MEK1	MAPK / ERK kinase 1
MLCK	Myosin light-chain kinase
NCAM	Neural cell adhesion molecule
NFκB	Nuclear factor κB
NGF	Nerve growth factor
NMR	Nuclear magnetic resonance
NO	Nitric oxide
NP-40	Nonidet P-40, Nonylphenyl-polyethylene glycol (Nonidet is a trademark of Shell Chemical Co.)
ORF	Open reading frame
p.a.	*Pro analysi* (per analysis)

PAGE	Polyacrylamide gel electrophoresis
Pak	p21-activated kinase
PBD	p21-binding domain
PBS	Phosphate buffered saline
PBST	PBS / TWEEN
PCR	Polymerase chain reaction
PDGF	Platelet-derived growth factor
PDK1	3-phosphoinositide-dependent kinase-1
PDL	poly-D-lysine
PDNF	Platelet derived neurotrophic factor
PDZ	PSD-95/Discs large/Z0-1
PFA	Paraformaldehyde
PH	Pleckstrin homology
PI3K	Phosphatidylinositol 3-kinase
PIP_2	Phosphatidylinositol 4,5-bisphosphate
PIX	Pak-interactive exchange factor
PKA	Protein kinase A
PKC	Protein kinase C
PLC_γ	Phospholipase C_γ
PMSF	Phenylmethylsulphonyl fluoride
POPX	Partner of PIX
PrP	Prion protein
PSA	Polysialic acid
RIPA	Radio immunoprecipitation assay
ROCK	Rho-kinase
Robo	Roundabout
rpm	Rotations per minute
RPTPα	Receptor-like protein tyrosine phosphatase α
SC	Synthetic complete
SDS	Sodium dodecyl sulfate
SEM	Standard error of the mean
SH2 domain	Src homology 2 domain
siRNA	Small interfering RNA
SOC	Super optimal broth with catabolite repression
SPR	SH3 domain-containing proline-rich protein
TAE	Tris acetate EDTA
TAG-1	Transient axonal glycoprotein-1
TBS	Tris buffered saline
TBST	TBS / TWEEN
TEMED	N,N,N′,N′-Tetramethylethylenediamine
TH	Tyrosine hydroxylase

Tris	Trishydroxymethylaminomethane
Triton X-100	4-(1,1,3,3-Tetramethylbutyl)phenyl-polyethylene glycol (Triton is a registered trademark of Union Carbide Corp.)
TWEEN 20	Polyethylene glycol sorbitan monolaurate (TWEEN is a registered trademark of Uniqema)
Tyr	Tyrosine
UV	Ultraviolet
VASE	Variable alternatively spliced exon

VII. REFERENCES

Acevedo, K., N. Moussi, R. Li, P. Soo, and O. Bernard. 2006. LIM kinase 2 is widely expressed in all tissues. *J Histochem Cytochem*. 54:487-501.

Adams, A.E., D.I. Johnson, R.M. Longnecker, B.F. Sloat, and J.R. Pringle. 1990. CDC42 and CDC43, two additional genes involved in budding and the establishment of cell polarity in the yeast Saccharomyces cerevisiae. *J Cell Biol*. 111:131-42.

Akiyama, S.K., S.S. Yamada, W.T. Chen, and K.M. Yamada. 1989. Analysis of fibronectin receptor function with monoclonal antibodies: roles in cell adhesion, migration, matrix assembly, and cytoskeletal organization. *J Cell Biol*. 109:863-75.

Albach, C., E. Damoc, T. Denzinger, M. Schachner, M. Przybylski, and B. Schmitz. 2004. Identification of N-glycosylation sites of the murine neural cell adhesion molecule NCAM by MALDI-TOF and MALDI-FTICR mass spectrometry. *Anal Bioanal Chem*. 378:1129-35.

Allen, K.M., J.G. Gleeson, S. Bagrodia, M.W. Partington, J.C. MacMillan, R.A. Cerione, J.C. Mulley, and C.A. Walsh. 1998. PAK3 mutation in nonsyndromic X-linked mental retardation. *Nat Genet*. 20:25-30.

Amaral, D.G., and M.P. Witter. 1989. The three-dimensional organization of the hippocampal formation: a review of anatomical data. *Neuroscience*. 31:571-91.

Ang, L.H., W. Chen, Y. Yao, R. Ozawa, E. Tao, J. Yonekura, T. Uemura, H. Keshishian, and H. Hing. 2006. Lim kinase regulates the development of olfactory and neuromuscular synapses. *Dev Biol*. 293:178-90.

Ang, L.H., J. Kim, V. Stepensky, and H. Hing. 2003. Dock and Pak regulate olfactory axon pathfinding in Drosophila. *Development*. 130:1307-16.

Angata, K., J.M. Long, O. Bukalo, W. Lee, A. Dityatev, A. Wynshaw-Boris, M. Schachner, M. Fukuda, and J.D. Marth. 2004. Sialyltransferase ST8Sia-II assembles a subset of polysialic acid that directs hippocampal axonal targeting and promotes fear behavior. *J Biol Chem*. 279:32603-13.

Arai, M., M. Itokawa, K. Yamada, T. Toyota, M. Arai, S. Haga, H. Ujike, I. Sora, K. Ikeda, and T. Yoshikawa. 2004. Association of neural cell adhesion molecule 1 gene polymorphisms with bipolar affective disorder in Japanese individuals. *Biol Psychiatry*. 55:804-10.

Arber, S., F.A. Barbayannis, H. Hanser, C. Schneider, C.A. Stanyon, O. Bernard, and P. Caroni. 1998. Regulation of actin dynamics through phosphorylation of cofilin by LIM-kinase. *Nature*. 393:805-9.

Arias-Romero, L.E., and J. Chernoff. 2008. A tale of two Paks. *Biol Cell*. 100:97-108.

Asrar, S., Y. Meng, Z. Zhou, Z. Todorovski, W.W. Huang, and Z. Jia. 2009. Regulation of hippocampal long-term potentiation by p21-activated protein kinase 1 (PAK1). *Neuropharmacology*. 56:73-80.

Bagrodia, S., D. Bailey, Z. Lenard, M. Hart, J.L. Guan, R.T. Premont, S.J. Taylor, and R.A. Cerione. 1999. A tyrosine-phosphorylated protein that binds to an important regulatory region on the cool family of p21-activated kinase-binding proteins. *J Biol Chem*. 274:22393-400.

Bagrodia, S., B. Derijard, R.J. Davis, and R.A. Cerione. 1995. Cdc42 and PAK-mediated signaling leads to Jun kinase and p38 mitogen-activated protein kinase activation. *J Biol Chem*. 270:27995-8.

Bagrodia, S., S.J. Taylor, K.A. Jordon, L. Van Aelst, and R.A. Cerione. 1998. A novel regulator of p21-activated kinases. *J Biol Chem*. 273:23633-6.

Bamburg, J.R., and B.W. Bernstein. 2008. ADF/cofilin. *Curr Biol*. 18:R273-5.

Bamburg, J.R., H.E. Harris, and A.G. Weeds. 1980. Partial purification and characterization of an actin depolymerizing factor from brain. *FEBS Lett*. 121:178-82.

Bamburg, J.R., A. McGough, and S. Ono. 1999. Putting a new twist on actin: ADF/cofilins modulate actin dynamics. *Trends Cell Biol*. 9:364-70.

Banerjee, M., D. Worth, D.M. Prowse, and M. Nikolic. 2002. Pak1 phosphorylation on t212 affects microtubules in cells undergoing mitosis. *Curr Biol*. 12:1233-9.

Bateman, J., and D. Van Vactor. 2001. The Trio family of guanine-nucleotide-exchange factors: regulators of axon guidance. *J Cell Sci*. 114:1973-80.

Beeser, A., Z.M. Jaffer, C. Hofmann, and J. Chernoff. 2005. Role of group A p21-activated kinases in activation of extracellular-regulated kinase by growth factors. *J Biol Chem*. 280:36609-15.

Beggs, H.E., S.C. Baragona, J.J. Hemperly, and P.F. Maness. 1997. NCAM140 interacts with the focal adhesion kinase p125(fak) and the SRC-related tyrosine kinase p59(fyn). *J Biol Chem*. 272:8310-9.

Beggs, H.E., P. Soriano, and P.F. Maness. 1994. NCAM-dependent neurite outgrowth is inhibited in neurons from Fyn-minus mice. *J Cell Biol*. 127:825-33.

Benner, G.E., P.B. Dennis, and R.A. Masaracchia. 1995. Activation of an S6/H4 kinase (PAK 65) from human placenta by intramolecular and intermolecular autophosphorylation. *J Biol Chem*. 270:21121-8.

Bernard, O., S. Ganiatsas, G. Kannourakis, and R. Dringen. 1994. Kiz-1, a protein with LIM zinc finger and kinase domains, is expressed mainly in neurons. *Cell Growth Differ*. 5:1159-71.

Bernards, A. 2003. GAPs galore! A survey of putative Ras superfamily GTPase activating proteins in man and Drosophila. *Biochim Biophys Acta*. 1603:47-82.

Beug, H., G. Gerisch, S. Kempff, V. Riedel, and G. Cremer. 1970. Specific inhibition of cell contact formation in Dictyostelium by univalent antibodies. *Exp Cell Res*. 63:147-58.

Bhat, S., and D.H. Silberberg. 1988. Developmental expression of neural cell adhesion molecules of oligodendrocytes in vivo and in culture. *J Neurochem*. 50:1830-8.

Bienvenu, T., V. des Portes, N. McDonell, A. Carrie, R. Zemni, P. Couvert, H.H. Ropers, C. Moraine, H. van Bokhoven, J.P. Fryns, K. Allen, C.A. Walsh, J. Boue, A. Kahn, J. Chelly, and C. Beldjord. 2000. Missense mutation in PAK3, R67C, causes X-linked nonspecific mental retardation. *Am J Med Genet*. 93:294-8.

Bock, E., K. Edvardsen, A. Gibson, D. Linnemann, J.M. Lyles, and O. Nybroe. 1987. Characterization of soluble forms of NCAM. *FEBS Lett*. 225:33-6.

Boda, B., L. Jourdain, and D. Muller. 2008. Distinct, but compensatory roles of PAK1 and PAK3 in spine morphogenesis. *Hippocampus*. 18:857-61.

Bodrikov, V., I. Leshchyns'ka, V. Sytnyk, J. Overvoorde, J. den Hertog, and M. Schachner. 2005. RPTPalpha is essential for NCAM-mediated p59fyn activation and neurite elongation. *J Cell Biol*. 168:127-39.

Bodrikov, V., V. Sytnyk, I. Leshchyns'ka, J. den Hertog, and M. Schachner. 2008. NCAM induces CaMKIIalpha-mediated RPTPalpha phosphorylation to enhance its catalytic activity and neurite outgrowth. *J Cell Biol*. 182:1185-200.

Bokoch, G.M. 2003. Biology of the p21-activated kinases. *Annu Rev Biochem*. 72:743-81.

Bokoch, G.M., A.M. Reilly, R.H. Daniels, C.C. King, A. Olivera, S. Spiegel, and U.G. Knaus. 1998. A GTPase-independent mechanism of p21-activated kinase activation. Regulation by sphingosine and other biologically active lipids. *J Biol Chem*. 273:8137-44.

Bokoch, G.M., Y. Wang, B.P. Bohl, M.A. Sells, L.A. Quilliam, and U.G. Knaus. 1996. Interaction of the Nck adapter protein with p21-activated kinase (PAK1). *J Biol Chem*. 271:25746-9.

Botto, L., M. Masserini, and P. Palestini. 2007. Changes in the composition of detergent-resistant membrane domains of cultured neurons following protein kinase C activation. *J Neurosci Res*. 85:443-50.

Bray, D. 1984. Axonal growth in response to experimentally applied mechanical tension. *Dev Biol*. 102:379-89.

Bray, D., and K. Chapman. 1985. Analysis of microspike movements on the neuronal growth cone. *J Neurosci*. 5:3204-13.

Brown, J.L., L. Stowers, M. Baer, J. Trejo, S. Coughlin, and J. Chant. 1996. Human Ste20 homologue hPAK1 links GTPases to the JNK MAP kinase pathway. *Curr Biol*. 6:598-605.

Bukalo, O., N. Fentrop, A.Y. Lee, B. Salmen, J.W. Law, C.T. Wotjak, M. Schweizer, A. Dityatev, and M. Schachner. 2004. Conditional ablation of the neural cell adhesion molecule reduces precision of spatial learning, long-term potentiation, and depression in the CA1 subfield of mouse hippocampus. *J Neurosci*. 24:1565-77.

Burbelo, P.D., D. Drechsel, and A. Hall. 1995. A conserved binding motif defines numerous candidate target proteins for both Cdc42 and Rac GTPases. *J Biol Chem*. 270:29071-4.

Burbelo, P.D., C.A. Kozak, A.A. Finegold, A. Hall, and D.M. Pirone. 1999. Cloning, central nervous system expression and chromosomal mapping of the mouse PAK-1 and PAK-3 genes. *Gene*. 232:209-15.

Burroughs, C.L., M. Watanabe, and D.E. Morse. 1991. Distribution of the neural cell adhesion molecule (NCAM) during heart development. *J Mol Cell Cardiol*. 23:1411-22.

Buttner, B., C. Kannicht, W. Reutter, and R. Horstkorte. 2003. The neural cell adhesion molecule is associated with major components of the cytoskeleton. *Biochem Biophys Res Commun*. 310:967-71.

Casey, P.J. 1995. Protein lipidation in cell signaling. *Science*. 268:221-5.

Cau, J., S. Faure, S. Vigneron, J.C. Labbe, C. Delsert, and N. Morin. 2000. Regulation of Xenopus p21-activated kinase (X-PAK2) by Cdc42 and maturation-promoting factor controls Xenopus oocyte maturation. *J Biol Chem*. 275:2367-75.

Cau, J., and A. Hall. 2005. Cdc42 controls the polarity of the actin and microtubule cytoskeletons through two distinct signal transduction pathways. *J Cell Sci*. 118:2579-87.

Causeret, F., M. Terao, T. Jacobs, Y.V. Nishimura, Y. Yanagawa, K. Obata, M. Hoshino, and M. Nikolic. 2008. The p21-Activated Kinase Is Required for Neuronal Migration in the Cerebral Cortex. *Cereb Cortex*.

Chahdi, A., B. Miller, and A. Sorokin. 2005. Endothelin 1 induces beta 1Pix translocation and Cdc42 activation via protein kinase A-dependent pathway. *J Biol Chem*. 280:578-84.

Chan, P.M., L. Lim, and E. Manser. 2008. PAK is regulated by PI3K, PIX, CDC42, and PP2Calpha and mediates focal adhesion turnover in the hyperosmotic stress-induced p38 pathway. *J Biol Chem*. 283:24949-61.

Chazal, G., P. Durbec, A. Jankovski, G. Rougon, and H. Cremer. 2000. Consequences of neural cell adhesion molecule deficiency on cell migration in the rostral migratory stream of the mouse. *J Neurosci*. 20:1446-57.

Chong, C., L. Tan, L. Lim, and E. Manser. 2001. The mechanism of PAK activation. Autophosphorylation events in both regulatory and kinase domains control activity. *J Biol Chem*. 276:17347-53.

Chung, W.W., C.F. Lagenaur, Y.M. Yan, and J.S. Lund. 1991. Developmental expression of neural cell adhesion molecules in the mouse neocortex and olfactory bulb. *J Comp Neurol*. 314:290-305.

Cremer, H., G. Chazal, A. Carleton, C. Goridis, J.D. Vincent, and P.M. Lledo. 1998. Long-term but not short-term plasticity at mossy fiber synapses is impaired in neural cell adhesion molecule-deficient mice. *Proc Natl*

Acad Sci U S A. 95:13242-7.
Cremer, H., G. Chazal, C. Goridis, and A. Represa. 1997. NCAM is essential for axonal growth and fasciculation in the hippocampus. *Mol Cell Neurosci*. 8:323-35.
Cremer, H., R. Lange, A. Christoph, M. Plomann, G. Vopper, J. Roes, R. Brown, S. Baldwin, P. Kraemer, S. Scheff, and et al. 1994. Inactivation of the N-CAM gene in mice results in size reduction of the olfactory bulb and deficits in spatial learning. *Nature*. 367:455-9.
Crossin, K.L., and L.A. Krushel. 2000. Cellular signaling by neural cell adhesion molecules of the immunoglobulin superfamily. *Dev Dyn*. 218:260-79.
Cullen, B.R. 1996. HIV-1: is Nef a PAK animal? *Curr Biol*. 6:1557-9.
Cunningham, B.A., S. Hoffman, U. Rutishauser, J.J. Hemperly, and G.M. Edelman. 1983. Molecular topography of the neural cell adhesion molecule N-CAM: surface orientation and location of sialic acid-rich and binding regions. *Proc Natl Acad Sci U S A*. 80:3116-20.
D'Eustachio, P., G.C. Owens, G.M. Edelman, and B.A. Cunningham. 1985. Chromosomal location of the gene encoding the neural cell adhesion molecule (N-CAM) in the mouse. *Proc Natl Acad Sci U S A*. 82:7631-5.
Dan, C., A. Kelly, O. Bernard, and A. Minden. 2001a. Cytoskeletal changes regulated by the PAK4 serine/threonine kinase are mediated by LIM kinase 1 and cofilin. *J Biol Chem*. 276:32115-21.
Dan, I., N.M. Watanabe, and A. Kusumi. 2001b. The Ste20 group kinases as regulators of MAP kinase cascades. *Trends Cell Biol*. 11:220-30.
Daniels, R.H., P.S. Hall, and G.M. Bokoch. 1998. Membrane targeting of p21-activated kinase 1 (PAK1) induces neurite outgrowth from PC12 cells. *Embo J*. 17:754-64.
Danielsen, E.M., and B. van Deurs. 1995. A transferrin-like GPI-linked iron-binding protein in detergent-insoluble noncaveolar microdomains at the apical surface of fetal intestinal epithelial cells. *J Cell Biol*. 131:939-50.
del Pozo, M.A., N.B. Alderson, W.B. Kiosses, H.H. Chiang, R.G. Anderson, and M.A. Schwartz. 2004. Integrins regulate Rac targeting by internalization of membrane domains. *Science*. 303:839-42.
Dharmawardhane, S., L.C. Sanders, S.S. Martin, R.H. Daniels, and G.M. Bokoch. 1997. Localization of p21-activated kinase 1 (PAK1) to pinocytic vesicles and cortical actin structures in stimulated cells. *J Cell Biol*. 138:1265-78.
Di Cesare, A., S. Paris, C. Albertinazzi, S. Dariozzi, J. Andersen, M. Mann, R. Longhi, and I. de Curtis. 2000. p95-APP1 links membrane transport to Rac-mediated reorganization of actin. *Nat Cell Biol*. 2:521-30.
Dickson, B.J. 2001. Rho GTPases in growth cone guidance. *Curr Opin Neurobiol*. 11:103-10.
Ditlevsen, D.K., V. Berezin, and E. Bock. 2007a. Signalling pathways underlying neural cell adhesion molecule-mediated survival of dopaminergic neurons. *Eur J Neurosci*. 25:1678-84.
Ditlevsen, D.K., L.B. Kohler, V. Berezin, and E. Bock. 2007b. Cyclic guanosine monophosphate signalling pathway plays a role in neural cell adhesion molecule-mediated neurite outgrowth and survival. *J Neurosci Res*. 85:703-11.
Ditlevsen, D.K., L.B. Kohler, M.V. Pedersen, M. Risell, K. Kolkova, M. Meyer, V. Berezin, and E. Bock. 2003. The role of phosphatidylinositol 3-kinase in neural cell adhesion molecule-mediated neuronal differentiation and survival. *J Neurochem*. 84:546-56.
Ditlevsen, D.K., G.K. Povlsen, V. Berezin, and E. Bock. 2008. NCAM-induced intracellular signaling revisited. *J Neurosci Res*. 86:727-43.
Doherty, P., S.V. Ashton, S.E. Moore, and F.S. Walsh. 1991a. Morphoregulatory activities of NCAM and N-cadherin can be accounted for by G protein-dependent activation of L- and N-type neuronal Ca2+ channels. *Cell*. 67:21-33.
Doherty, P., J. Cohen, and F.S. Walsh. 1990a. Neurite outgrowth in response to transfected N-CAM changes during development and is modulated by polysialic acid. *Neuron*. 5:209-19.
Doherty, P., M. Fruns, P. Seaton, G. Dickson, C.H. Barton, T.A. Sears, and F.S. Walsh. 1990b. A threshold effect of the major isoforms of NCAM on neurite outgrowth. *Nature*. 343:464-6.
Doherty, P., L.H. Rowett, S.E. Moore, D.A. Mann, and F.S. Walsh. 1991b. Neurite outgrowth in response to transfected N-CAM and N-cadherin reveals fundamental differences in neuronal responsiveness to CAMs. *Neuron*. 6:247-58.
Doherty, P., E. Williams, and F.S. Walsh. 1995. A soluble chimeric form of the L1 glycoprotein stimulates neurite outgrowth. *Neuron*. 14:57-66.
Drazba, J., and V. Lemmon. 1990. The role of cell adhesion molecules in neurite outgrowth on Muller cells. *Dev Biol*. 138:82-93.
Eblen, S.T., J.K. Slack, M.J. Weber, and A.D. Catling. 2002. Rac-PAK signaling stimulates extracellular signal-regulated kinase (ERK) activation by regulating formation of MEK1-ERK complexes. *Mol Cell Biol*. 22:6023-33.
Eckhardt, M., O. Bukalo, G. Chazal, L. Wang, C. Goridis, M. Schachner, R. Gerardy-Schahn, H. Cremer, and A. Dityatev. 2000. Mice deficient in the polysialyltransferase ST8SiaIV/PST-1 allow discrimination of the roles of neural cell adhesion molecule protein and polysialic acid in neural development and synaptic plasticity. *J Neurosci*. 20:5234-44.
Edelman, G.M. 1985. Cell adhesion and the molecular processes of morphogenesis. *Annu Rev Biochem*.

54:135-69.
Edelman, G.M., and M.D. Poulik. 1961. Studies on structural units of the gamma-globulins. *J Exp Med*. 113:861-84.
Edidin, M. 2001. Shrinking patches and slippery rafts: scales of domains in the plasma membrane. *Trends Cell Biol*. 11:492-6.
Edwards, D.C., and G.N. Gill. 1999. Structural features of LIM kinase that control effects on the actin cytoskeleton. *J Biol Chem*. 274:11352-61.
Edwards, D.C., L.C. Sanders, G.M. Bokoch, and G.N. Gill. 1999. Activation of LIM-kinase by Pak1 couples Rac/Cdc42 GTPase signalling to actin cytoskeletal dynamics. *Nat Cell Biol*. 1:253-9.
Fan, X., J.P. Labrador, H. Hing, and G.J. Bashaw. 2003. Slit stimulation recruits Dock and Pak to the roundabout receptor and increases Rac activity to regulate axon repulsion at the CNS midline. *Neuron*. 40:113-27.
Finne, J., U. Finne, H. Deagostini-Bazin, and C. Goridis. 1983. Occurrence of alpha 2-8 linked polysialosyl units in a neural cell adhesion molecule. *Biochem Biophys Res Commun*. 112:482-7.
Foletta, V.C., N. Moussi, P.D. Sarmiere, J.R. Bamburg, and O. Bernard. 2004. LIM kinase 1, a key regulator of actin dynamics, is widely expressed in embryonic and adult tissues. *Exp Cell Res*. 294:392-405.
Frangiskakis, J.M., A.K. Ewart, C.A. Morris, C.B. Mervis, J. Bertrand, B.F. Robinson, B.P. Klein, G.J. Ensing, L.A. Everett, E.D. Green, C. Proschel, N.J. Gutowski, M. Noble, D.L. Atkinson, S.J. Odelberg, and M.T. Keating. 1996. LIM-kinase1 hemizygosity implicated in impaired visuospatial constructive cognition. *Cell*. 86:59-69.
Frey, D., T. Laux, L. Xu, C. Schneider, and P. Caroni. 2000. Shared and unique roles of CAP23 and GAP43 in actin regulation, neurite outgrowth, and anatomical plasticity. *J Cell Biol*. 149:1443-54.
Frost, J.A., S. Xu, M.R. Hutchison, S. Marcus, and M.H. Cobb. 1996. Actions of Rho family small G proteins and p21-activated protein kinases on mitogen-activated protein kinase family members. *Mol Cell Biol*. 16:3707-13.
Gatti, A., Z. Huang, P.T. Tuazon, and J.A. Traugh. 1999. Multisite autophosphorylation of p21-activated protein kinase gamma-PAK as a function of activation. *J Biol Chem*. 274:8022-8.
Gillian, A.M., J.P. Brion, and K.C. Breen. 1994. Expression of the neural cell adhesion molecule (NCAM) in Alzheimer's disease. *Neurodegeneration*. 3:283-91.
Goldberg, D.J., and D.W. Burmeister. 1986. Stages in axon formation: observations of growth of Aplysia axons in culture using video-enhanced contrast-differential interference contrast microscopy. *J Cell Biol*. 103:1921-31.
Goridis, C., H. Deagostini-Bazin, M. Hirn, M.R. Hirsch, G. Rougon, R. Sadoul, O.K. Langley, G. Gombos, and J. Finne. 1983. Neural surface antigens during nervous system development. *Cold Spring Harb Symp Quant Biol*. 48 Pt 2:527-37.
Goslin, K., D.J. Schreyer, J.H. Skene, and G. Banker. 1988. Development of neuronal polarity: GAP-43 distinguishes axonal from dendritic growth cones. *Nature*. 336:672-4.
Gower, H.J., C.H. Barton, V.L. Elsom, J. Thompson, S.E. Moore, G. Dickson, and F.S. Walsh. 1988. Alternative splicing generates a secreted form of N-CAM in muscle and brain. *Cell*. 55:955-64.
Guthrie, C., and G.R. Fink. 1991. Guide to yeast genetics and molecular biology. Academic Press, San Diego.
Harden, N., J. Lee, H.Y. Loh, Y.M. Ong, I. Tan, T. Leung, E. Manser, and L. Lim. 1996. A Drosophila homolog of the Rac- and Cdc42-activated serine/threonine kinase PAK is a potential focal adhesion and focal complex protein that colocalizes with dynamic actin structures. *Mol Cell Biol*. 16:1896-908.
Hart, M.J., A. Eva, D. Zangrilli, S.A. Aaronson, T. Evans, R.A. Cerione, and Y. Zheng. 1994. Cellular transformation and guanine nucleotide exchange activity are catalyzed by a common domain on the dbl oncogene product. *J Biol Chem*. 269:62-5.
Hayashi, K., T. Ohshima, M. Hashimoto, and K. Mikoshiba. 2007. Pak1 regulates dendritic branching and spine formation. *Dev Neurobiol*. 67:655-69.
Hayashi, K., T. Ohshima, and K. Mikoshiba. 2002. Pak1 is involved in dendrite initiation as a downstream effector of Rac1 in cortical neurons. *Mol Cell Neurosci*. 20:579-94.
Hayashi, M.L., S.Y. Choi, B.S. Rao, H.Y. Jung, H.K. Lee, D. Zhang, S. Chattarji, A. Kirkwood, and S. Tonegawa. 2004. Altered cortical synaptic morphology and impaired memory consolidation in forebrain- specific dominant-negative PAK transgenic mice. *Neuron*. 42:773-87.
He, H.T., J. Barbet, J.C. Chaix, and C. Goridis. 1986. Phosphatidylinositol is involved in the membrane attachment of NCAM-120, the smallest component of the neural cell adhesion molecule. *Embo J*. 5:2489-94.
He, Q., E.W. Dent, and K.F. Meiri. 1997. Modulation of actin filament behavior by GAP-43 (neuromodulin) is dependent on the phosphorylation status of serine 41, the protein kinase C site. *J Neurosci*. 17:3515-24.
He, Q., and K.F. Meiri. 2002. Isolation and characterization of detergent-resistant microdomains responsive to NCAM-mediated signaling from growth cones. *Mol Cell Neurosci*. 19:18-31.
Hemperly, J.J., G.M. Edelman, and B.A. Cunningham. 1986a. cDNA clones of the neural cell adhesion molecule (N-CAM) lacking a membrane-spanning region consistent with evidence for membrane attachment via a phosphatidylinositol intermediate. *Proc Natl Acad Sci U S A*. 83:9822-6.
Hemperly, J.J., B.A. Murray, G.M. Edelman, and B.A. Cunningham. 1986b. Sequence of a cDNA clone encoding

the polysialic acid-rich and cytoplasmic domains of the neural cell adhesion molecule N-CAM. *Proc Natl Acad Sci U S A*. 83:3037-41.

Heredia, L., P. Helguera, S. de Olmos, G. Kedikian, F. Sola Vigo, F. LaFerla, M. Staufenbiel, J. de Olmos, J. Busciglio, A. Caceres, and A. Lorenzo. 2006. Phosphorylation of actin-depolymerizing factor/cofilin by LIM-kinase mediates amyloid beta-induced degeneration: a potential mechanism of neuronal dystrophy in Alzheimer's disease. *J Neurosci*. 26:6533-42.

Hing, H., J. Xiao, N. Harden, L. Lim, and S.L. Zipursky. 1999. Pak functions downstream of Dock to regulate photoreceptor axon guidance in Drosophila. *Cell*. 97:853-63.

Hinkle, C.L., S. Diestel, J. Lieberman, and P.F. Maness. 2006. Metalloprotease-induced ectodomain shedding of neural cell adhesion molecule (NCAM). *J Neurobiol*. 66:1378-95.

Hinsby, A.M., L. Lundfald, D.K. Ditlevsen, I. Korshunova, L. Juhl, S.O. Meakin, V. Berezin, and E. Bock. 2004. ShcA regulates neurite outgrowth stimulated by neural cell adhesion molecule but not by fibroblast growth factor 2: evidence for a distinct fibroblast growth factor receptor response to neural cell adhesion molecule activation. *J Neurochem*. 91:694-703.

Hoffman, S., B.C. Sorkin, P.C. White, R. Brackenbury, R. Mailhammer, U. Rutishauser, B.A. Cunningham, and G.M. Edelman. 1982. Chemical characterization of a neural cell adhesion molecule purified from embryonic brain membranes. *J Biol Chem*. 257:7720-9.

Holst, B.D., P.W. Vanderklish, L.A. Krushel, W. Zhou, R.B. Langdon, J.R. McWhirter, G.M. Edelman, and K.L. Crossin. 1998. Allosteric modulation of AMPA-type glutamate receptors increases activity of the promoter for the neural cell adhesion molecule, N-CAM. *Proc Natl Acad Sci U S A*. 95:2597-602.

Horstkorte, R., M. Schachner, J.P. Magyar, T. Vorherr, and B. Schmitz. 1993. The fourth immunoglobulin-like domain of NCAM contains a carbohydrate recognition domain for oligomannosidic glycans implicated in association with L1 and neurite outgrowth. *J Cell Biol*. 121:1409-21.

Hummel, T., M.L. Vasconcelos, J.C. Clemens, Y. Fishilevich, L.B. Vosshall, and S.L. Zipursky. 2003. Axonal targeting of olfactory receptor neurons in Drosophila is controlled by Dscam. *Neuron*. 37:221-31.

Ibsen, S., V. Berezin, B. Norgaard-Pedersen, and E. Bock. 1983. Quantification of the D2-glycoprotein in amniotic fluid and serum from pregnancies with fetal neural tube defects. *J Neurochem*. 41:363-6.

Jacobs, T., F. Causeret, Y.V. Nishimura, M. Terao, A. Norman, M. Hoshino, and M. Nikolic. 2007. Localized activation of p21-activated kinase controls neuronal polarity and morphology. *J Neurosci*. 27:8604-15.

Jaffer, Z.M., and J. Chernoff. 2002. p21-activated kinases: three more join the Pak. *Int J Biochem Cell Biol*. 34:713-7.

Jalink, K., E.J. van Corven, T. Hengeveld, N. Morii, S. Narumiya, and W.H. Moolenaar. 1994. Inhibition of lysophosphatidate- and thrombin-induced neurite retraction and neuronal cell rounding by ADP ribosylation of the small GTP-binding protein Rho. *J Cell Biol*. 126:801-10.

Jessen, U., V. Novitskaya, N. Pedersen, P. Serup, V. Berezin, and E. Bock. 2001. The transcription factors CREB and c-Fos play key roles in NCAM-mediated neuritogenesis in PC12-E2 cells. *J Neurochem*. 79:1149-60.

Jones, N.P., and M. Katan. 2007. Role of phospholipase Cgamma1 in cell spreading requires association with a beta-Pix/GIT1-containing complex, leading to activation of Cdc42 and Rac1. *Mol Cell Biol*. 27:5790-805.

Jorgensen, O.S., and E. Bock. 1974. Brain specific synaptosomal membrane proteins demonstrated by crossed immunoelectrophoresis. *J Neurochem*. 23:879-80.

Juliano, R.L. 2002. Signal transduction by cell adhesion receptors and the cytoskeleton: functions of integrins, cadherins, selectins, and immunoglobulin-superfamily members. *Annu Rev Pharmacol Toxicol*. 42:283-323.

Juliano, R.L., P. Reddig, S. Alahari, M. Edin, A. Howe, and A. Aplin. 2004. Integrin regulation of cell signalling and motility. *Biochem Soc Trans*. 32:443-6.

Kim, M.D., P. Kolodziej, and A. Chiba. 2002. Growth cone pathfinding and filopodial dynamics are mediated separately by Cdc42 activation. *J Neurosci*. 22:1794-806.

Kim, S., T. Kim, D. Lee, S.H. Park, H. Kim, and D. Park. 2000. Molecular cloning of neuronally expressed mouse betaPix isoforms. *Biochem Biophys Res Commun*. 272:721-5.

Kim, S., S.H. Lee, and D. Park. 2001. Leucine zipper-mediated homodimerization of the p21-activated kinase-interacting factor, beta Pix. Implication for a role in cytoskeletal reorganization. *J Biol Chem*. 276:10581-4.

King, C.C., E.M. Gardiner, F.T. Zenke, B.P. Bohl, A.C. Newton, B.A. Hemmings, and G.M. Bokoch. 2000a. p21-activated kinase (PAK1) is phosphorylated and activated by 3-phosphoinositide-dependent kinase-1 (PDK1). *J Biol Chem*. 275:41201-9.

King, C.C., F.T. Zenke, P.E. Dawson, E.M. Dutil, A.C. Newton, B.A. Hemmings, and G.M. Bokoch. 2000b. Sphingosine is a novel activator of 3-phosphoinositide-dependent kinase 1. *J Biol Chem*. 275:18108-13.

Kiryushko, D., I. Korshunova, V. Berezin, and E. Bock. 2006. Neural cell adhesion molecule induces intracellular signaling via multiple mechanisms of Ca2+ homeostasis. *Mol Biol Cell*. 17:2278-86.

Kiselyov, V.V., G. Skladchikova, A.M. Hinsby, P.H. Jensen, N. Kulahin, V. Soroka, N. Pedersen, V. Tsetlin, F.M. Poulsen, V. Berezin, and E. Bock. 2003. Structural basis for a direct interaction between FGFR1 and

NCAM and evidence for a regulatory role of ATP. *Structure*. 11:691-701.
Kiselyov, V.V., V. Soroka, V. Berezin, and E. Bock. 2005. Structural biology of NCAM homophilic binding and activation of FGFR. *J Neurochem*. 94:1169-79.
Knaus, U.G., S. Morris, H.J. Dong, J. Chernoff, and G.M. Bokoch. 1995. Regulation of human leukocyte p21-activated kinases through G protein--coupled receptors. *Science*. 269:221-3.
Knaus, U.G., Y. Wang, A.M. Reilly, D. Warnock, and J.H. Jackson. 1998. Structural requirements for PAK activation by Rac GTPases. *J Biol Chem*. 273:21512-8.
Koh, C.G., E. Manser, Z.S. Zhao, C.P. Ng, and L. Lim. 2001. Beta1PIX, the PAK-interacting exchange factor, requires localization via a coiled-coil region to promote microvillus-like structures and membrane ruffles. *J Cell Sci*. 114:4239-51.
Koh, C.G., E.J. Tan, E. Manser, and L. Lim. 2002. The p21-activated kinase PAK is negatively regulated by POPX1 and POPX2, a pair of serine/threonine phosphatases of the PP2C family. *Curr Biol*. 12:317-21.
Kolkova, K., V. Novitskaya, N. Pedersen, V. Berezin, and E. Bock. 2000. Neural cell adhesion molecule-stimulated neurite outgrowth depends on activation of protein kinase C and the Ras-mitogen-activated protein kinase pathway. *J Neurosci*. 20:2238-46.
Korshunova, I., V. Novitskaya, D. Kiryushko, N. Pedersen, K. Kolkova, E. Kropotova, M. Mosevitsky, M. Rayko, J.S. Morrow, I. Ginzburg, V. Berezin, and E. Bock. 2007. GAP-43 regulates NCAM-180-mediated neurite outgrowth. *J Neurochem*. 100:1599-612.
Kramer, E.M., C. Klein, T. Koch, M. Boytinck, and J. Trotter. 1999. Compartmentation of Fyn kinase with glycosylphosphatidylinositol-anchored molecules in oligodendrocytes facilitates kinase activation during myelination. *J Biol Chem*. 274:29042-9.
Kranenburg, O., M. Poland, F.P. van Horck, D. Drechsel, A. Hall, and W.H. Moolenaar. 1999. Activation of RhoA by lysophosphatidic acid and Galpha12/13 subunits in neuronal cells: induction of neurite retraction. *Mol Biol Cell*. 10:1851-7.
Krog, L., M. Olsen, A.M. Dalseg, J. Roth, and E. Bock. 1992. Characterization of soluble neural cell adhesion molecule in rat brain, CSF, and plasma. *J Neurochem*. 59:838-47.
Ku, G.M., D. Yablonski, E. Manser, L. Lim, and A. Weiss. 2001. A PAK1-PIX-PKL complex is activated by the T-cell receptor independent of Nck, Slp-76 and LAT. *Embo J*. 20:457-65.
Kuhn, T.B., M.D. Brown, and J.R. Bamburg. 1998. Rac1-dependent actin filament organization in growth cones is necessary for beta1-integrin-mediated advance but not for growth on poly-D-lysine. *J Neurobiol*. 37:524-40.
Lamoureux, P., Z.F. Altun-Gultekin, C. Lin, J.A. Wagner, and S.R. Heidemann. 1997. Rac is required for growth cone function but not neurite assembly. *J Cell Sci*. 110 (Pt 5):635-41.
Lamoureux, P., R.E. Buxbaum, and S.R. Heidemann. 1989. Direct evidence that growth cones pull. *Nature*. 340:159-62.
Laux, T., K. Fukami, M. Thelen, T. Golub, D. Frey, and P. Caroni. 2000. GAP43, MARCKS, and CAP23 modulate PI(4,5)P(2) at plasmalemmal rafts, and regulate cell cortex actin dynamics through a common mechanism. *J Cell Biol*. 149:1455-72.
Lee, S.J., and E.N. Benveniste. 1999. Adhesion molecule expression and regulation on cells of the central nervous system. *J Neuroimmunol*. 98:77-88.
Leeuw, T., C. Wu, J.D. Schrag, M. Whiteway, D.Y. Thomas, and E. Leberer. 1998. Interaction of a G-protein beta-subunit with a conserved sequence in Ste20/PAK family protein kinases. *Nature*. 391:191-5.
Lei, M., W. Lu, W. Meng, M.C. Parrini, M.J. Eck, B.J. Mayer, and S.C. Harrison. 2000. Structure of PAK1 in an autoinhibited conformation reveals a multistage activation switch. *Cell*. 102:387-97.
Leshchyns'ka, I., V. Sytnyk, J.S. Morrow, and M. Schachner. 2003. Neural cell adhesion molecule (NCAM) association with PKCbeta2 via betaI spectrin is implicated in NCAM-mediated neurite outgrowth. *J Cell Biol*. 161:625-39.
Lewis, A.K., and P.C. Bridgman. 1992. Nerve growth cone lamellipodia contain two populations of actin filaments that differ in organization and polarity. *J Cell Biol*. 119:1219-43.
Li, W., and K.L. Guan. 2004. The Down syndrome cell adhesion molecule (DSCAM) interacts with and activates Pak. *J Biol Chem*. 279:32824-31.
Lindner, J., G. Zinser, W. Werz, C. Goridis, B. Bizzini, and M. Schachner. 1986. Experimental modification of postnatal cerebellar granule cell migration in vitro. *Brain Res*. 377:298-304.
Little, E.B., G.M. Edelman, and B.A. Cunningham. 1998. Palmitoylation of the cytoplasmic domain of the neural cell adhesion molecule N-CAM serves as an anchor to cellular membranes. *Cell Adhes Commun*. 6:415-30.
Loo, T.H., Y.W. Ng, L. Lim, and E. Manser. 2004. GIT1 activates p21-activated kinase through a mechanism independent of p21 binding. *Mol Cell Biol*. 24:3849-59.
Lu, W., S. Katz, R. Gupta, and B.J. Mayer. 1997. Activation of Pak by membrane localization mediated by an SH3 domain from the adaptor protein Nck. *Curr Biol*. 7:85-94.
Luo, L. 2000. Rho GTPases in neuronal morphogenesis. *Nat Rev Neurosci*. 1:173-80.
Luo, L. 2002. Actin cytoskeleton regulation in neuronal morphogenesis and structural plasticity. *Annu Rev Cell*

Dev Biol. 18:601-35.
Luo, L., Y.J. Liao, L.Y. Jan, and Y.N. Jan. 1994. Distinct morphogenetic functions of similar small GTPases: Drosophila Drac1 is involved in axonal outgrowth and myoblast fusion. *Genes Dev*. 8:1787-802.
Madaule, P., and R. Axel. 1985. A novel ras-related gene family. *Cell*. 41:31-40.
Maekawa, M., T. Ishizaki, S. Boku, N. Watanabe, A. Fujita, A. Iwamatsu, T. Obinata, K. Ohashi, K. Mizuno, and S. Narumiya. 1999. Signaling from Rho to the actin cytoskeleton through protein kinases ROCK and LIM-kinase. *Science*. 285:895-8.
Maness, P.F., and M. Schachner. 2007. Neural recognition molecules of the immunoglobulin superfamily: signaling transducers of axon guidance and neuronal migration. *Nat Neurosci*. 10:19-26.
Manser, E., H.Y. Huang, T.H. Loo, X.Q. Chen, J.M. Dong, T. Leung, and L. Lim. 1997. Expression of constitutively active alpha-PAK reveals effects of the kinase on actin and focal complexes. *Mol Cell Biol*. 17:1129-43.
Manser, E., T. Leung, H. Salihuddin, Z.S. Zhao, and L. Lim. 1994. A brain serine/threonine protein kinase activated by Cdc42 and Rac1. *Nature*. 367:40-6.
Manser, E., T.H. Loo, C.G. Koh, Z.S. Zhao, X.Q. Chen, L. Tan, I. Tan, T. Leung, and L. Lim. 1998. PAK kinases are directly coupled to the PIX family of nucleotide exchange factors. *Mol Cell*. 1:183-92.
McCoy, R.D., E.R. Vimr, and F.A. Troy. 1985. CMP-NeuNAc:poly-alpha-2,8-sialosyl sialyltransferase and the biosynthesis of polysialosyl units in neural cell adhesion molecules. *J Biol Chem*. 260:12695-9.
Meberg, P.J., S. Ono, L.S. Minamide, M. Takahashi, and J.R. Bamburg. 1998. Actin depolymerizing factor and cofilin phosphorylation dynamics: response to signals that regulate neurite extension. *Cell Motil Cytoskeleton*. 39:172-90.
Meiri, K.F., J.L. Saffell, F.S. Walsh, and P. Doherty. 1998. Neurite outgrowth stimulated by neural cell adhesion molecules requires growth-associated protein-43 (GAP-43) function and is associated with GAP-43 phosphorylation in growth cones. *J Neurosci*. 18:10429-37.
Meng, Y., H. Takahashi, J. Meng, Y. Zhang, G. Lu, S. Asrar, T. Nakamura, and Z. Jia. 2004. Regulation of ADF/cofilin phosphorylation and synaptic function by LIM-kinase. *Neuropharmacology*. 47:746-54.
Meng, Y., Y. Zhang, V. Tregoubov, C. Janus, L. Cruz, M. Jackson, W.Y. Lu, J.F. MacDonald, J.Y. Wang, D.L. Falls, and Z. Jia. 2002. Abnormal spine morphology and enhanced LTP in LIMK-1 knockout mice. *Neuron*. 35:121-33.
Michaely, P.A., C. Mineo, Y.S. Ying, and R.G. Anderson. 1999. Polarized distribution of endogenous Rac1 and RhoA at the cell surface. *J Biol Chem*. 274:21430-6.
Milev, P., P. Maurel, M. Haring, R.K. Margolis, and R.U. Margolis. 1996. TAG-1/axonin-1 is a high-affinity ligand of neurocan, phosphacan/protein-tyrosine phosphatase-zeta/beta, and N-CAM. *J Biol Chem*. 271:15716-23.
Mira, J.P., V. Benard, J. Groffen, L.C. Sanders, and U.G. Knaus. 2000. Endogenous, hyperactive Rac3 controls proliferation of breast cancer cells by a p21-activated kinase-dependent pathway. *Proc Natl Acad Sci U S A*. 97:185-9.
Mizuno, K., I. Okano, K. Ohashi, K. Nunoue, K. Kuma, T. Miyata, and T. Nakamura. 1994. Identification of a human cDNA encoding a novel protein kinase with two repeats of the LIM/double zinc finger motif. *Oncogene*. 9:1605-12.
Moller, C.J., A.G. Byskov, J. Roth, J.E. Celis, and E. Bock. 1991. NCAM in developing mouse gonads and ducts. *Anat Embryol (Berl)*. 184:541-8.
Morreale, A., M. Venkatesan, H.R. Mott, D. Owen, D. Nietlispach, P.N. Lowe, and E.D. Laue. 2000. Structure of Cdc42 bound to the GTPase binding domain of PAK. *Nat Struct Biol*. 7:384-8.
Mott, H.R., D. Nietlispach, K.A. Evetts, and D. Owen. 2005. Structural analysis of the SH3 domain of beta-PIX and its interaction with alpha-p21 activated kinase (PAK). *Biochemistry*. 44:10977-83.
Neiiendam, J.L., L.B. Kohler, C. Christensen, S. Li, M.V. Pedersen, D.K. Ditlevsen, M.K. Kornum, V.V. Kiselyov, V. Berezin, and E. Bock. 2004. An NCAM-derived FGF-receptor agonist, the FGL-peptide, induces neurite outgrowth and neuronal survival in primary rat neurons. *J Neurochem*. 91:920-35.
Neugebauer, K.M., K.J. Tomaselli, J. Lilien, and L.F. Reichardt. 1988. N-cadherin, NCAM, and integrins promote retinal neurite outgrowth on astrocytes in vitro. *J Cell Biol*. 107:1177-87.
Newsome, T.P., S. Schmidt, G. Dietzl, K. Keleman, B. Asling, A. Debant, and B.J. Dickson. 2000. Trio combines with dock to regulate Pak activity during photoreceptor axon pathfinding in Drosophila. *Cell*. 101:283-94.
Nguyen, C., M.G. Mattei, J.F. Mattei, M.J. Santoni, C. Goridis, and B.R. Jordan. 1986. Localization of the human NCAM gene to band q23 of chromosome 11: the third gene coding for a cell interaction molecule mapped to the distal portion of the long arm of chromosome 11. *J Cell Biol*. 102:711-5.
Niethammer, P., M. Delling, V. Sytnyk, A. Dityatev, K. Fukami, and M. Schachner. 2002. Cosignaling of NCAM via lipid rafts and the FGF receptor is required for neuritogenesis. *J Cell Biol*. 157:521-32.
Nikolic, M. 2002. The role of Rho GTPases and associated kinases in regulating neurite outgrowth. *Int J Biochem Cell Biol*. 34:731-45.
Nikolic, M., M.M. Chou, W. Lu, B.J. Mayer, and L.H. Tsai. 1998. The p35/Cdk5 kinase is a neuron-specific Rac

effector that inhibits Pak1 activity. *Nature*. 395:194-8.
Nishida, E., S. Maekawa, and H. Sakai. 1984. Cofilin, a protein in porcine brain that binds to actin filaments and inhibits their interactions with myosin and tropomyosin. *Biochemistry*. 23:5307-13.
Niwa, R., K. Nagata-Ohashi, M. Takeichi, K. Mizuno, and T. Uemura. 2002. Control of actin reorganization by Slingshot, a family of phosphatases that dephosphorylate ADF/cofilin. *Cell*. 108:233-46.
Nobes, C.D., and A. Hall. 1995. Rho, rac, and cdc42 GTPases regulate the assembly of multimolecular focal complexes associated with actin stress fibers, lamellipodia, and filopodia. *Cell*. 81:53-62.
Noble, M., M. Albrechtsen, C. Moller, J. Lyles, E. Bock, C. Goridis, M. Watanabe, and U. Rutishauser. 1985. Glial cells express N-CAM/D2-CAM-like polypeptides in vitro. *Nature*. 316:725-8.
Obermeier, A., S. Ahmed, E. Manser, S.C. Yen, C. Hall, and L. Lim. 1998. PAK promotes morphological changes by acting upstream of Rac. *Embo J*. 17:4328-39.
Oestreicher, A.B., P.N. De Graan, W.H. Gispen, J. Verhaagen, and L.H. Schrama. 1997. B-50, the growth associated protein-43: modulation of cell morphology and communication in the nervous system. *Prog Neurobiol*. 53:627-86.
Oh, W.K., J.C. Yoo, D. Jo, Y.H. Song, M.G. Kim, and D. Park. 1997. Cloning of a SH3 domain-containing proline-rich protein, p85SPR, and its localization in focal adhesion. *Biochem Biophys Res Commun*. 235:794-8.
Olenik, C., H. Barth, I. Just, K. Aktories, and D.K. Meyer. 1997. Gene expression of the small GTP-binding proteins RhoA, RhoB, Rac1, and Cdc42 in adult rat brain. *Brain Res Mol Brain Res*. 52:263-9.
Olofsson, B. 1999. Rho guanine dissociation inhibitors: pivotal molecules in cellular signalling. *Cell Signal*. 11:545-54.
Ong, E., M. Suzuki, F. Belot, J.C. Yeh, I. Franceschini, K. Angata, O. Hindsgaul, and M. Fukuda. 2002a. Biosynthesis of HNK-1 glycans on O-linked oligosaccharides attached to the neural cell adhesion molecule (NCAM): the requirement for core 2 beta 1,6-N-acetylglucosaminyltransferase and the muscle-specific domain in NCAM. *J Biol Chem*. 277:18182-90.
Ong, W.Y., X.S. Wang, and E. Manser. 2002b. Differential distribution of alpha and beta isoforms of p21-activated kinase in the monkey cerebral neocortex and hippocampus. *Exp Brain Res*. 144:189-99.
Osmani, N., N. Vitale, J.P. Borg, and S. Etienne-Manneville. 2006. Scrib controls Cdc42 localization and activity to promote cell polarization during astrocyte migration. *Curr Biol*. 16:2395-405.
Pak, C.W., K.C. Flynn, and J.R. Bamburg. 2008. Actin-binding proteins take the reins in growth cones. *Nat Rev Neurosci*. 9:136-47.
Paratcha, G., F. Ledda, and C.F. Ibanez. 2003. The neural cell adhesion molecule NCAM is an alternative signaling receptor for GDNF family ligands. *Cell*. 113:867-79.
Park, H.S., S.H. Lee, D. Park, J.S. Lee, S.H. Ryu, W.J. Lee, S.G. Rhee, and Y.S. Bae. 2004. Sequential activation of phosphatidylinositol 3-kinase, beta Pix, Rac1, and Nox1 in growth factor-induced production of H2O2. *Mol Cell Biol*. 24:4384-94.
Parrini, M.C., M. Lei, S.C. Harrison, and B.J. Mayer. 2002. Pak1 kinase homodimers are autoinhibited in trans and dissociated upon activation by Cdc42 and Rac1. *Mol Cell*. 9:73-83.
Pawson, T., and J.D. Scott. 1997. Signaling through scaffold, anchoring, and adaptor proteins. *Science*. 278:2075-80.
Pedersen, M.V., L.B. Kohler, D.K. Ditlevsen, S. Li, V. Berezin, and E. Bock. 2004. Neuritogenic and survival-promoting effects of the P2 peptide derived from a homophilic binding site in the neural cell adhesion molecule. *J Neurosci Res*. 75:55-65.
Penzes, P., A. Beeser, J. Chernoff, M.R. Schiller, B.A. Eipper, R.E. Mains, and R.L. Huganir. 2003. Rapid induction of dendritic spine morphogenesis by trans-synaptic ephrinB-EphB receptor activation of the Rho-GEF kalirin. *Neuron*. 37:263-74.
Persohn, E., G.E. Pollerberg, and M. Schachner. 1989. Immunoelectron-microscopic localization of the 180 kD component of the neural cell adhesion molecule N-CAM in postsynaptic membranes. *J Comp Neurol*. 288:92-100.
Pfenninger, K.H., L. Ellis, M.P. Johnson, L.B. Friedman, and S. Somlo. 1983. Nerve growth cones isolated from fetal rat brain: subcellular fractionation and characterization. *Cell*. 35:573-84.
Pike, L.J. 2006. Rafts defined: a report on the Keystone Symposium on Lipid Rafts and Cell Function. *J Lipid Res*. 47:1597-8.
Plioplys, A.V., S.E. Hemmens, and C.M. Regan. 1990. Expression of a neural cell adhesion molecule serum fragment is depressed in autism. *J Neuropsychiatry Clin Neurosci*. 2:413-7.
Pollerberg, G.E., K. Burridge, K.E. Krebs, S.R. Goodman, and M. Schachner. 1987. The 180-kD component of the neural cell adhesion molecule N-CAM is involved in cell-cell contacts and cytoskeleton-membrane interactions. *Cell Tissue Res*. 250:227-36.
Pollerberg, G.E., M. Schachner, and J. Davoust. 1986. Differentiation state-dependent surface mobilities of two forms of the neural cell adhesion molecule. *Nature*. 324:462-5.
Poltorak, M., I. Khoja, J.J. Hemperly, J.R. Williams, R. el-Mallakh, and W.J. Freed. 1995. Disturbances in cell recognition molecules (N-CAM and L1 antigen) in the CSF of patients with schizophrenia. *Exp Neurol*.

131:266-72.
Polverino, A., J. Frost, P. Yang, M. Hutchison, A.M. Neiman, M.H. Cobb, and S. Marcus. 1995. Activation of mitogen-activated protein kinase cascades by p21-activated protein kinases in cell-free extracts of Xenopus oocytes. *J Biol Chem*. 270:26067-70.
Ponimaskin, E., G. Dityateva, M.O. Ruonala, M. Fukata, Y. Fukata, F. Kobe, F.S. Wouters, M. Delling, D.S. Bredt, M. Schachner, and A. Dityatev. 2008. Fibroblast growth factor-regulated palmitoylation of the neural cell adhesion molecule determines neuronal morphogenesis. *J Neurosci*. 28:8897-907.
Ponniah, S., D.Z. Wang, K.L. Lim, and C.J. Pallen. 1999. Targeted disruption of the tyrosine phosphatase PTPalpha leads to constitutive downregulation of the kinases Src and Fyn. *Curr Biol*. 9:535-8.
Price, L.S., J. Leng, M.A. Schwartz, and G.M. Bokoch. 1998. Activation of Rac and Cdc42 by integrins mediates cell spreading. *Mol Biol Cell*. 9:1863-71.
Probstmeier, R., K. Kuhn, and M. Schachner. 1989. Binding properties of the neural cell adhesion molecule to different components of the extracellular matrix. *J Neurochem*. 53:1794-801.
Puto, L.A., K. Pestonjamasp, C.C. King, and G.M. Bokoch. 2003. p21-activated kinase 1 (PAK1) interacts with the Grb2 adapter protein to couple to growth factor signaling. *J Biol Chem*. 278:9388-93.
Rashid, T., M. Banerjee, and M. Nikolic. 2001. Phosphorylation of Pak1 by the p35/Cdk5 kinase affects neuronal morphology. *J Biol Chem*. 276:49043-52.
Resh, M.D. 1999. Fatty acylation of proteins: new insights into membrane targeting of myristoylated and palmitoylated proteins. *Biochim Biophys Acta*. 1451:1-16.
Ridley, A.J., and A. Hall. 1992. The small GTP-binding protein rho regulates the assembly of focal adhesions and actin stress fibers in response to growth factors. *Cell*. 70:389-99.
Ridley, A.J., H.F. Paterson, C.L. Johnston, D. Diekmann, and A. Hall. 1992. The small GTP-binding protein rac regulates growth factor-induced membrane ruffling. *Cell*. 70:401-10.
Rietveld, A., S. Neutz, K. Simons, and S. Eaton. 1999. Association of sterol- and glycosylphosphatidylinositol-linked proteins with Drosophila raft lipid microdomains. *J Biol Chem*. 274:12049-54.
Rodriguez, M.M., D. Ron, K. Touhara, C.H. Chen, and D. Mochly-Rosen. 1999. RACK1, a protein kinase C anchoring protein, coordinates the binding of activated protein kinase C and select pleckstrin homology domains in vitro. *Biochemistry*. 38:13787-94.
Ronn, L.C., S. Dissing, A. Holm, V. Berezin, and E. Bock. 2002. Increased intracellular calcium is required for neurite outgrowth induced by a synthetic peptide ligand of NCAM. *FEBS Lett*. 518:60-6.
Rosenberger, G., and K. Kutsche. 2006. AlphaPIX and betaPIX and their role in focal adhesion formation. *Eur J Cell Biol*. 85:265-74.
Rossman, K.L., C.J. Der, and J. Sondek. 2005. GEF means go: turning on RHO GTPases with guanine nucleotide-exchange factors. *Nat Rev Mol Cell Biol*. 6:167-80.
Rutishauser, U., A. Acheson, A.K. Hall, D.M. Mann, and J. Sunshine. 1988. The neural cell adhesion molecule (NCAM) as a regulator of cell-cell interactions. *Science*. 240:53-7.
Rutishauser, U., J.P. Thiery, R. Brackenbury, and G.M. Edelman. 1978. Adhesion among neural cells of the chick embryo. III. Relationship of the surface molecule CAM to cell adhesion and the development of histotypic patterns. *J Cell Biol*. 79:371-81.
Rutishauser, U., J.P. Thiery, R. Brackenbury, B.A. Sela, and G.M. Edelman. 1976. Mechanisms of adhesion among cells from neural tissues of the chick embryo. *Proc Natl Acad Sci U S A*. 73:577-81.
Sadoul, R., M. Hirn, H. Deagostini-Bazin, G. Rougon, and C. Goridis. 1983. Adult and embryonic mouse neural cell adhesion molecules have different binding properties. *Nature*. 304:347-9.
Saffell, J.L., E.J. Williams, I.J. Mason, F.S. Walsh, and P. Doherty. 1997. Expression of a dominant negative FGF receptor inhibits axonal growth and FGF receptor phosphorylation stimulated by CAMs. *Neuron*. 18:231-42.
Sakakibara, A., and A.F. Horwitz. 2006. Mechanism of polarized protrusion formation on neuronal precursors migrating in the developing chicken cerebellum. *J Cell Sci*. 119:3583-92.
Sambrook, J., E.F. Fritsch, and T. Maniatis. 1989. Molecular cloning: A Labroatory Manual. Cold Spring Harbor Laboratory Press, Cold Spring Harbor, NY.
Sanes, J.R., M. Schachner, and J. Covault. 1986. Expression of several adhesive macromolecules (N-CAM, L1, J1, NILE, uvomorulin, laminin, fibronectin, and a heparan sulfate proteoglycan) in embryonic, adult, and denervated adult skeletal muscle. *J Cell Biol*. 102:420-31.
Santuccione, A., V. Sytnyk, I. Leshchyns'ka, and M. Schachner. 2005. Prion protein recruits its neuronal receptor NCAM to lipid rafts to activate p59fyn and to enhance neurite outgrowth. *J Cell Biol*. 169:341-54.
Sargiacomo, M., M. Sudol, Z. Tang, and M.P. Lisanti. 1993. Signal transducing molecules and glycosyl-phosphatidylinositol-linked proteins form a caveolin-rich insoluble complex in MDCK cells. *J Cell Biol*. 122:789-807.
Sasaki, T., and Y. Takai. 1998. The Rho small G protein family-Rho GDI system as a temporal and spatial determinant for cytoskeletal control. *Biochem Biophys Res Commun*. 245:641-5.
Scheffzek, K., M.R. Ahmadian, and A. Wittinghofer. 1998. GTPase-activating proteins: helping hands to

complement an active site. *Trends Biochem Sci*. 23:257-62.
Schlessinger, J. 2000. Cell signaling by receptor tyrosine kinases. *Cell*. 103:211-25.
Schmid, R.S., R.D. Graff, M.D. Schaller, S. Chen, M. Schachner, J.J. Hemperly, and P.F. Maness. 1999. NCAM stimulates the Ras-MAPK pathway and CREB phosphorylation in neuronal cells. *J Neurobiol*. 38:542-58.
Schmid, R.S., and P.F. Maness. 2008. L1 and NCAM adhesion molecules as signaling coreceptors in neuronal migration and process outgrowth. *Curr Opin Neurobiol*. 18:245-50.
Schmid, R.S., B.R. Midkiff, V.P. Kedar, and P.F. Maness. 2004. Adhesion molecule L1 stimulates neuronal migration through Vav2-Pak1 signaling. *Neuroreport*. 15:2791-4.
Schmitt-Ulms, G., G. Legname, M.A. Baldwin, H.L. Ball, N. Bradon, P.J. Bosque, K.L. Crossin, G.M. Edelman, S.J. DeArmond, F.E. Cohen, and S.B. Prusiner. 2001. Binding of neural cell adhesion molecules (N-CAMs) to the cellular prion protein. *J Mol Biol*. 314:1209-25.
Schmucker, D., J.C. Clemens, H. Shu, C.A. Worby, J. Xiao, M. Muda, J.E. Dixon, and S.L. Zipursky. 2000. Drosophila Dscam is an axon guidance receptor exhibiting extraordinary molecular diversity. *Cell*. 101:671-84.
Schuch, U., M.J. Lohse, and M. Schachner. 1989. Neural cell adhesion molecules influence second messenger systems. *Neuron*. 3:13-20.
Schuster, T., M. Krug, H. Hassan, and M. Schachner. 1998. Increase in proportion of hippocampal spine synapses expressing neural cell adhesion molecule NCAM180 following long-term potentiation. *J Neurobiol*. 37:359-72.
Seilheimer, B., and M. Schachner. 1988. Studies of adhesion molecules mediating interactions between cells of peripheral nervous system indicate a major role for L1 in mediating sensory neuron growth on Schwann cells in culture. *J Cell Biol*. 107:341-51.
Sells, M.A., U.G. Knaus, S. Bagrodia, D.M. Ambrose, G.M. Bokoch, and J. Chernoff. 1997. Human p21-activated kinase (Pak1) regulates actin organization in mammalian cells. *Curr Biol*. 7:202-10.
Shamah, S.M., M.Z. Lin, J.L. Goldberg, S. Estrach, M. Sahin, L. Hu, M. Bazalakova, R.L. Neve, G. Corfas, A. Debant, and M.E. Greenberg. 2001. EphA receptors regulate growth cone dynamics through the novel guanine nucleotide exchange factor ephexin. *Cell*. 105:233-44.
Shapiro, L., J. Love, and D.R. Colman. 2007. Adhesion molecules in the nervous system: structural insights into function and diversity. *Annu Rev Neurosci*. 30:451-74.
Sheu, F.S., R.M. Marais, P.J. Parker, N.G. Bazan, and A. Routtenberg. 1990. Neuron-specific protein F1/GAP-43 shows substrate specificity for the beta subtype of protein kinase C. *Biochem Biophys Res Commun*. 171:1236-43.
Shin, E.Y., K.S. Shin, C.S. Lee, K.N. Woo, S.H. Quan, N.K. Soung, Y.G. Kim, C.I. Cha, S.R. Kim, D. Park, G.M. Bokoch, and E.G. Kim. 2002. Phosphorylation of p85 beta PIX, a Rac/Cdc42-specific guanine nucleotide exchange factor, via the Ras/ERK/PAK2 pathway is required for basic fibroblast growth factor-induced neurite outgrowth. *J Biol Chem*. 277:44417-30.
Simons, K., and E. Ikonen. 1997. Functional rafts in cell membranes. *Nature*. 387:569-72.
Singer, S.J., and G.L. Nicolson. 1972. The fluid mosaic model of the structure of cell membranes. *Science*. 175:720-31.
Slack-Davis, J.K., S.T. Eblen, M. Zecevic, S.A. Boerner, A. Tarcsafalvi, H.B. Diaz, M.S. Marshall, M.J. Weber, J.T. Parsons, and A.D. Catling. 2003. PAK1 phosphorylation of MEK1 regulates fibronectin-stimulated MAPK activation. *J Cell Biol*. 162:281-91.
Stanyon, C.A., and O. Bernard. 1999. LIM-kinase1. *Int J Biochem Cell Biol*. 31:389-94.
Stork, O., H. Welzl, D. Wolfer, T. Schuster, N. Mantei, S. Stork, D. Hoyer, H. Lipp, K. Obata, and M. Schachner. 2000. Recovery of emotional behaviour in neural cell adhesion molecule (NCAM) null mutant mice through transgenic expression of NCAM180. *Eur J Neurosci*. 12:3291-306.
Sullivan, P.F., R.S. Keefe, L.A. Lange, E.M. Lange, T.S. Stroup, J. Lieberman, and P.F. Maness. 2007. NCAM1 and neurocognition in schizophrenia. *Biol Psychiatry*. 61:902-10.
Sumi, T., K. Matsumoto, Y. Takai, and T. Nakamura. 1999. Cofilin phosphorylation and actin cytoskeletal dynamics regulated by rho- and Cdc42-activated LIM-kinase 2. *J Cell Biol*. 147:1519-32.
Sundberg-Smith, L.J., J.T. Doherty, C.P. Mack, and J.M. Taylor. 2005. Adhesion stimulates direct PAK1/ERK2 association and leads to ERK-dependent PAK1 Thr212 phosphorylation. *J Biol Chem*. 280:2055-64.
Suter, D.M., and P. Forscher. 2000. Substrate-cytoskeletal coupling as a mechanism for the regulation of growth cone motility and guidance. *J Neurobiol*. 44:97-113.
Sytnyk, V., I. Leshchyns'ka, M. Delling, G. Dityateva, A. Dityatev, and M. Schachner. 2002. Neural cell adhesion molecule promotes accumulation of TGN organelles at sites of neuron-to-neuron contacts. *J Cell Biol*. 159:649-61.
Sytnyk, V., I. Leshchyns'ka, A.G. Nikonenko, and M. Schachner. 2006. NCAM promotes assembly and activity-dependent remodeling of the postsynaptic signaling complex. *J Cell Biol*. 174:1071-85.
Tanaka, E., T. Ho, and M.W. Kirschner. 1995. The role of microtubule dynamics in growth cone motility and axonal growth. *J Cell Biol*. 128:139-55.

Tang, Y., Z. Chen, D. Ambrose, J. Liu, J.B. Gibbs, J. Chernoff, and J. Field. 1997. Kinase-deficient Pak1 mutants inhibit Ras transformation of Rat-1 fibroblasts. *Mol Cell Biol*. 17:4454-64.

Tang, Y., H. Zhou, A. Chen, R.N. Pittman, and J. Field. 2000. The Akt proto-oncogene links Ras to Pak and cell survival signals. *J Biol Chem*. 275:9106-9.

Teo, M., E. Manser, and L. Lim. 1995. Identification and molecular cloning of a p21cdc42/rac1-activated serine/threonine kinase that is rapidly activated by thrombin in platelets. *J Biol Chem*. 270:26690-7.

Teramoto, H., O.A. Coso, H. Miyata, T. Igishi, T. Miki, and J.S. Gutkind. 1996. Signaling from the small GTP-binding proteins Rac1 and Cdc42 to the c-Jun N-terminal kinase/stress-activated protein kinase pathway. A role for mixed lineage kinase 3/protein-tyrosine kinase 1, a novel member of the mixed lineage kinase family. *J Biol Chem*. 271:27225-8.

Thiel, D.A., M.K. Reeder, A. Pfaff, T.R. Coleman, M.A. Sells, and J. Chernoff. 2002. Cell cycle-regulated phosphorylation of p21-activated kinase 1. *Curr Biol*. 12:1227-32.

Thiery, J.P., R. Brackenbury, U. Rutishauser, and G.M. Edelman. 1977. Adhesion among neural cells of the chick embryo. *Prog Clin Biol Res*. 15:199-206.

Thompson, C., C.H. Lin, and P. Forscher. 1996. An Aplysia cell adhesion molecule associated with site-directed actin filament assembly in neuronal growth cones. *J Cell Sci*. 109 (Pt 12):2843-54.

Thompson, G., D. Owen, P.A. Chalk, and P.N. Lowe. 1998. Delineation of the Cdc42/Rac-binding domain of p21-activated kinase. *Biochemistry*. 37:7885-91.

Tomasiewicz, H., K. Ono, D. Yee, C. Thompson, C. Goridis, U. Rutishauser, and T. Magnuson. 1993. Genetic deletion of a neural cell adhesion molecule variant (N-CAM-180) produces distinct defects in the central nervous system. *Neuron*. 11:1163-74.

Tsakiridis, T., C. Taha, S. Grinstein, and A. Klip. 1996. Insulin activates a p21-activated kinase in muscle cells via phosphatidylinositol 3-kinase. *J Biol Chem*. 271:19664-7.

Tsoory, M., A. Guterman, and G. Richter-Levin. 2008. Exposure to stressors during juvenility disrupts development-related alterations in the PSA-NCAM to NCAM expression ratio: potential relevance for mood and anxiety disorders. *Neuropsychopharmacology*. 33:378-93.

Turner, C.E., M.C. Brown, J.A. Perrotta, M.C. Riedy, S.N. Nikolopoulos, A.R. McDonald, S. Bagrodia, S. Thomas, and P.S. Leventhal. 1999. Paxillin LD4 motif binds PAK and PIX through a novel 95-kD ankyrin repeat, ARF-GAP protein: A role in cytoskeletal remodeling. *J Cell Biol*. 145:851-63.

Tursun, B., A. Schluter, M.A. Peters, B. Viehweger, H.P. Ostendorff, J. Soosairajah, A. Drung, M. Bossenz, S.A. Johnsen, M. Schweizer, O. Bernard, and I. Bach. 2005. The ubiquitin ligase Rnf6 regulates local LIM kinase 1 levels in axonal growth cones. *Genes Dev*. 19:2307-19.

Vadlamudi, R.K., and R. Kumar. 2003. P21-activated kinases in human cancer. *Cancer Metastasis Rev*. 22:385-93.

Vadlamudi, R.K., F. Li, L. Adam, D. Nguyen, Y. Ohta, T.P. Stossel, and R. Kumar. 2002. Filamin is essential in actin cytoskeletal assembly mediated by p21-activated kinase 1. *Nat Cell Biol*. 4:681-90.

Vadlamudi, R.K., F. Li, C.J. Barnes, R. Bagheri-Yarmand, and R. Kumar. 2004. p41-Arc subunit of human Arp2/3 complex is a p21-activated kinase-1-interacting substrate. *EMBO Rep*. 5:154-60.

Vetter, I.R., and A. Wittinghofer. 2001. The guanine nucleotide-binding switch in three dimensions. *Science*. 294:1299-304.

Vikis, H.G., W. Li, and K.L. Guan. 2002. The plexin-B1/Rac interaction inhibits PAK activation and enhances Sema4D ligand binding. *Genes Dev*. 16:836-45.

Vutskits, L., Z. Djebbara-Hannas, H. Zhang, J.P. Paccaud, P. Durbec, G. Rougon, D. Muller, and J.Z. Kiss. 2001. PSA-NCAM modulates BDNF-dependent survival and differentiation of cortical neurons. *Eur J Neurosci*. 13:1391-402.

Walmod, P.S., K. Kolkova, V. Berezin, and E. Bock. 2004. Zippers make signals: NCAM-mediated molecular interactions and signal transduction. *Neurochem Res*. 29:2015-35.

Walsh, F.S., R.B. Parekh, S.E. Moore, G. Dickson, C.H. Barton, H.J. Gower, R.A. Dwek, and T.W. Rademacher. 1989. Tissue specific O-linked glycosylation of the neural cell adhesion molecule (N-CAM). *Development*. 105:803-11.

Walsh, F.S., W. Putt, J.G. Dickson, C.A. Quinn, R.D. Cox, M. Webb, N. Spurr, and P.N. Goodfellow. 1986. Human N-CAM gene: mapping to chromosome 11 by analysis of somatic cell hybrids with mouse and human cDNA probes. *Brain Res*. 387:197-200.

Wang, J., C.T. Zugates, I.H. Liang, C.H. Lee, and T. Lee. 2002. Drosophila Dscam is required for divergent segregation of sister branches and suppresses ectopic bifurcation of axons. *Neuron*. 33:559-71.

Weinhold, B., R. Seidenfaden, I. Rockle, M. Muhlenhoff, F. Schertzinger, S. Conzelmann, J.D. Marth, R. Gerardy-Schahn, and H. Hildebrandt. 2005. Genetic ablation of polysialic acid causes severe neurodevelopmental defects rescued by deletion of the neural cell adhesion molecule. *J Biol Chem*. 280:42971-7.

Wen, Z., and J.Q. Zheng. 2006. Directional guidance of nerve growth cones. *Curr Opin Neurobiol*. 16:52-8.

Wherlock, M., and H. Mellor. 2002. The Rho GTPase family: a Racs to Wrchs story. *J Cell Sci*. 115:239-40.

Whitehead, I.P., S. Campbell, K.L. Rossman, and C.J. Der. 1997. Dbl family proteins. *Biochim Biophys Acta*. 1332:F1-23.

Williams, E.J., J. Furness, F.S. Walsh, and P. Doherty. 1994a. Activation of the FGF receptor underlies neurite outgrowth stimulated by L1, N-CAM, and N-cadherin. *Neuron*. 13:583-94.

Williams, E.J., B. Mittal, F.S. Walsh, and P. Doherty. 1995. A Ca2+/calmodulin kinase inhibitor, KN-62, inhibits neurite outgrowth stimulated by CAMs and FGF. *Mol Cell Neurosci*. 6:69-79.

Williams, E.J., F.S. Walsh, and P. Doherty. 1994b. The production of arachidonic acid can account for calcium channel activation in the second messenger pathway underlying neurite outgrowth stimulated by NCAM, N-cadherin, and L1. *J Neurochem*. 62:1231-4.

Williams, R.W., and K. Herrup. 1988. The control of neuron number. *Annu Rev Neurosci*. 11:423-53.

Worby, C.A., N. Simonson-Leff, J.C. Clemens, R.P. Kruger, M. Muda, and J.E. Dixon. 2001. The sorting nexin, DSH3PX1, connects the axonal guidance receptor, Dscam, to the actin cytoskeleton. *J Biol Chem*. 276:41782-9.

y Cajal, S.R. 1890a. Notas anatómicas. I. Sobre la aparición de las expansiones celulares en la médula embrionaria. *Gac Sanit Barc* 12:413-419.

y Cajal, S.R. 1890b. A quelle époque apparaissent les expansions des cellules nerveuses de la moelle épinière du poulet. *Anat Anz* 5:609-613.

Yang, N., O. Higuchi, K. Ohashi, K. Nagata, A. Wada, K. Kangawa, E. Nishida, and K. Mizuno. 1998. Cofilin phosphorylation by LIM-kinase 1 and its role in Rac-mediated actin reorganization. *Nature*. 393:809-12.

Yu, J.S., W.J. Chen, M.H. Ni, W.H. Chan, and S.D. Yang. 1998. Identification of the regulatory autophosphorylation site of autophosphorylation-dependent protein kinase (auto-kinase). Evidence that auto-kinase belongs to a member of the p21-activated kinase family. *Biochem J*. 334 (Pt 1):121-31.

Zalcman, G., O. Dorseuil, J.A. Garcia-Ranea, G. Gacon, and J. Camonis. 1999. RhoGAPs and RhoGDIs, (His)stories of two families. *Prog Mol Subcell Biol*. 22:85-113.

Zebda, N., O. Bernard, M. Bailly, S. Welti, D.S. Lawrence, and J.S. Condeelis. 2000. Phosphorylation of ADF/cofilin abolishes EGF-induced actin nucleation at the leading edge and subsequent lamellipod extension. *J Cell Biol*. 151:1119-28.

Zecchini, S., and U. Cavallaro. 2008. Neural Cell Adhesion Molecule in Cancer: Expression and Mechanisms. *Neurochem Res*.

Zegers, M.M., M.A. Forget, J. Chernoff, K.E. Mostov, M.B. ter Beest, and S.H. Hansen. 2003. Pak1 and PIX regulate contact inhibition during epithelial wound healing. *Embo J*. 22:4155-65.

Zenke, F.T., C.C. King, B.P. Bohl, and G.M. Bokoch. 1999. Identification of a central phosphorylation site in p21-activated kinase regulating autoinhibition and kinase activity. *J Biol Chem*. 274:32565-73.

Zhan, Q., Q. Ge, T. Ohira, T. Van Dyke, and J.A. Badwey. 2003. p21-activated kinase 2 in neutrophils can be regulated by phosphorylation at multiple sites and by a variety of protein phosphatases. *J Immunol*. 171:3785-93.

Zhang, H., L. Vutskits, V. Calaora, P. Durbec, and J.Z. Kiss. 2004. A role for the polysialic acid-neural cell adhesion molecule in PDGF-induced chemotaxis of oligodendrocyte precursor cells. *J Cell Sci*. 117:93-103.

Zhang, H., D.J. Webb, H. Asmussen, S. Niu, and A.F. Horwitz. 2005. A GIT1/PIX/Rac/PAK signaling module regulates spine morphogenesis and synapse formation through MLC. *J Neurosci*. 25:3379-88.

Zhang, S., J. Han, M.A. Sells, J. Chernoff, U.G. Knaus, R.J. Ulevitch, and G.M. Bokoch. 1995. Rho family GTPases regulate p38 mitogen-activated protein kinase through the downstream mediator Pak1. *J Biol Chem*. 270:23934-6.

Zhao, Z.S., and E. Manser. 2005. PAK and other Rho-associated kinases--effectors with surprisingly diverse mechanisms of regulation. *Biochem J*. 386:201-14.

Zhao, Z.S., E. Manser, X.Q. Chen, C. Chong, T. Leung, and L. Lim. 1998. A conserved negative regulatory region in alphaPAK: inhibition of PAK kinases reveals their morphological roles downstream of Cdc42 and Rac1. *Mol Cell Biol*. 18:2153-63.

Zhao, Z.S., E. Manser, and L. Lim. 2000a. Interaction between PAK and nck: a template for Nck targets and role of PAK autophosphorylation. *Mol Cell Biol*. 20:3906-17.

Zhao, Z.S., E. Manser, T.H. Loo, and L. Lim. 2000b. Coupling of PAK-interacting exchange factor PIX to GIT1 promotes focal complex disassembly. *Mol Cell Biol*. 20:6354-63.

Zheng, X.M., Y. Wang, and C.J. Pallen. 1992. Cell transformation and activation of pp60c-src by overexpression of a protein tyrosine phosphatase. *Nature*. 359:336-9.

Zheng, Y. 2001. Dbl family guanine nucleotide exchange factors. *Trends Biochem Sci*. 26:724-32.

Zheng, Y., D. Zangrilli, R.A. Cerione, and A. Eva. 1996. The pleckstrin homology domain mediates transformation by oncogenic dbl through specific intracellular targeting. *J Biol Chem*. 271:19017-20.

Zhong, J.L., M.D. Banerjee, and M. Nikolic. 2003. Pak1 and its T212 phosphorylated form accumulate in neurones and epithelial cells of the developing rodent. *Dev Dyn*. 228:121-7.

VIII. ACKNOWLEDGEMENT

The present study was performed in the Institute for Biosynthesis of Neuronal Structures of the Centre for Molecular Neurobiology (ZMNH) at the University of Hamburg. I owe my deepest gratitude to my supervisor Prof. Dr. Melitta Schachner whose valuable advice, continuous enthusiasm and broad knowledge have been of great value.

I want to express my gratitude to Dr. Vladimir Sytnyk and Dr. Iryna Leshchyns'ka for introducing me into the magic field of neuroscience. Their smart guidance, methodological advice and instructive comments have been essential for the completion of my work.

Many thanks to Prof. Dr. Thorsten Burmester for taking me as his ph.D. student in the biology department of Hamburg University. All the personnel of the biology department are sincerely acknowledged for all their help and guidance. I wish to thank all the faculty and staff at ZMNH.

I wish to express my gratitude to Dr. Toshima Ohshima, (Laboratory for Developmental Neurobiology, Brain Science Institute, Saitama, Japan) for providing me the mutant Pak1 constructs.

I express my gratitude to all my colleagues in ZMNH for nice conversations and creating and supporting the most valuable team spirit. The relaxing atmosphere among the group members has helped me carry out the thesis work greatly.

I want to thank all my friends for their help and support during the course of this study. The time spent together has been a great counter balance to work and given me so many precious memories that will have a place in my heart for ever.

My parents Mingchao Li and Guimin Zhang, as well as my sister Bo Li, are warmly acknowledged for always being there for me. Their encouragement, support and love have been essential for me during this work and throughout my life.

Finally, I want to express my deepest gratitude to all who have helped and cared me.